NATURAL CONVECTION IN AN ENCLOSED GAS HEATED BY LOCAL LASER RADIATION

Air Force Aero Propulsion Laboratory
Wright-Patterson Air Force Base, Ohio

March 1976

DISCLAIMER NOTICE

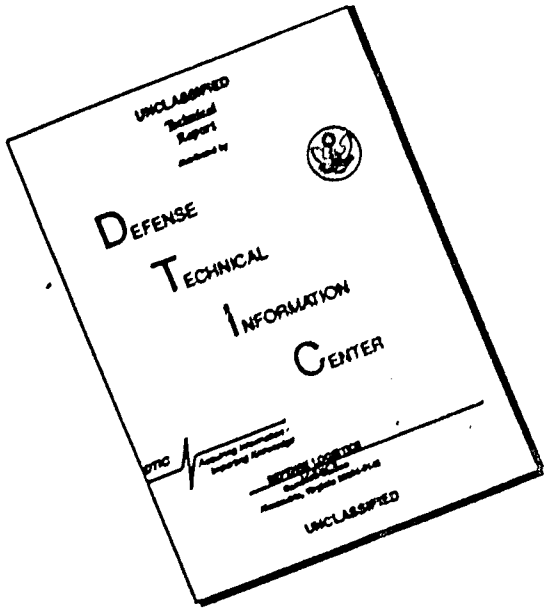

THIS DOCUMENT IS BEST QUALITY AVAILABLE. THE COPY FURNISHED TO DTIC CONTAINED A SIGNIFICANT NUMBER OF PAGES WHICH DO NOT REPRODUCE LEGIBLY.

AFAPL-TR-76-11

NATURAL CONVECTION IN AN ENCLOSED GAS HEATED BY LOCAL LASER RADIATION

FIRE PROTECTION BRANCH
FUELS AND LUBRICATION DIVISION

MARCH 1976

TECHNICAL REPORT AFAPL-TR-76-11
FINAL REPORT FOR PERIOD 1 JANUARY 1974 – 1 DECEMBER 1975

AIR FORCE AERO-PROPULSION LABORATORY
AIR FORCE WRIGHT AERONAUTICAL LABORATORIES
Air Force Systems Command
Wright-Patterson Air Force Base, Ohio 45433

NOTICE

When Government drawings, specifications, or other data are used for any purpose other than in connection with a definitely related Government procurement operation, the United States Government thereby incurs no responsibility nor any obligation whatsoever; and the fact that the government may have formulated, furnished, or in any way supplied the said drawings, specifications, or other data, is not to be regarded by implication or otherwise as in any manner licensing the holder or any other person or corporation, or conveying any rights or permission to manufacture, use, or sell any patented invention that may in any way be related thereto.

This report contains the results of an effort to model the convective motion of a gas being heated by local laser radiation. This work was performed in the Fire Protection Branch of the Air Force Aero-Propulsion Laboratory, Air Force Systems Command, Wright-Patterson AFB, Ohio under Project 3048, Task 304807, and Work Unit 30480774. This effort was conducted by Mr. Allan Ferrenberg (AFAPL/SFH) with the assistance of Dr. Kervyn Mach (AFAPL/TBC) during the period of January 1974 to December 1975.

The authors would like to express their appreciation for the advice and assistance of Professor Lit S. Han of the Ohio State University, the programming assistance of Ms. Beth Simons (engineer's assistant) of Systems Research Laboratories, Dayton, Ohio, and the secretarial efforts of Ms. Mary Huttsell of the Air Force Aero-Propulsion Laboratory.

This report has been reviewed by the information office, ASD/OIP, and is releasable to the National Technical Information Service [NTIS]. At NTIS, it will be available to the general public, including foreign nationals.

This technical report has been reviewed and is approved for publication.

Allan J. Ferrenberg
ALLAN J. FERRENBERG
Project Engineer
Fire Protection Branch
Fuels and Lubrication Division
Air Force Aero-Propulsion Laboratory

Kervyn D Mach
DR. KERVYN MACH
Components Branch
Turbine Engine Division
Air Force Aero-Propulsion Laboratory

Benito P Botteri
BENITO P. BOTTERI
Chief, Fire Protection Branch
Fuels and Lubrication Division
Air Force Aero-Propulsion Laboratory

AIR FORCE - 2 APRIL 1976 - 150

UNCLASSIFIED

SECURITY CLASSIFICATION OF THIS PAGE *(When Data Entered)*

REPORT DOCUMENTATION PAGE		READ INSTRUCTIONS BEFORE COMPLETING FORM
1. REPORT NUMBER AFAPL-TR-76-11	2. GOVT ACCESSION NO.	3. RECIPIENT'S CATALOG NUMBER
4. TITLE *(and Subtitle)* Natural Convection In An Enclosed Gas Heated By Local Laser Radiation		5. TYPE OF REPORT & PERIOD COVERED Final (1 Jan 74 to 1 Dec 75) 6. PERFORMING ORG. REPORT NUMBER
7. AUTHOR(s) Allan J. Ferrenberg Kervyn Mach, PhD		8. CONTRACT OR GRANT NUMBER(s)
9. PERFORMING ORGANIZATION NAME AND ADDRESS Fire Protection Branch (AFAPL/SFH) Air Force Aero-Propulsion Laboratory Wright-Patterson AFB, OH 45433		10. PROGRAM ELEMENT, PROJECT, TASK AREA & WORK UNIT NUMBERS 30480774
11. CONTROLLING OFFICE NAME AND ADDRESS Fire Protection Branch (AFAPL/SFH) Air Force Aero-Propulsion Laboratory Wright-Patterson AFB, OH 45433		12. REPORT DATE March 1976 13. NUMBER OF PAGES 109
14. MONITORING AGENCY NAME & ADDRESS *(if different from Controlling Office)*		15. SECURITY CLASS. *(of this report)* UNCLASSIFIED 15a. DECLASSIFICATION DOWNGRADING SCHEDULE

16. DISTRIBUTION STATEMENT *(of this Report)*

Approved for Public Release; Distribution Unlimited

17. DISTRIBUTION STATEMENT *(of the abstract entered in Block 20, if different from Report)*

18. SUPPLEMENTARY NOTES

19. KEY WORDS *(Continue on reverse side if necessary and identify by block number)*

1. Laser
2. Convection
3. Laser Propagation
4. Laser Effects

20. ABSTRACT *(Continue on reverse side if necessary and identify by block number)*

This report describes a technique by which the thermal effects of heating a gas by laser radiation absorption can be modelled. This is accomplished via a two-dimensional computer program which couples the equations of motion, energy, and continuity. The program models the convective motion of the gas during the irradiation period and predicts thermal and velocity distribution in the gas mixture. Any partially absorbing gas mixture can be considered, as long as sufficient thermophysical properties and absorption coefficients are known. Energy absorbed from the laser as a function of time can also be determined.

DD FORM 1 JAN 73 1473 EDITION OF 1 NOV 65 IS OBSOLETE

UNCLASSIFIED

SECURITY CLASSIFICATION OF THIS PAGE *(When Data Entered)*

TABLE OF CONTENTS

LIST OF ILLUSTRATIONS

I. INTRODUCTION/PHYSICAL DESCRIPTION OF THE PROBLEM

With the rapidly increasing development of higher power lasers, and the growing number of applications of these devices, a number of new and transient heat transfer problems require solutions. One such set of problems involves the absorption of energy from a laser beam by the gas through which the beam is passing. This report describes a numerical technique by which the various energy transfer and gas motion phenomena in such an irradiated gas can be modeled. The problem consists of a gas mixture enclosed in a vessel of square cross-section. The beam passes through the gas mixture along the center of the square section as shown in Figure 1. The container is considered to be well insulated and sealed. This implies that the laser energy is incident through a sealed window or an open hole in the container which is very small compared to the volume of the container. Thus the pressure within the enclosure is unrelieved and increases as the gas is heated. The beam diameter is small compared to the cross-section dimensions of the enclosure and the amount of energy absorbed is relatively small.

The medium or fluid being heated consists of a homogeneous mixture of gases. The gas composition and chemical properties do not change. The energy absorbed is assumed to manifest itself only as a change in the temperature of the gas with no chemical change. For longer wavelength radiation, the absence of chemical change due to photochemical effects is probably a reasonable assumption. However, as the gas mixture becomes hotter, some chemical changes will begin to occur. The temperatures at which these chemical effects become significant

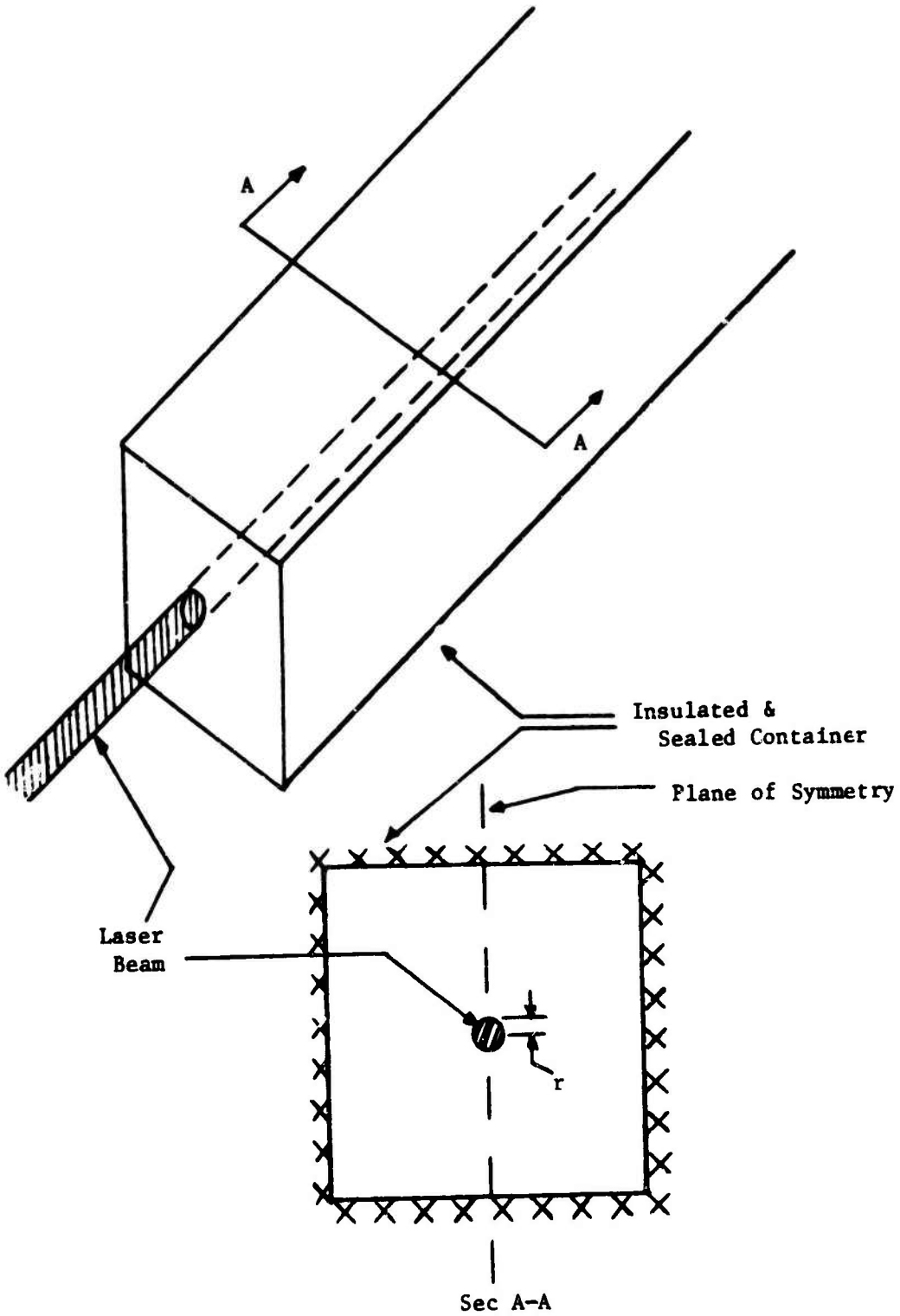

FIGURE 1: PROBLEM CONFIGURATION

depends upon the reactivity of the gases in the mixture. Therefore, this analysis is not applicable where temperatures are high enough to cause chemical changes in the gas mixture. The mixture considered in this analysis is a normal hydrocarbon vapor in air. Absorption coefficients for these vapors are extracted from Reference 1, and the air is assumed to be completely transparent to the laser radiation. (The ratio of the absorption coefficients of air to pentane is 10^{-5}.) These absorption coefficients apply to 10.6 micron radiation as would be produced by a carbon dioxide laser, and are assumed to be directly proportional to the gas density (i.e., number of molecules in beam path). As a first order approximation, the absorption coefficient is assumed to be independent of temperature. Other gas mixtures can be included in this analysis if sufficient thermal properties and absorption coefficients at the specified wavelength are known for each constituent. Similarly, other wavelength laser radiation can be considered.

This analysis of the problem consists of the construction of a computer program which models the heat transfer effects occurring in the gas (i.e., convection, conduction, and absorption of the laser radiation). Re-radiation from the gas is not considered. This should not be a problem at the relatively low temperatures to which the gases are heated. Since only a very small amount of energy is removed from the beam as it passes through the gas, the gas mixture temperature gradients and incident energy gradients along the beam axis are very small. Therefore, the problem is assumed to be two-dimensional. Furthermore, symmetry about a vertical plane through the center of the beam is assumed.

Two different types of laser beams, characterized by different spatial energy distributions, are considered. The first of these is the "flat-top" or "square" beam which has a constant power density versus radial distance from the beam center distribution, as shown in Figure 2. The second type of beam considered has a Gaussian power density distribution truncated at the defined radius. This is also shown in Figure 2. The laser output power is assumed to be constant with time, i.e., continuous wave (CW) output.

II. MATHEMATICAL DESCRIPTION OF THE PROBLEM

The coordinate system utilized in this analysis is shown in Figure 3. Terms used in this report are defined in Appendix 1.

A. ASSUMPTIONS:

The problem is assumed to be two-dimensional and symmetric about a vertical plane through the laser beam axis. The beam passes through the center of the square enclosure. Only the right side of the cross-section of the enclosure will be considered as shown in Figure 3. The enclosure is assumed to be insulated and the system is therefore adiabatic, with the exception of the volumetric heating of the gas by absorption of energy from the laser beam. The density of the gas is assumed to remain constant except in the absorption coefficient calculation and in the bouyancy term in the vertical equation of motion. This assumption is discussed in Appendix 3. The heating occurs in a sealed enclosure. Thus, there is

"Flattop" Beam

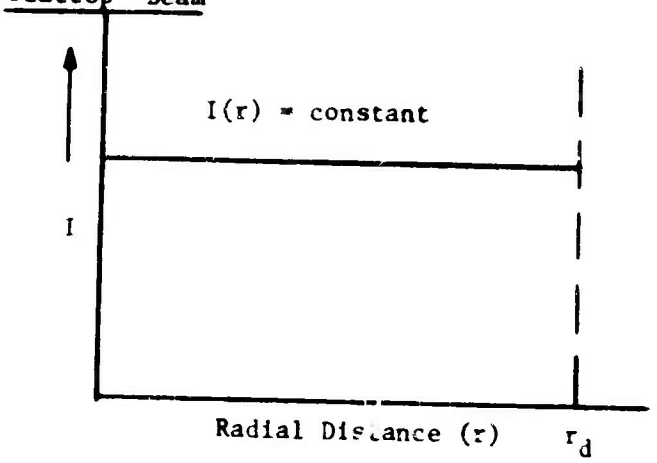

r_d = defined beam radius
I = power per unit area

Gaussian Beam

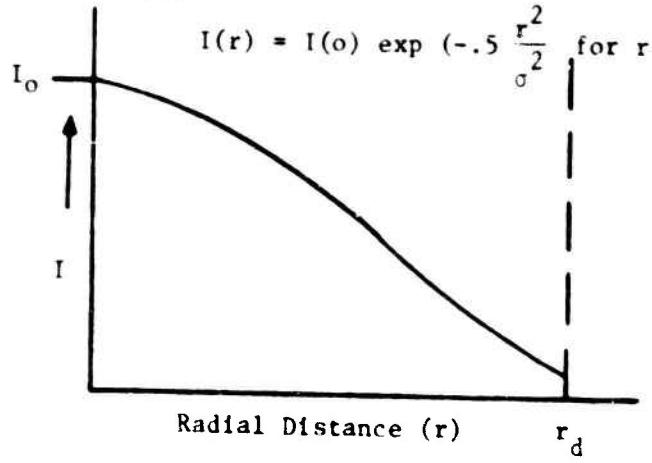

I(o) = 2 x average power per unit area

$$I(o) = \frac{\text{Total output power of laser x 2}}{\pi r_d^2}$$

$$\sigma = \frac{r_d}{2}$$

FIGURE 2: LASER BEAM POWER DISTRIBUTIONS

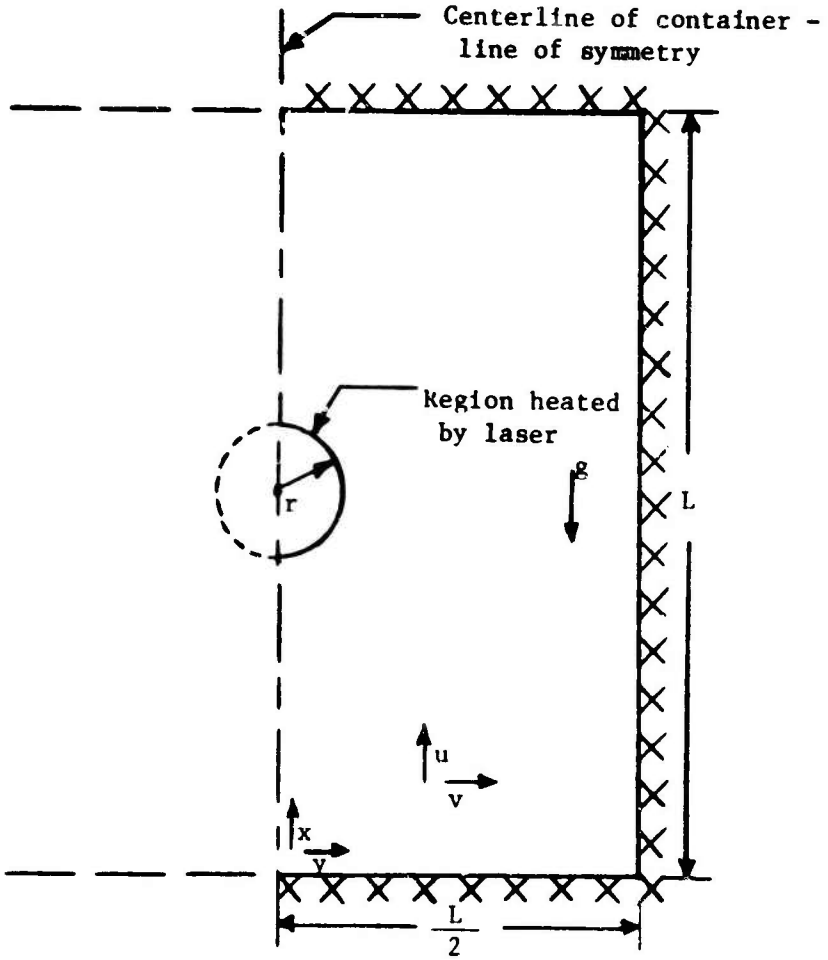

u = velocity in x direction

v = velocity in y direction

g = force of gravity

FIGURE 3: COORDINATE DEFINITIONS

no pressure relief. The average gas density ($\bar{\rho}$) in the enclosure remains constant and equal to the initial gas density (ρ_o). The specific heat, thermal conductivity, viscosity, and absorption coefficient of the gas mixture remain constant. The gas mixture is assumed to act as a perfect gas, and the viscous energy dissipation terms in the energy equation are neglected.

B. INITIAL AND BOUNDARY CONDITIONS

The gas mixture is initially at rest and at initial temperature (θ_o), pressure (P_o), and density (ρ_o). At time t = 0 the laser beam is turned on. The boundary conditions are:

1. Zero velocity at walls

   at x = 0 and x = L: $u = v = 0$

   at y = L/2: $u = v = 0$

2. Zero temperature gradient at walls (adiabatic)

   at x = 0 and x = L: $\frac{\partial \theta}{\partial x} = 0$

   at y = L/2: $\frac{\partial \theta}{\partial y} = 0$

3. Zero mass flow and zero gradients of temperature and vertical velocity across line of symmetry

   at y = 0: $v = 0, \frac{\partial u}{\partial y} = 0, \frac{\partial \theta}{\partial y} = 0$

C. EQUATIONS

1. x component of motion equation:

$$\bar{\rho}\left(\frac{\partial u}{\partial t} + u\frac{\partial u}{\partial x} + v\frac{\partial u}{\partial y}\right) = -\frac{\partial P}{\partial x} - \rho g + \mu\left(\frac{\partial^2 u}{\partial x^2} + \frac{\partial^2 u}{\partial y^2}\right)$$

2. y component of motion equation:

$$\bar{\rho}\left(\frac{\partial v}{\partial t} + u\frac{\partial v}{\partial x} + v\frac{\partial v}{\partial y}\right) = -\frac{\partial P}{\partial y} + \mu\left(\frac{\partial^2 v}{\partial x^2} + \frac{\partial^2 v}{\partial y^2}\right)$$

3. Continuity equation:

$$\frac{\partial u}{\partial x} + \frac{\partial v}{\partial y} = 0$$

4. Energy equation:

$$\frac{\partial \theta}{\partial t} + u \frac{\partial \theta}{\partial x} + v \frac{\partial \theta}{\partial y} = \frac{k}{\bar{\rho} c} \left(\frac{\partial^2 \theta}{\partial x^2} + \frac{\partial^2 \theta}{\partial y^2} \right) + \frac{q}{\bar{\rho} c}$$

III. METHOD OF SOLUTION:

A. DERIVATION OF EQUATIONS

The method of deriving the required equations is similar to that of Reference 2. Differentiating the x component of the equation of motion with respect to y, yields:

$$\bar{\rho} \left(\frac{\partial^2 u}{\partial t \partial x} + \frac{\partial^2 u}{\partial y \partial x} + u \frac{\partial^2 u}{\partial y \partial x} + \frac{\partial v}{\partial y} \frac{\partial u}{\partial y} + v \frac{\partial^2 u}{\partial y^2} \right)$$

$$= - \frac{\partial^2 P}{\partial x \partial y} - g \frac{\partial \rho}{\partial y} + \mu \frac{\partial}{\partial y} \left(\frac{\partial^2 u}{\partial x^2} + \frac{\partial^2 u}{\partial y^2} \right) \qquad \text{(Eq. 1)}$$

Similarly, differentiating the y component of the equation of motion with respect to x, yields:

$$\bar{\rho} \left(\frac{\partial^2 v}{\partial t \partial x} + \frac{\partial u}{\partial x} \frac{\partial v}{\partial x} + u \frac{\partial^2 v}{\partial x^2} + \frac{\partial^2 v}{\partial x \partial y} + v \frac{\partial^2 v}{\partial x \partial y} \right)$$

$$= - \frac{\partial^2 P}{\partial x \partial y} + \mu \frac{\partial}{\partial x} \left(\frac{\partial^2 v}{\partial x^2} + \frac{\partial^2 v}{\partial y^2} \right) \qquad \text{(Eq. 2)}$$

Subtracting equation 2 from equation 1:

$$\bar{\rho} \left[\frac{\partial}{\partial t} \left(\frac{\partial u}{\partial y} - \frac{\partial v}{\partial x} \right) + \frac{\partial u}{\partial x} \left(\frac{\partial u}{\partial y} - \frac{\partial v}{\partial x} \right) + u \left(\frac{\partial^2 u}{\partial x \partial y} - \frac{\partial^2 v}{\partial x^2} \right) \right.$$

$$\left. + \frac{\partial v}{\partial y} \left(\frac{\partial u}{\partial y} - \frac{\partial v}{\partial x} \right) + v \left(\frac{\partial^2 u}{\partial y^2} - \frac{\partial^2 v}{\partial x \partial y} \right) \right] = -g \frac{\partial \rho}{\partial y}$$

$$+ \mu \left[\frac{\partial}{\partial y} \left(\frac{\partial^2 u}{\partial x^2} + \frac{\partial^2 u}{\partial y^2} \right) - \frac{\partial}{\partial x} \left(\frac{\partial^2 v}{\partial x^2} + \frac{\partial^2 v}{\partial y^2} \right) \right]$$

Since $\frac{\partial u}{\partial x} + \frac{\partial v}{\partial y} = 0$ (continuity equation), we see that the second and fourth terms on the left side of the equation cancel, yielding:

$$\bar{\rho} \left[\frac{\partial}{\partial t} \left(\frac{\partial u}{\partial y} - \frac{\partial v}{\partial x} \right) + u \left(\frac{\partial^2 u}{\partial x \partial y} - \frac{\partial^2 v}{\partial x^2} \right) + v \left(\frac{\partial^2 u}{\partial y^2} - \frac{\partial^2 v}{\partial x \partial y} \right) \right]$$

$$= -g \frac{\partial \rho}{\partial y} + \mu \left[\frac{\partial}{\partial y} \left(\frac{\partial^2 u}{\partial x^2} + \frac{\partial^2 u}{\partial y^2} \right) - \frac{\partial}{\partial x} \left(\frac{\partial^2 v}{\partial x^2} + \frac{\partial^2 v}{\partial y^2} \right) \right] \qquad \text{(Eq. 3)}$$

This equation of motion and the energy equation will now be non-dimensional via the following relationships:

$$\text{Coordinates: } X = \frac{x}{r} \qquad Y = \frac{y}{r}$$

$$\text{Velocities: } U = \frac{ur}{\nu} \qquad V = \frac{vr}{\nu}$$

$$\text{Temperature: } T = \frac{\theta}{\theta_o} - 1$$

$$\text{Time: } \tau = \frac{t\nu}{r^2}$$

$$\text{Density: } \phi = \frac{\rho}{\rho_o} = \frac{\rho}{\bar{\rho}}$$

$$\text{Heating rate: } Q = \frac{q}{\rho c} \frac{r^2}{\nu \theta_o}$$

Applying these relationships to equation 3 yields:

$$\bar{\rho} \left[\frac{\nu}{r^2} \frac{\partial}{\partial \tau} \left(\frac{\nu}{r^2} \frac{\partial U}{\partial Y} - \frac{\nu}{r^2} \frac{\partial V}{\partial X}\right) + \frac{\nu}{r} U \left(\frac{\nu}{r^3} \frac{\partial^2 U}{\partial X \partial Y} - \frac{\nu}{r^3} \frac{\partial^2 V}{\partial X^2}\right)\right.$$

$$\left. + \frac{\nu}{r} V \left(\frac{\nu}{r^3} \frac{\partial^2 U}{\partial Y^2} - \frac{\nu}{r^3} \frac{\partial^2 V}{\partial X \partial Y}\right)\right] = -g \frac{\bar{\rho}}{r} \frac{\partial \phi}{\partial Y} + \mu \left[\frac{1}{r} \frac{\partial}{\partial Y} \left(\frac{\nu}{r^3} \frac{\partial^2 U}{\partial X^2}\right.\right.$$

$$\left.\left. + \frac{\nu}{r^3} \frac{\partial^2 U}{\partial Y^2}\right) - \frac{1}{r} \frac{\partial}{\partial X} \left(\frac{\nu}{r^3} \frac{\partial^2 V}{\partial X^2} + \frac{\nu}{r^3} \frac{\partial^2 V}{\partial Y^2}\right)\right]$$

Simplifying and using $\frac{\mu}{\bar{\rho}} = \nu$

$$\frac{\partial}{\partial \tau} \left(\frac{\partial U}{\partial Y} - \frac{\partial V}{\partial X}\right) + U \left(\frac{\partial^2 U}{\partial X \partial Y} - \frac{\partial^2 V}{\partial X^2}\right) + V \left(\frac{\partial^2 U}{\partial Y^2} - \frac{\partial^2 V}{\partial X \partial Y}\right)$$

$$= -\frac{gr^3}{\nu^2} \frac{\partial \phi}{\partial Y} + \frac{\partial}{\partial Y} \left(\frac{\partial^2 U}{\partial X^2} + \frac{\partial^2 U}{\partial Y^2}\right) - \frac{\partial}{\partial X} \left(\frac{\partial^2 V}{\partial X^2} - \frac{\partial^2 V}{\partial Y^2}\right) \qquad \text{(Eq. 4)}$$

Applying the non-dimensionalizing relationships to the energy equation produces:

$$\frac{\nu \theta_o}{r^2} \frac{\partial T}{\partial \tau} + \frac{\nu}{r} U \frac{\theta_o}{r} \frac{\partial T}{\partial X} + \frac{\nu}{r} V \frac{\theta_o}{r} \frac{\partial T}{\partial Y} = \frac{k}{\rho c} \left(\frac{\theta_o}{r^2} \frac{\partial^2 T}{\partial X^2} + \frac{\theta_o}{r^2} \frac{\partial^2 T}{\partial Y^2}\right)$$

$$+ \frac{1}{r^2} Q \nu \theta_o$$

Simplifying again using the definition of kinematic viscosity, and using the Prandtl number ($N_{PR} = \frac{\mu c}{k}$), yields

$$\frac{\partial T}{\partial \tau} + U \frac{\partial T}{\partial X} + V \frac{\partial T}{\partial Y} = \frac{1}{N_{PR}} \left(\frac{\partial^2 T}{\partial X^2} + \frac{\partial^2 T}{\partial Y^2}\right) + Q \qquad \text{(Eq. 5)}$$

Finally, applying the non-dimensionalizing relationships to the initial and boundary conditions produces the following:

at $\tau = 0$: $U = V = 0$, $T = 0$

at $X = 0$ and $X = \frac{L}{r}$: $U = V = 0$, $\frac{\partial T}{\partial X} = 0$

at $Y = \frac{L}{2r}$: $U = V = 0$, $\frac{\partial T}{\partial Y} = 0$

at $Y = 0$: $\frac{\partial T}{\partial Y} = 0$, $\frac{\partial}{\partial} = 0$, $V = 0$

The stream function (ψ) and vorticity (ζ) are now introduced:

$$U = \frac{\partial \psi}{\partial Y} \quad \text{(Eq. 6)} \qquad V = -\frac{\partial \psi}{\partial X} \quad \text{(Eq. 7)}$$

$$\zeta = -\nabla^2 \psi = -\frac{\partial^2 \psi}{\partial X^2} - \frac{\partial^2 \psi}{\partial Y^2} \quad \text{(Eq. 8)}$$

Applying these stream function and vorticity equations to the motion equation (equation 4) yields:

$$\frac{\partial \zeta}{\partial \tau} + U \frac{\partial \zeta}{\partial X} + V \frac{\partial \zeta}{\partial Y} = \frac{gr^3}{\nu^2} \frac{\partial \phi}{\partial Y} + \nabla^2 \zeta \quad \text{(Eq. 9)}$$

Equations 5 through 9 describe the problem, and the boundary and initial conditions have now become the following:

at $\tau = 0$: $U = V = \zeta = 0$, $T = 0$

at $X = 0$ and $X = \frac{L}{r}$: $U = V = 0$, $\frac{\partial T}{\partial X} = 0$

at $Y = \frac{L}{2r}$: $U = V = 0$, $\frac{\partial T}{\partial Y} = 0$

at $Y = 0$: $\frac{\partial T}{\partial Y} = 0$, $V = \frac{\partial U}{\partial Y} = \frac{\partial V}{\partial X} = \zeta = 0$

B. SOLUTION OF THE EQUATIONS

Laser Heating Function Q

Equations 5-9 can now be solved via a series of finite

difference approximations advancing in time. The driving function is the non-dimensional volumetric heating rate term (Q) in the energy equation. For small absorption coefficients, the actual volumetric heating rate (q) is approximately the product of the incident power density, I(X,Y) and the absorption coefficient $\alpha(X,Y,\tau)$. I(X,Y) (watts/cm^2) varies with location in accordance with the formulas in Figure 2. The absorption coefficient (α, cm^{-1}) is assumed to be dependent only on the local gas density, $\rho(X,Y,\tau)$, which varies with location and time. Thus, the actual volumetric heating rate must be calculated at each grid point (X, Y) in the beam radius and at each time τ. The local density distribution at time τ is used to calculate the heating rate distribution at time $(\tau + \Delta\tau)$.

$$q\ (X,Y,\ \tau\ +\Delta\tau\ ) = I(X,Y)\ \alpha\ (X,Y,\tau\ )$$

q is then non-dimensionalized via the previously mentioned formula:

$$Q\ (X,Y,\ \tau\ +\ \Delta\tau)\ =\ \frac{r^2}{\bar{\rho} c \nu \theta_o}\ q\ (X,Y,\ \tau\ +\ \Delta\tau) \qquad \text{(Eq. 10)}$$

Energy Equation

The next step requires the solution of the energy equation to find the new distribution of local temperatures at time $(\tau + \Delta\tau)$. Using standard finite difference approximations with a forward differenced time derivative, centered-difference spatial derivatives, and a Taylor series approximation for the second order terms, the energy equation (equation 5) can be expressed as:

$$\frac{1}{\Delta\tau}\ [T(X,Y,\ \tau\ +\ \Delta\tau)\ -\ T(X,Y,\tau)]\ \ +\ U\ (X,Y,\tau)\ \frac{1}{2\Delta X}\ [T(X\ +\ \Delta X,Y,\tau)$$

$$-\ T(X\ -\ \Delta X,Y,\tau)]\ +\ V\ (X,Y,\tau)\ \frac{1}{2\Delta Y}\ [T(X,Y\ +\ \Delta Y,\tau)\ -\ T(X,Y\ -\ \Delta Y,\tau)]$$

$$=\ \frac{1}{N_{PR}}\ \ \frac{1}{(\Delta X)^2}\ [T(X\ +\ \Delta X,Y,\tau)\ +\ T(X\ -\ \Delta X,Y,\tau)\ +\ T(X,Y\ +\ \Delta Y,\tau)$$

$$+ T(X,Y - \Delta Y,\tau) - 4T(X,Y,\tau)] + Q(X,Y, \tau + \Delta\tau)$$

where $\Delta X = \Delta Y$

Since the distributions of all the variables are known at time τ, and $Q(X,Y, \tau+ \Delta\tau)$ can be determined from equation 10, we may solve for $T(X,Y,\tau + \Delta\tau)$.

$$T(X,Y, \tau + \Delta\tau) = \frac{\Delta\tau}{N_{PR}} \frac{1}{(\Delta X)^2} [T(X + \Delta X,Y,\tau) + T(X - \Delta X,Y,\tau)$$

$$+ T(X,Y + \Delta Y,\tau) + T(X,Y - \Delta Y,\tau) - 4T(X,Y,\tau)] + \Delta\tau Q(X,Y,\tau + \Delta\tau)$$

$$- U(X,Y,\tau) \frac{\Delta\tau}{2\Delta X} [T(X + \Delta X,Y,\tau) - T(X - \Delta X,Y,\tau)]$$

$$-V (X,Y,\tau) \frac{\Delta\tau}{2\Delta Y} [T(X,Y + \Delta Y,\tau) - T(X,Y - \Delta Y,\tau)] + T(X,Y,\tau) \quad \text{(Eq. 11)}$$

Since the first derivative of T at the walls and across the line of symmetry is zero, the values of T along these boundaries may be defined by using a standard "mirror image" technique. [e.g., at $T(X,o,\tau)$: $T(X,Y + \Delta Y, \tau) = T(X,Y - \Delta Y, \tau)$].

Density Function

An average pressure term, $P(\tau)$, is determined at time $\tau + \Delta\tau$ in the following manner:

Assuming the gas mixture to be a perfect gas,

$$P(\tau + \Delta\tau) - P(\tau) = \frac{mR}{M\bar{V}} [\bar{\theta}(\tau + \Delta\tau) - \bar{\theta}(\tau)] \quad \text{(Eq. 12)}$$

where $\bar{\theta}$ is the mass average temperature of the total mass of the gas (m) in the enclosure having a constant volume $\bar{V}$. This implies that the pressure is homogeneous within the enclosure or that pressure equalization occurs much more rapidly than temperature equalization.

Furthermore, the total heat input during any particular time

interval, Δt, is $\Delta t \int\int_{Y\ X} q(X,Y,\tau+\Delta\tau)dXdY$, which can also be expressed

$$\Delta t \sum_{Y} \sum_{X} q(X,Y,\tau + \Delta\tau)$$

This total heat input can be related to the mass average temperature rise in the following manner:

$$\sum_{Y} \sum_{X} q(X,Y, \tau + \Delta\tau) = \frac{mc}{\Delta t} [\bar{\theta}(\tau + \Delta\tau) - \bar{\theta}(\tau)] \qquad \text{(Eq. 13)}$$

Substituting for $m [\bar{\theta} (\tau + \Delta\tau) - \bar{\theta}(\tau)]$ in equations 12 and 13, and simplifying, yields:

$$P(\tau + \Delta\tau) - P(\tau) = \frac{\Delta t R}{M\bar{V}c} \sum_{Y} \sum_{X} q(X,Y,\tau + \Delta\tau) \qquad \text{(Eq. 14)}$$

which can be solved for $P(\tau + \Delta\tau)$.

Now,

$$\phi(X,Y, \tau + \Delta\tau) = \frac{\rho(X,Y, \tau + \Delta\tau)}{\rho_o} = \frac{P(\tau + \Delta\tau)\ \theta_o}{P_o\ \theta(X,Y, \tau + \Delta\tau)}$$

from $T = \frac{\theta}{\theta_o} - 1$, it is clear that $\frac{\theta_o}{\theta} = [T(X,Y, \tau + \Delta\tau) + 1]^{-1}$

substituting into the equation for ϕ, there follows:

$$\phi(X,Y, \tau + \Delta\tau) = \frac{P(\tau + \Delta\tau)}{P_o[T(X,Y, \tau + \Delta\tau) + 1]} \qquad \text{(Eq. 15)}$$

Vorticity Equation

Equations 10, 11, 14, and 15 can be evaluated in succession to yield values of Q, T, P, and ϕ, respectively, at the advanced time $\tau + \Delta\tau$. The vorticity function (X,Y,τ) is now advanced to time $\tau + \Delta\tau$ via the motion equation. The motion equation (eq. 9) can be expressed numerically in the following manner:

$$\frac{1}{\Delta\tau} [\zeta(X,Y, \tau + \Delta\tau) - \zeta(X,Y,\tau)] + U(X,Y,\tau) \frac{1}{2\Delta X} [\zeta(X + \Delta X,Y,\tau)$$

$$- \zeta(X - \Delta X,Y,\tau)] + V(X,Y,\tau) \frac{1}{2\Delta Y} [\zeta(X,Y + \Delta Y,\tau) - \zeta(X,Y - \Delta Y,\tau)]$$

$$= \frac{gr^3}{\nu^2} \frac{1}{2\Delta Y} [\phi(X,Y + \Delta Y,\tau) - \phi(X,Y - \Delta Y,\tau)] + \frac{1}{(\Delta X)^2} [\zeta(X + \Delta X,Y,\tau)$$

$$+ \zeta(X - \Delta X,Y,\tau) + \zeta(X,Y + \Delta Y,\tau) + \zeta(X,Y - \Delta Y,\tau) - 4\zeta(X,Y,\tau)]$$

This can be solved for $\zeta(X,Y,\ \tau + \Delta\tau)$.

$$\zeta(X,Y,\ \tau + \Delta\tau) = \zeta(X,Y,\tau) - \frac{\Delta\tau}{2\Delta X}\ U(X,Y,\tau)[\zeta(X + \Delta X,Y,\tau) - \zeta(X - \Delta X,Y,\tau)] - \frac{\Delta\tau}{2\Delta Y}\ V(X,Y,\tau)\ [\zeta(X,Y + \Delta Y,\tau) - \zeta(X,Y - \Delta Y,\tau)]$$

$$+ \frac{gr^3}{\nu^2}\ \frac{\Delta\tau}{2\Delta Y}\ [\phi(X,Y + \Delta Y,\ \tau + \Delta\tau) - \phi(X,Y - \Delta Y,\ \tau + \Delta\tau)\ + \frac{\Delta\tau}{(\Delta X)^2}$$

$$[\zeta(X+\Delta X,Y,\tau) + \zeta(X-\Delta X,Y,\tau) + \zeta(X,Y+\Delta Y,\tau) + \zeta(X,Y-\Delta Y,\tau) - 4\zeta(X,Y,\tau)]$$

(Eq. 16)

Equation 16 can be solved to find the values of vorticity at all interior points. Along the line of symmetry, the vorticity function is zero. A parabolic extrapolation of the vorticity values approaching any of the three walls is used to establish vorticity values along these walls. This extrapolation technique is described below and was used in Reference 3.

Consider the ζ values approaching the vertical wall for a constant X value, as shown below:

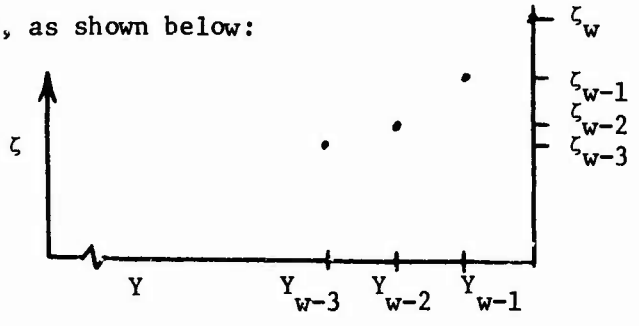

where the separation between each of the Y values is ΔY. A parabola can be constructed to intersect the three points $(\zeta_w,\ Y_w)$, (ζ_{w-1}, Y_{w-1}), $(\zeta_{w-2},\ Y_{w-2})$. This parabola can be defined by the following equation:

$$\zeta(Y) = \frac{(Y - Y_{w-1})\ (Y - Y_w)\ \zeta(Y_{w-2})}{2(\Delta Y)^2} - \frac{(Y - Y_{w-2})\ (Y - Y_w)\ \zeta(Y_{w-1})}{(\Delta Y)^2} + \frac{(Y - Y_{w-2})\ (Y - Y_{w-1})\ \zeta(Y_w)}{2(\Delta Y)^2}$$

Differentiation of this equation yields:

$$\zeta'(Y) = \frac{(2Y - Y_{w-1} - Y_w)\ \zeta(Y_{w-2})}{2(\Delta Y)^2}$$

$$- \frac{(2Y - Y_{w-2} - Y_w)\ \zeta(Y_{w-1})}{(\Delta Y)^2} + \frac{(2Y - Y_{w-2} - Y_{w-1})\ \zeta(Y_w)}{2(\Delta Y)^2}$$

This equation can now be used to determine $\zeta'(Y)$ at $Y = Y_{w-2}$.

$$\zeta'(Y_{w-2}) = \frac{(2Y_{w-2} - Y_{w-1} - Y_w)\ \zeta(Y_{w-2})}{2(\Delta Y)^2}$$

$$- \frac{(2Y_{w-2} - Y_{w-2} - Y_w)\ \zeta(Y_{w-1})}{(\Delta Y)^2} + \frac{(2Y_{w-2} - Y_{w-2} - Y_{w-1})\ \zeta(Y_w)}{2(\Delta Y)^2}$$

Utilizing a centered difference approximation for ζ' - i.e., $\zeta'(Y_{w-2}) = \frac{1}{2(\Delta Y)}\ [\zeta(Y_{w-1}) - \zeta(Y_{w-3})]$ and remembering that

$$Y_w - Y_{w-2} = 2\Delta Y$$

$$Y_w - Y_{w-1} = \Delta Y$$

$$Y_{w-1} - Y_{w-2} = \Delta Y$$

the equation is simplified to produce:

$$\frac{1}{2\Delta Y}\ [\zeta(Y_{w-1}) - \zeta(Y_{w-3})] = -\frac{3}{2\Delta Y}\ \zeta(Y_{w-2}) + \frac{2}{\Delta Y}\ \zeta(Y_{w-1}) - \frac{1}{2\Delta Y}\ \zeta(Y_w)$$

Solving this equation for $\zeta(Y_w)$, one obtains:

$$\zeta(Y_w) = 3\zeta(Y_{w-1}) - 3\zeta(Y_{w-2}) + \zeta(Y_{w-3}) \qquad \text{(Eq. 17)}$$

Thus, the value of the vorticity is determined along the vertical wall. A similar procedure is used for the lower and upper walls.

Stream Function

Now that the values of vorticity are known at time $\tau + \Delta\tau$, the stream function (ψ) can be determined. This is done by numerically solving the defining equation for vorticity (eq. 8), for ψ. Using

truncated Taylor series approximations for the second order terms, equation 8 can be expressed as:

$$\zeta(X,Y,\tau) = -\frac{1}{(\Delta X)^2}\left[\psi(X+\Delta X,Y,\tau) + \psi(X-\Delta X,\ Y,\tau) - 2\psi(X,Y,\tau)\right]$$

$$-\frac{1}{(\Delta Y)^2}\left[\psi(X,Y+\Delta Y,\tau) + \psi(X,Y-\Delta Y,\tau) - 2\psi(X,Y,\tau)\right]$$

Although the above equation can be solved via the explicit "relaxation" technique, the number of calculations required before suitable convergence occurs is excessive. Thus, an alternating direction implicit (ADI) method was used to solve the equation for ψ. This ADI method is used to find a solution to the equation

$$\frac{\partial\psi}{\partial\gamma} = \frac{\partial^2\psi}{\partial X^2} + \frac{\partial^2\psi}{\partial Y^2} + \zeta$$

where the term γ is analogous to a time term. The objective is to perform iterations until the term $\frac{\partial\psi}{\partial\gamma}$ approaches zero (analogous to a steady-state solution), thereby providing a solution to the vorticity equation $\zeta = -\nabla^2\psi$.

The ADI computation proceeds in steps of $\frac{1}{2}\Delta\gamma$. The partial differential equation is written in finite difference form, looking forward with respect to γ and implicit in the X direction during the first step of $\frac{1}{2}\Delta\gamma$. A second equation, implicit in the Y direction, is then used for the second step of $\frac{1}{2}\Delta\gamma$. The procedure is repeated until the change in ψ across a pair of steps of $\frac{1}{2}\Delta\gamma$ is sufficiently close to zero, thereby yielding a steady-state solution with respect to γ. We now introduce $\psi^{(o)}$, $\psi^{(\frac{1}{2}\Delta\gamma)}$, and $\psi^{(\Delta\gamma)}$, representing the value of ψ at time τ, the value of ψ after solution of the first ADI equation, and the value of ψ after solution of the second ADI equation, respectively. Thus the two ADI equations are as shown below.

Implicit in X direction:

$$\frac{\psi^{(\frac{1}{2}\Delta\gamma)}(X,Y) - \psi^{(o)}(X,Y)}{\frac{1}{2}\Delta\gamma} = \frac{\psi^{(\frac{1}{2}\Delta\gamma)}(X+\Delta X,Y) - 2\psi^{(\frac{1}{2}\Delta\gamma)}(X,Y) + \psi^{(\frac{1}{2}\Delta\gamma)}(X-\Delta X,Y)}{(\Delta X)^2}$$

$$+ \frac{\psi^{(o)}(X,Y+\Delta Y) - 2\psi^{(o)}(X,Y) + \psi^{(o)}(X,Y-\Delta Y)}{(\Delta Y)^2} + \zeta(X,Y,\tau+\Delta\tau) \qquad \text{(Eq. 18)}$$

Implicit in Y direction:

$$\frac{\psi^{(\Delta\gamma)}(X,Y) - \psi^{(\frac{1}{2}\Delta\gamma)}(X,Y)}{\frac{1}{2}\Delta\gamma} = \frac{\psi^{(\frac{1}{2}\Delta\gamma)}(X+\Delta X,Y) - 2\psi^{(\frac{1}{2}\Delta\gamma)}(X,Y) + \psi^{(\frac{1}{2}\Delta\gamma)}(X-\Delta X,Y)}{(\Delta X)^2}$$

$$+ \frac{\psi^{(\Delta\gamma)}(X,Y+\Delta Y) - 2\psi^{(\Delta\gamma)}(X,Y) + \psi^{(\Delta\gamma)}(X,Y-\Delta Y)}{(\Delta Y)^2} + \zeta(X,Y,\tau+\Delta\tau) \qquad \text{(Eq. 19)}$$

Equation 18 can be solved for $\psi^{(\frac{1}{2}\Delta\gamma)}$, and the results used in equation 19 to determine $\psi^{(\Delta\gamma)}$. If $\psi^{(\Delta\gamma)}(X,Y) - \psi^{(o)}(X,Y)$ is sufficiently small, then $\psi(X,Y,\tau+\Delta\tau)$ is set equal to $\psi^{(\Delta\gamma)}(X,Y)$. If $\psi^{(\Delta\gamma)}(X,Y) - \psi^{(o)}(X,Y)$ is too great, then $\psi^{(o)}(X,Y)$ is set equal to $\psi^{(\Delta\gamma)}(X,Y)$ and the calculation is repeated. An arbitrary value of $\Delta\gamma$ may be chosen; however, an optimum value exists at which computation time will be minimized. The method by which equations 18 and 19 are solved will now be described.

Multiplying equation 18 by $(\Delta X)^2$ (remembering that $\Delta X = \Delta Y$) and collecting like terms, we obtain:

$$\psi^{(\frac{1}{2}\Delta\gamma)}(X+\Delta X,Y) - 2\left(1 + \frac{(\Delta X)^2}{\Delta\gamma}\right)\psi^{(\frac{1}{2}\Delta\gamma)}(X,Y) + \psi^{(\frac{1}{2}\Delta\gamma)}(X-\Delta X,Y)$$

$$= (\Delta X)^2\,\zeta(X,Y,\tau+\Delta\tau) - \psi^{(o)}(X,Y+\Delta Y) - 2\left(\frac{(\Delta X)^2}{\Delta\gamma} - 1\right)\psi^{(o)}(X,Y) - \psi^{(o)}(X,Y-\Delta Y)$$

(Eq. 20)

This equation will be solved over a column of grid points (Y = constant). Thus, the series of equations is of the following form:

$$\psi^{(\frac{1}{2}\Delta\gamma)}(X_i+\Delta X,Y) - B\psi^{(\frac{1}{2}\Delta\gamma)}(X_i,Y) + \psi^{(\frac{1}{2}\Delta\gamma)}(X_i-\Delta X,Y) = c(X_i) \qquad i = 1,M \qquad \text{(Eq. 21)}$$

where $B = 2\left(1 + \frac{(\Delta X)^2}{\Delta\gamma}\right)$, a known constant

C = right hand side of eq. 20, a known constant for each X_i and $M = \frac{L}{\Delta x} + 1$, the number of grid points in the column.

Thus, there is a set of M simultaneous linear equations with M unknown values of $\psi(X_i, Y)$ at $\tau + \frac{1}{2}\Delta\tau$. Since the velocities at the walls are zero, ψ = constant along the walls. Furthermore, since the line Y = 0 is a line of symmetry, $-\psi(X,Y,\tau) = \psi(X,-Y,\tau)$, which implies that $\psi(X,0,\tau) = 0$. Since the line of symmetry intersects the walls which have ψ = constant, it follows that the value of ψ along the walls is also zero. Thus, the values of $\psi(X_i, Y)$ at $\tau + \frac{1}{2}\Delta\tau$ in equation 21 are already known for i = 1 and i = M. The set of equations represented by equation 21 may be written:

$$
\begin{aligned}
0 - B\psi(X_2,Y) + \psi(X_3,Y) &= c_2 \\
\psi(X_2,Y) - B\psi(X_3,Y) + \psi(X_4,Y) &= c_3 \\
&\vdots \\
\psi(X_{M-3},Y) - B\psi(X_{M-2},Y) + \psi(X_{M-1},Y) &= c_{M-2} \\
\psi(X_{M-2},Y) - B\psi(X_{M-1},Y) + 0 &= c_{M-1}
\end{aligned}
$$

which can be expressed in matrix form as:

$$
\begin{bmatrix}
-B & 1 & 0 & 0 & \cdots & 0 \\
1 & -B & 1 & 0 & \cdots & 0 \\
0 & 1 & -B & 1 & \cdots & 0 \\
\vdots & & & & & \vdots \\
0 & \cdots & & 1 & -B & 1 \\
0 & \cdots & & 0 & 1 & -B
\end{bmatrix}
\begin{bmatrix}
\psi(X_2,Y) \\ \psi(X_3,Y) \\ \vdots \\ \psi(X_{M-1},Y)
\end{bmatrix}
=
\begin{bmatrix}
c_2 \\ c_3 \\ c_4 \\ \vdots \\ c_{M-1}
\end{bmatrix}
$$

The tri-diagonal square matrix can then be inverted and values of $\psi^{(\frac{1}{2}\Delta Y)}(X_i, Y)$ can be obtained for a given column. Equation 19 may be solved in exactly the same manner to obtain $\psi^{(\Delta Y)}(X,Y)$ in terms of $\psi^{(\frac{1}{2}\Delta Y)}(X,Y_j)$ along rows (X = constant, j = 1 to $\frac{L}{2\Delta y} + 1$). The procedure is repeated until a steady-state solution occurs, at which point the new stream function $\psi^{(\Delta Y)}(X,Y,\tau+\Delta\tau)$ is set equal to $\psi(X,Y)$.

Velocity Function

The final step in the solution of this set of equations for a single time step advancement $\Delta\tau$, is the determination of the non-dimensional velocities from the stream function ψ. This is accomplished via solution of equations 6 and 7. A centered-difference approximation is used and the equations to be solved are as shown below:

$$U(X,Y,\tau+\Delta\tau) = \frac{1}{2\Delta Y}\left[\psi(X,Y+\Delta Y,\tau+\Delta\tau) - \psi(X,Y-\Delta Y,\tau+\Delta\tau)\right] \quad \text{(Eq. 22)}$$

$$V(X,Y,\tau+\Delta\tau) = \frac{1}{2\Delta X}\left[\psi(X+\Delta X,Y,\tau+\Delta\tau) - \psi(X-\Delta X,Y,\tau+\Delta\tau)\right] \quad \text{(Eq. 23)}$$

At this point, all parameters have been advanced to the new time $\tau + \Delta\tau$, and the cycle is ready to begin again. A flow chart of this procedure is shown in Figure 4.

Conservative and Upwind Differencing

Several runs were made with 51 x 26 and 101 x 51 grids representing four inch and eight inch cross-sectional areas respectively ($\Delta x = \Delta y = .08$"). Beam diameters were varied from one to three inches, and time steps ($\Delta\tau$) of from .0001 to .001 seconds were used. Although the overall solutions appeared reasonable, apparent discretization errors did occur, producing unreasonably cool regions in the temperature arrays. The most obvious remedy to this problem would be the introduction of still finer grids and/or smaller time steps. However,

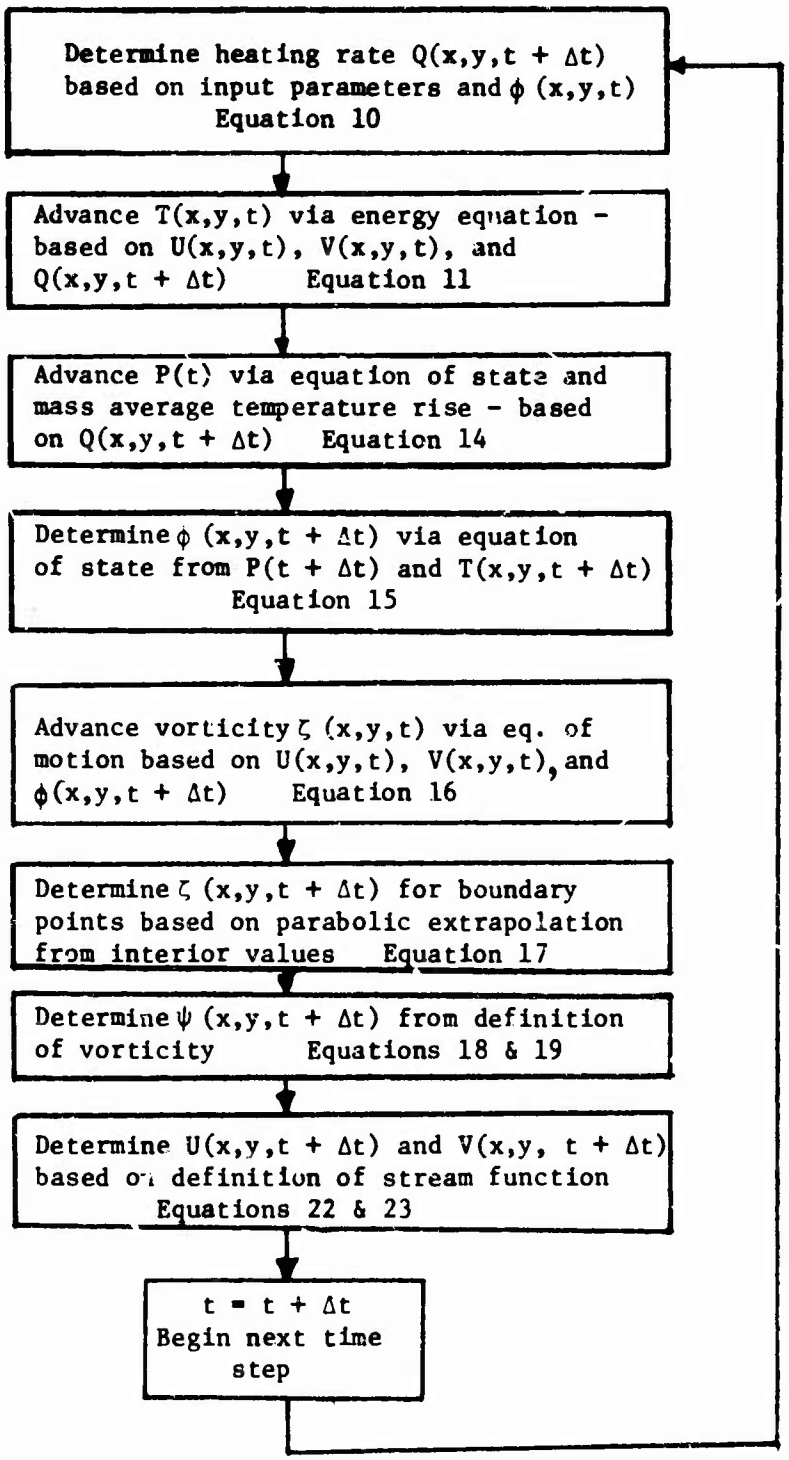

FIGURE 4: SOLUTION METHOD FLOW CHART

because the memory storage required for all these arrays and the computer time required was already quite large, another approach was taken. This approach consisted of the addition of conservative and upwind differencing numerical approximations to the energy and motion equations.

The conservative difference approximation is derived from the product rule for differentiation, and incorporates the condition of mass conservation in the differentiation process. To demonstrate its application, let us consider the second and third terms in the non-dimensionalized energy equation (eq. 5), $U \frac{\partial T}{\partial X} + V \frac{\partial T}{\partial Y}$. Utilizing the product rule for differentiation,

$$U \frac{\partial T}{\partial X} + V \frac{\partial T}{\partial Y} = \frac{\partial}{\partial X} (UT) - T \frac{\partial U}{\partial X} + \frac{\partial}{\partial Y} (VT) - T \frac{\partial V}{\partial Y}$$

and since $\frac{\partial U}{\partial X} + \frac{\partial V}{\partial Y} = 0$ from continuity,

$$U \frac{\partial T}{\partial X} + V \frac{\partial T}{\partial Y} = \frac{\partial (UT)}{\partial X} + \frac{\partial (VT)}{\partial Y}$$

which may be expressed numerically as:

$$\frac{1}{2\Delta X} [U(X+\Delta X,Y,\tau)\ T(X+\Delta X,Y,\tau) - U(X-\Delta X,Y,\tau)\ T(X-\Delta X,Y,\tau)]$$

$$+ \frac{1}{2\Delta Y} [V(X,Y+\Delta Y,\tau)\ T(X,Y+\Delta Y,\tau) - V(X,Y-\Delta Y,\tau)\ T(X,Y-\Delta Y,\tau)]$$

The above expression can now be substituted into the energy equation (eq. 11). The second and third terms on the right hand side of the equation of motion (eq. 16), representing $U \frac{\partial \zeta}{\partial X} + V \frac{\partial \zeta}{\partial Y}$ are similarly converted to the conservative numerical form.

The upwind differencing technique is also applied to the same terms of the energy and motion equations. This technique replaces the conservative, centered-difference, numerical approximation with a backward looking (with respect to velocity), conservative, numerical approximation. That is, the derivative is taken in the direction

"from which the wind is blowing". For example, the term $\frac{\partial(UT)}{\partial X}$ is approximated by

$$\frac{1}{\Delta X}\left[U(X,Y,\tau)\ T(X,Y,\tau) - U(X-\Delta X,Y,\tau)\ T(X-\Delta X,Y,\tau)\right]$$

if $U(x,y,\tau)$ is positive, and

$$\frac{1}{\Delta X}\left[U(X+\Delta X,Y,\tau)\ T(X+\Delta X,Y,\tau) - U(X,Y,\tau)\ T(X,Y,\tau)\right]$$

if $U(x,y,\tau)$ is negative.

The application of the upwind, conservative, numerical approximations to the appropriate terms of the energy and motion equations, resulted in smoother and physically reasonable temperature and vorticity arrays. The unreasonably cool zones in the temperature distribution were eliminated and the lines of constant vorticity became smoother.

C. GAS MIXTURE PROPERTIES

One portion of the input data requirements is the properties of the gas mixture. The properties of each component (up to ten components) are input to the program and are used to calculate properties of the mixture. The following are the properties of each component which are input:

Density (ρ) at initial temperature (T_o) and pressure (P_o)

Absorption coefficient (α) per psi per volume percent at initial density (ρ_o)

Thermal conductivity (k)

Molecular weight (M)

Molar concentration (mole fraction) (n)

Kinematic Viscosity (ν)

Specific Heat (c)

The method by which these properties are used to calculate the gas mixture properties will now be described. In the following

discussion, the subscripts i and j refer to the individual gas mixture components' properties, while m refers to the mixture properties.

$$\mu_i = \rho_i \nu_i \quad \text{where } \mu \text{ is viscosity}$$

$$\rho_m = \frac{P_o}{R\theta_o} \sum_{i=1}^{N} n_i M_i = \rho_o \qquad N = \text{no. of components}$$

$$M_m = \sum_{i=1}^{N} n_i M_i \qquad \alpha = 100\, P_o \sum_{i=1}^{N} n_i \alpha_i$$

$$c_m = \frac{1}{M_m} \sum_{i=1}^{N} c_i n_i M_i$$

The viscosity of the mixture is determined via the semi-empirical formula of Wilke as described in Reference 4. That is;

$$\mu_m = \sum_{i=1}^{N} \frac{n_i \mu_i}{\sum_{j=1}^{N} n_j A_{ij}}$$

where

$$A_{ij} = \frac{1}{8}\left(1 + \frac{M_i}{M_j}\right)^{-\frac{1}{2}} \left[1 + \left(\frac{\mu_i}{\mu_j}\right)^{\frac{1}{2}} \left(\frac{M_j}{M_i}\right)^{\frac{1}{4}}\right]^2$$

and of course,

$$\nu_m = \frac{\mu_m}{\rho_m}$$

The thermal conductivity of the mixture is determined by a similar method, attributed to Mason and Saxena, and also described in Reference 4. That is;

$$k_m = \sum_{i=1}^{N} \frac{n_i k_i}{\sum_{j=1}^{N} n_i A_{ij}}$$

where A_{ij} is the same as in the viscosity equation.

IV. APPLICATION EXAMPLES

This section consists of a sample set of input data and the results of four runs made with slight variations in this data. Appendix 2 is a listing of the main program and the four primary subroutines. Instructions for the use of this program are given in Appendix 4.

A. SAMPLE PROBLEM INPUT/OUTPUT:

Input data can be divided into two subsets: problem parameters and gas mixture constituents' properties. These are listed in Figure 5, along with the values assigned for the first sample problem. Since the thermal conductivity, viscosity, and specific heat remain fixed throughout the program, despite local temperature increases of a several hundreds of degrees Rankine, the values of those three properties shown in Figure 5 are actual and/or estimated values at approximately 672°R (100°C). The universal gas constant and the acceleration of gravity are constant values contained within the program. Only very minor changes are required to vary the acceleration of gravity or the spatial power distribution as is done in two of the examples.

Output data is presented both graphically and in tabular form. The tabular output data presented in the following example problems are the properties of the gas mixture, the actual beam power and area used in the calculations (which are different from the input conditions due to approximations to the heated area and due to truncation of Gaussian power distribution beams), the average power density or intensity (watts/cm^2), the pressure in the enclosure, and the rate at which the beam is heating a one-inch thick section of the gas mixture. The graphical output data consists of contour plots of temperature, stream function (streamlines) and vorticity within the enclosure, and of vertical velocity along three horizontal lines of constant X. All of the above information can be obtained at any time after irradiation has begun.

B. SAMPLE PROBLEM NO. 1:

This problem is described by the input data values listed in

PROBLEM PARAMETERS:

Initial Temperature (deg. rankine)	520.
Laser Beam Power (watts)	63675.
Beam Radius (inches)	1.5
Time Interval - Δt (sec)	.001
Initial Pressure (psia)	14.7
Number of Components in the Gas Mixture	2
Grid Spacing - Δx or Δy	.08
Enclosure Size - length of side of square cross-section (inches)	8.00
Beam Duration (sec)	.8

GAS MIXTURE CONSTITUENTS' PROPERTIES:

Property	Gas 1	Gas 2
Name	Pentane	Air
Density (lbm/cu. ft.)	.183	.0735
Absorption Coefficient (cm^{-1} per psi per volume percent)	1.39×10^{-5}	0
Thermal Conductivity (btu/hr. ft °R)	.0096	.017
Molecular Weight	72.15	28.97
Concentration (mole fraction)	.03	.97
Kinematic Viscosity (sq. ft/sec)	3.1×10^{-5}	2.18×10^{-4}
Specific Heat (btu/lbm °R)	.409	.24

FIGURE 5: INPUT PARAMETERS & SAMPLE PROBLEM VALUES

Figure 5. In addition, the standard acceleration of gravity and a Gaussian power distribution within the beam are used. The calculated properties of the gas mixture are listed below:

Density = .07974 lbm/cu ft

Absorption Coefficient = .000613 cm^{-1}

Thermal Conductivity = .01628 btu/(hr ft °R)

Molecular Weight = 30.265

Kinematic Viscosity = .000189 sq ft/sec

Specific Heat = .252 btu/(lbm °R)

The program assumes heating to occur at each grid point which lies within the defined beam radius. Thus the heated area only approximates a semi-circle. This heated area is shown in the graphical output. Also, the Gaussian beam is truncated at the defined radius. Thus, approximately 13% of the Gaussian laser beam power is omitted from the calculation. As a result of these approximations and truncations, the actual power used was 57,586.8 watts, the actual heated area was 7.283 sq inches, and the resulting power density (intensity), averaged over the entire heated area was 1225.86 watts/sq cm.

Figures 6 through 15 are the graphical output for this problem. The roughly semi-circular area drawn on these plots represents the heated area. The contours of each of the variables plotted are identified by symbols. The line identified by the octagon represents the value of the function that lies ten percent of the difference between the maximum value and the minimum value of that function, above the minimum value. For example, after .151 seconds of irradiation, the element with the highest temperature has a temperature of 785.2°R. Since the lowest temperature of any element at .151

seconds is 520°R (the initial temperature), the temperature that lies ten percent of the way from the lowest value to the highest is 546.52°R. An isotherm of 546.52°R is therefore drawn and is identified by an octagon. Similarly, the thirty percent, fifty percent, seventy percent, and ninety percent isotherms are identified by a triangle, a plus sign, an x, and a diamond, respectively. Streamlines and lines of constant vorticity are similarly labelled. The plot of upward velocity is actually a three-dimensional drawing relating the non-dimensionalized upward velocity at all Y values along three lines of constant X. The three lines precisely quarter the half cross-sectional area. Coordinates and the approximate beam boundary are shown in the first of these plots to assist in visualization.

At .151 seconds (Figures 6 and 7), the isotherms appear to be nearly concentric about the centerpoint of the line of symmetry, as would be expected with a Gaussian power beam. However, there is a slight upward displacement of these isotherms due to the convective motion of the gas which is now beginning to influence the pattern. The plots of upward velocity and stream function demonstrate this convective motion. Note that the highest value lines of constant stream function and vorticity are approximately centered about a point near the outermost horizontal point of the heated region.

At .294 seconds (Figures 8 and 9), the effects of convection begin to appear. The regions of highest temperature, stream function, and vorticity have been displaced upward. The upward velocities have increased significantly within and above the heated region. At this time the maximum temperature of 892°R was attained. This high temperature existed for approximately .02 seconds and then began to

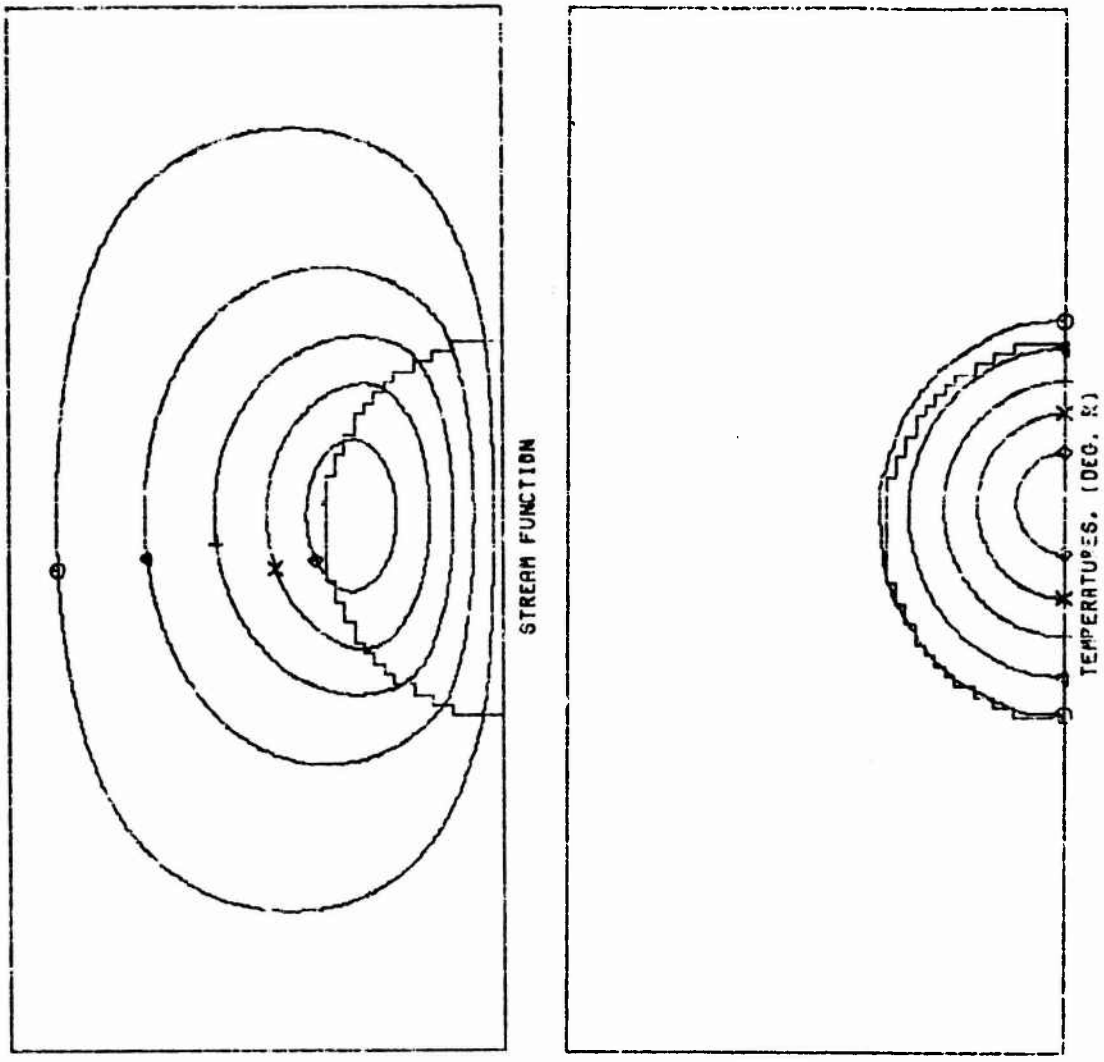

Stream Function (Non-dimensional)	Temperature (°R)	Symbol
15.6	546.5	Octagon
46.8	599.6	Triangle
78.0	652.6	+
109.2	705.6	X
140.4	758.7	Diamond

FIGURE 6: STREAM FUNCTION & TEMPERATURE AT .151 SECONDS OF PROBLEM 1

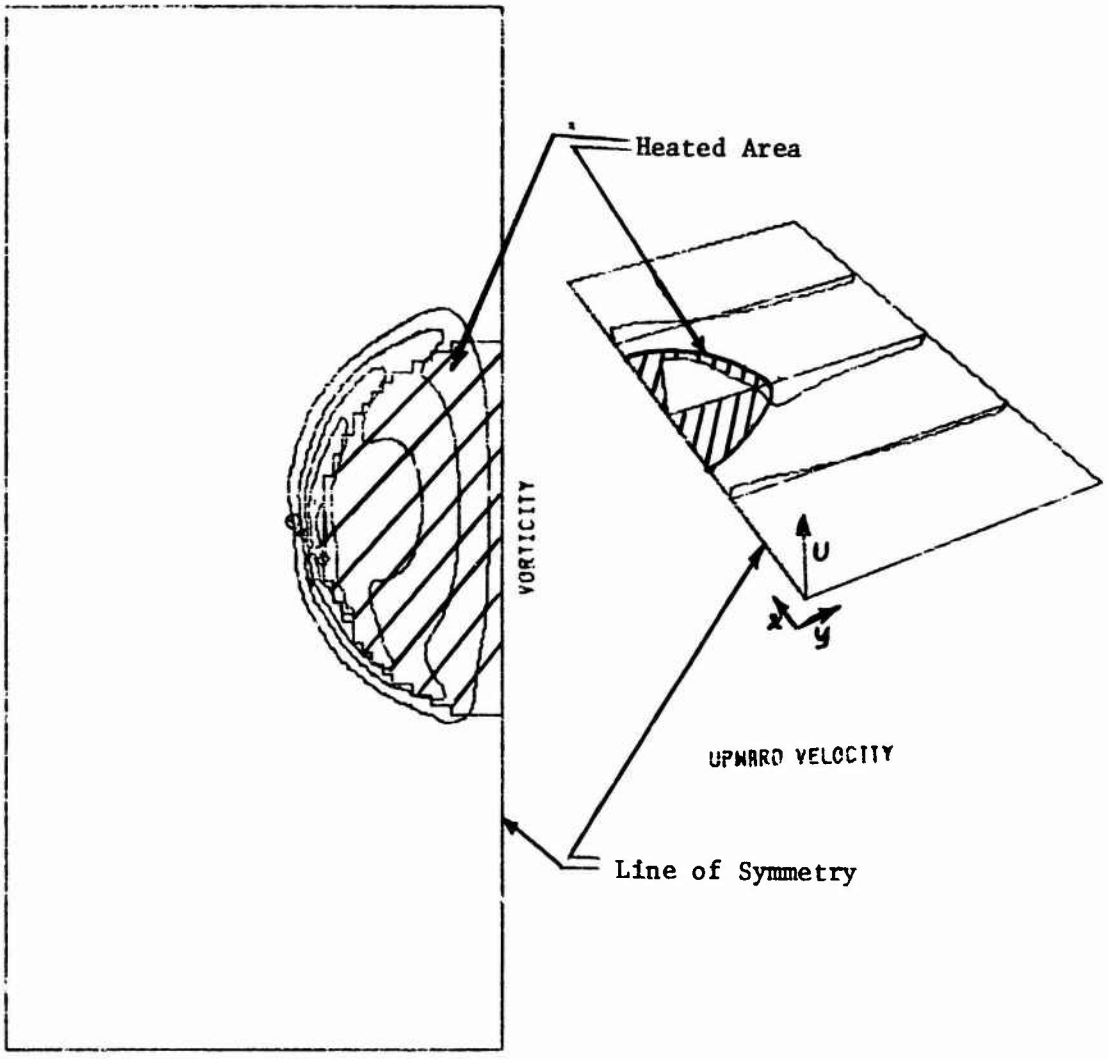

Vorticity (Non-dimensional)	Symbol
124.1	Octagon
372.3	Triangle
620.5	+
868.7	X
1116.9	Diamond

FIGURE 7: VORTICITY AND UPWARD VELOCITY AT .151 SECONDS OF PROBLEM 1

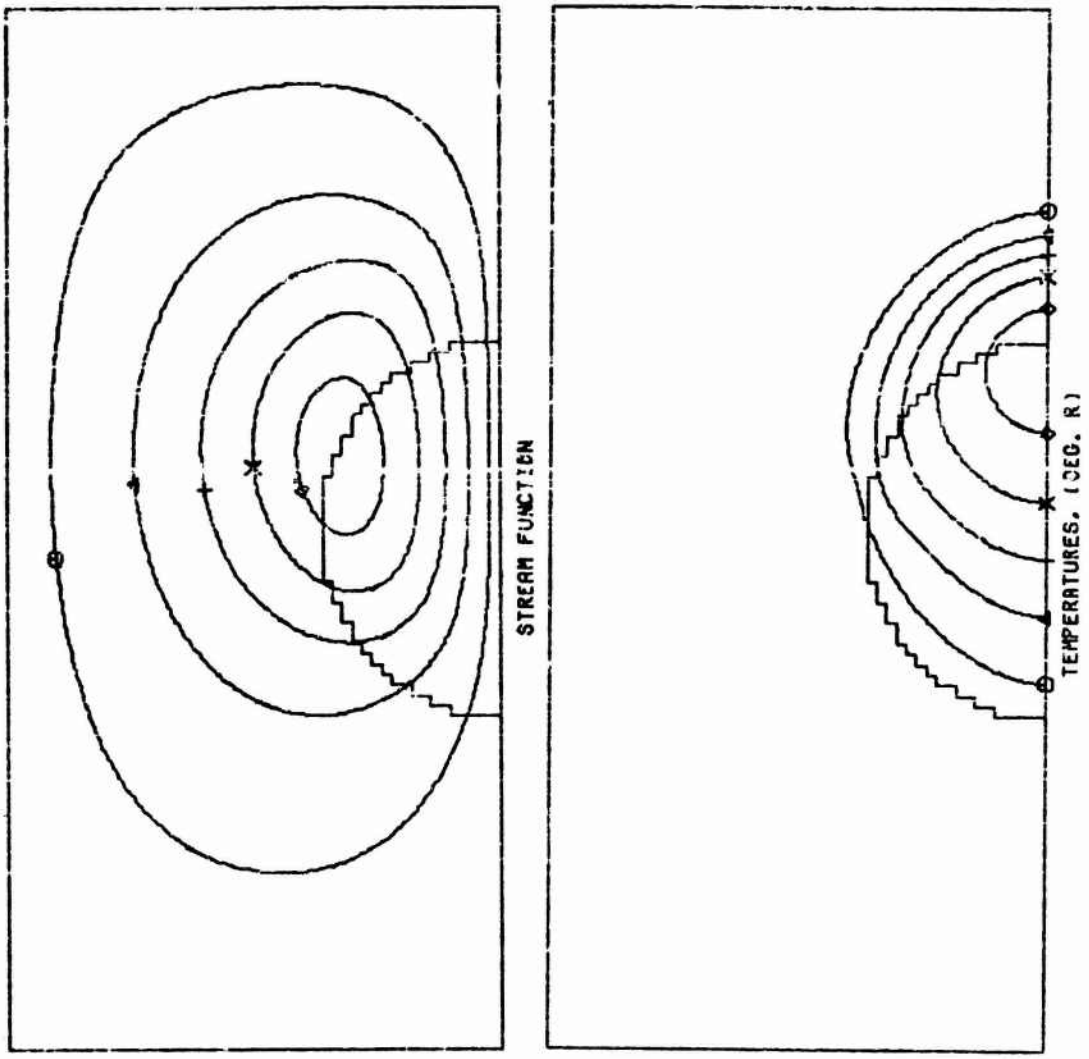

Stream Function (Non-dimensional)	Temperature (°R)	Symbol
46.2	557.1	Octagon
138.6	631.4	Triangle
231.0	705.6	+
323.4	779.9	X
415.8	854.2	Diamond

FIGURE 8: STREAM FUNCTION & TEMPERATURE AT .294 SECONDS OF PROBLEM 1

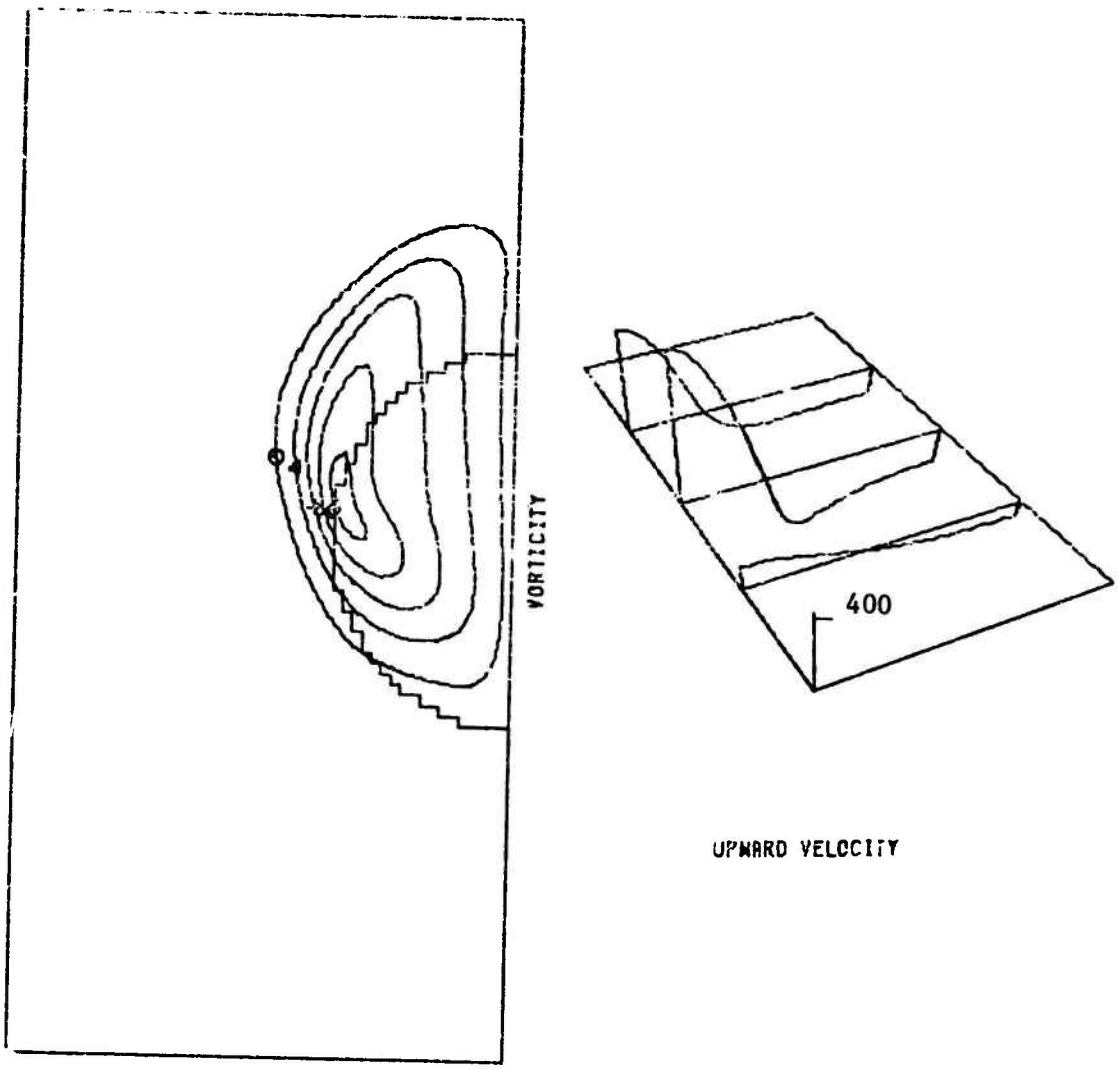

Vorticity (Non-dimensional)	Symbol
276	Octagon
828	Triangle
1380	+
1932	X
2484	Diamond

FIGURE 9: VORTICITY AND UPWARD VELOCITY AT .294 SECONDS OF PROBLEM 1

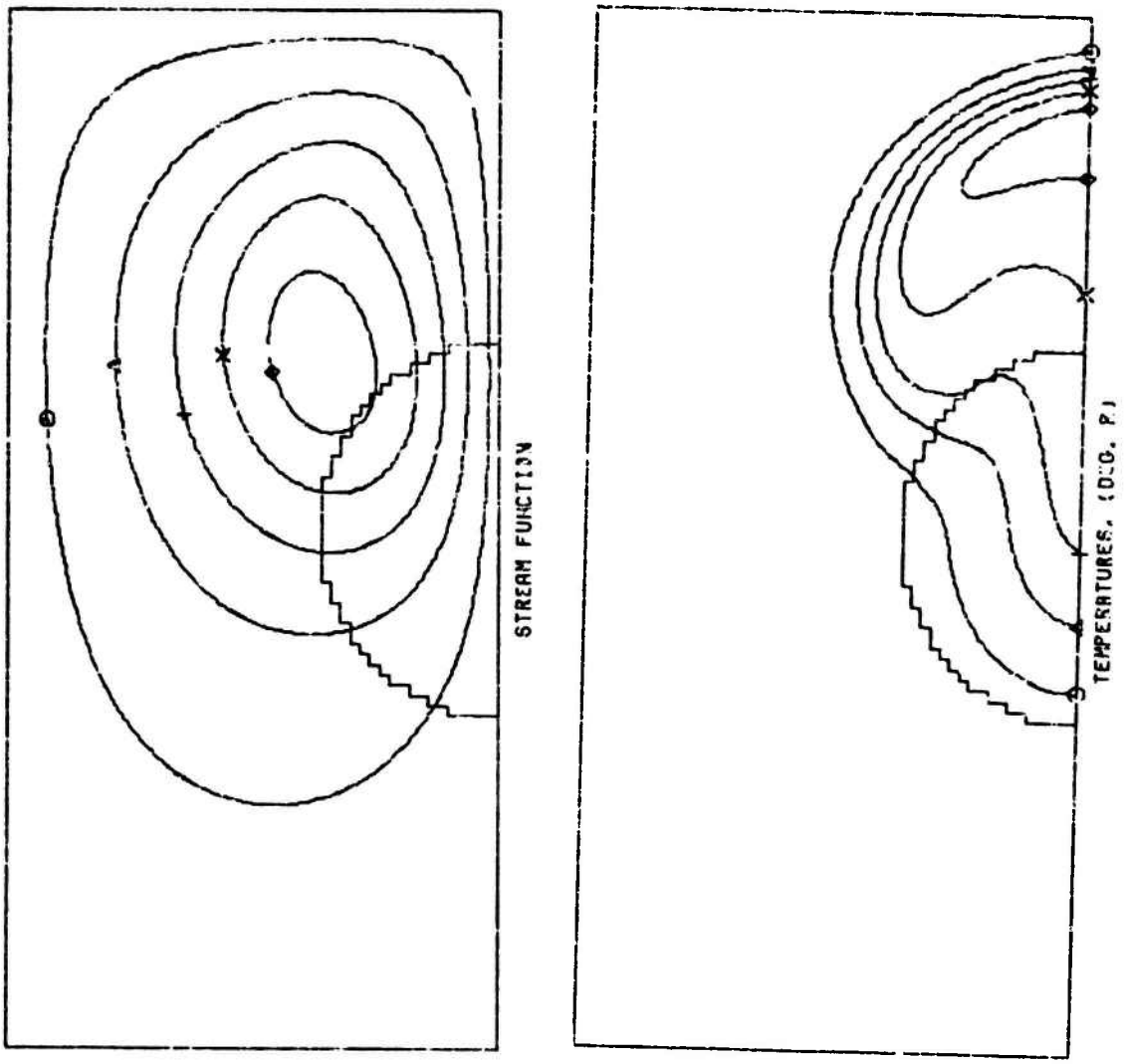

Stream Function (Non-dimensional)	Temperature (°R)	Symbol
81.4	553.1	Octagon
244.2	619.2	Triangle
407.0	685.4	+
569.8	751.5	X
732.6	817.6	Diamond

FIGURE 10: STREAM FUNCTION AND TEMPERATURE AT .45[illegible] SECONDS OF PROBLEM 1

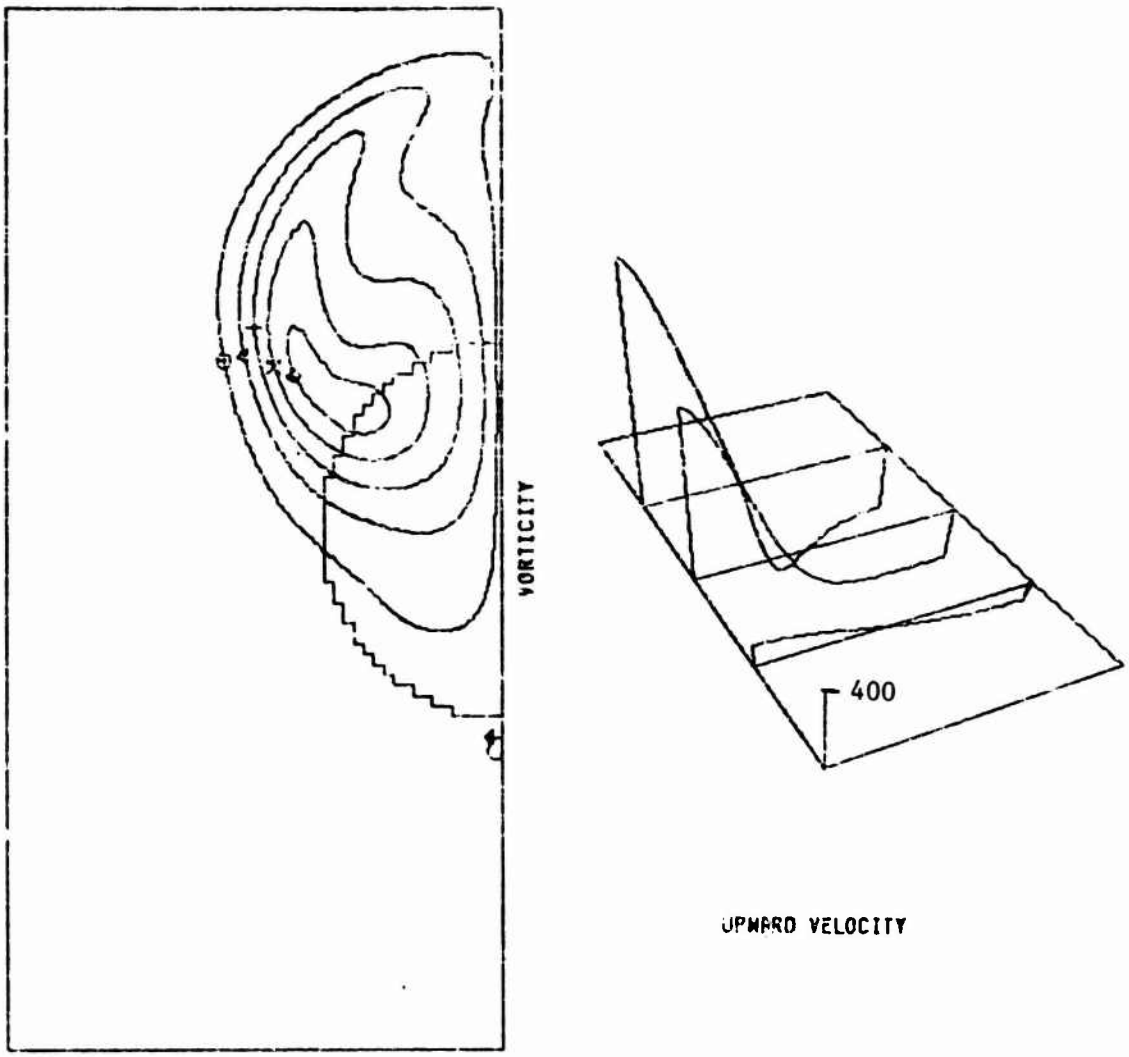

Vorticity (Non-dimensional)	Symbol
350.5	Octagon
1051.5	Triangle
1752.5	+
2453.5	X
3154.5	Diamond

FIGURE 11: VORTICITY AND UPWARD VELOCITY AT .451 SECONDS OF PROBLEM 1

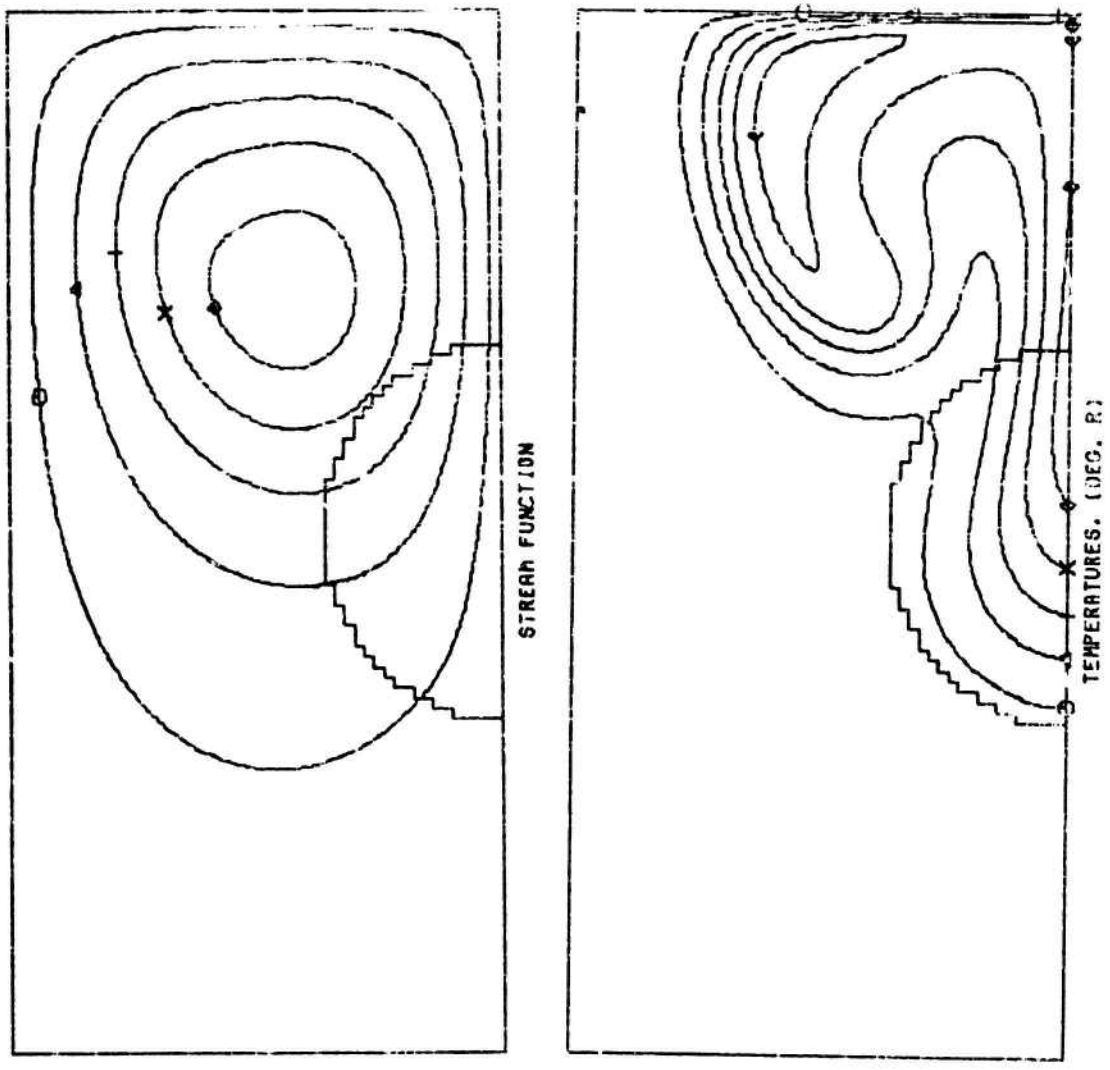

Stream Function (Non-dimensional)	Temperature (°R)	Symbol
98.8	545.0	Octagon
296.4	595.0	Triangle
494.0	645.1	+
691.6	695.1	X
889.2	745.1	Diamond

FIGURE 12: STREAM FUNCTION AND TEMPERATURE AT .601 SECONDS OF PROBLEM 1

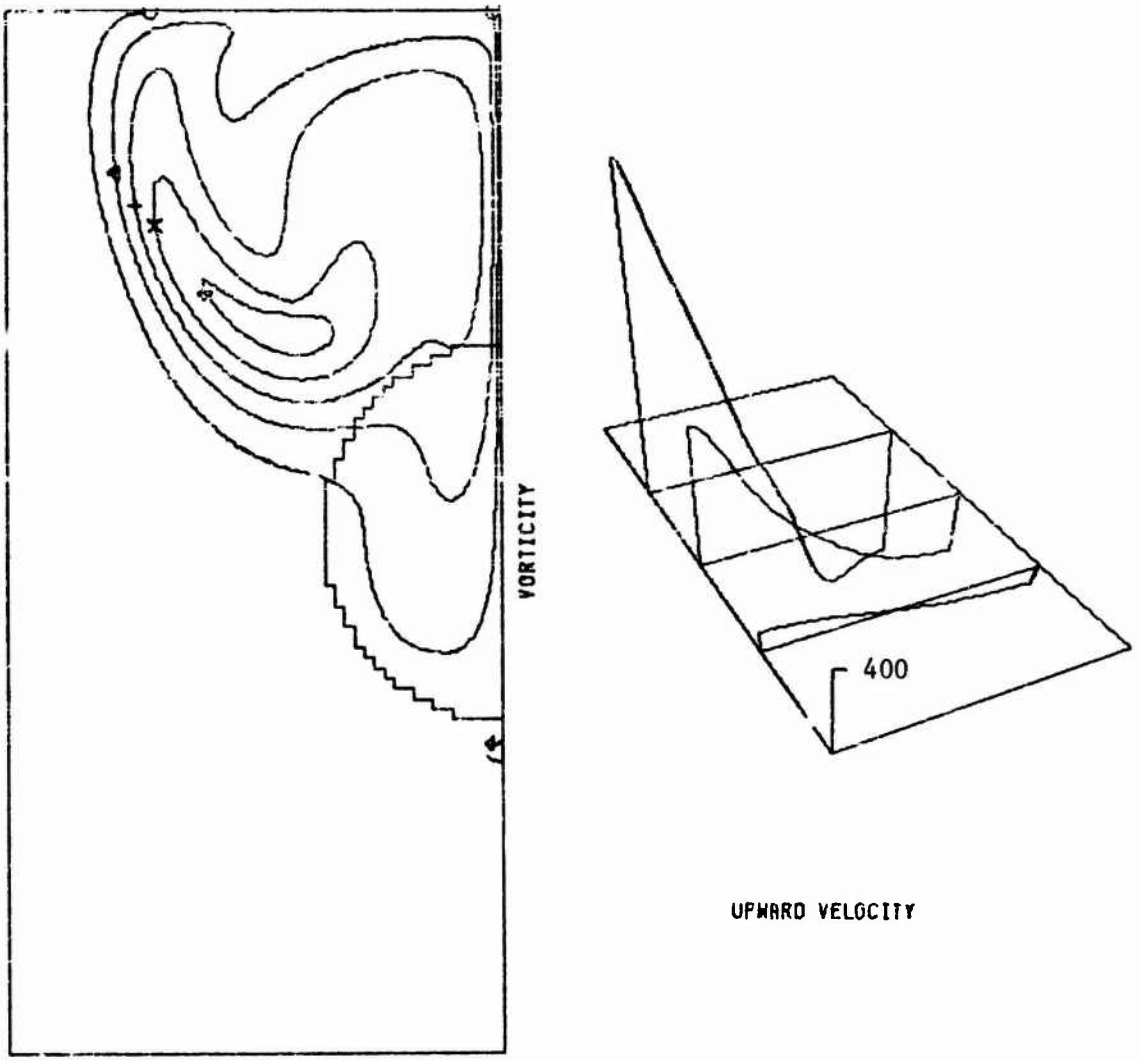

Vorticity (Non-dimensional)	Symbol
340.5	Octagon
1021.5	Triangle
1702.5	+
2383.5	X
3064.5	Diamond
0.0	Pine Tree

FIGURE 13: VORTICITY AND UPWARD VELOCITY AT .601 SECONDS OF PROBLEM 1

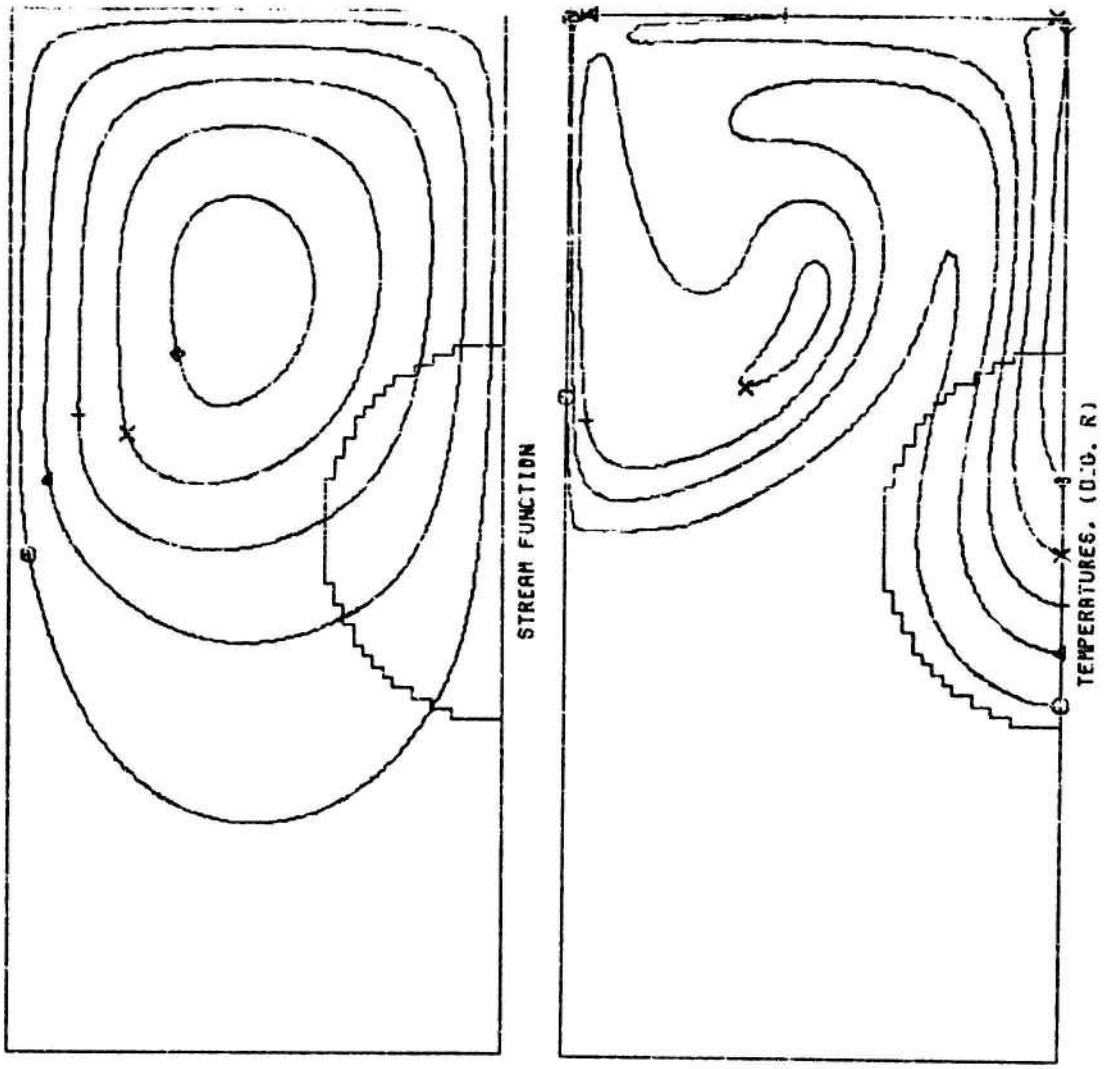

Stream Function (Non-dimensional)	Temperature (°R)	Symbol
93.0	547.2	Octagon
279.0	601.7	Triangle
465.0	656.2	+
651.0	710.7	X
837.0	765.2	Diamond

FIGURE 14: STREAM FUNCTION AND TEMPERATURE AT .801 SECONDS OF PROBLEM 1

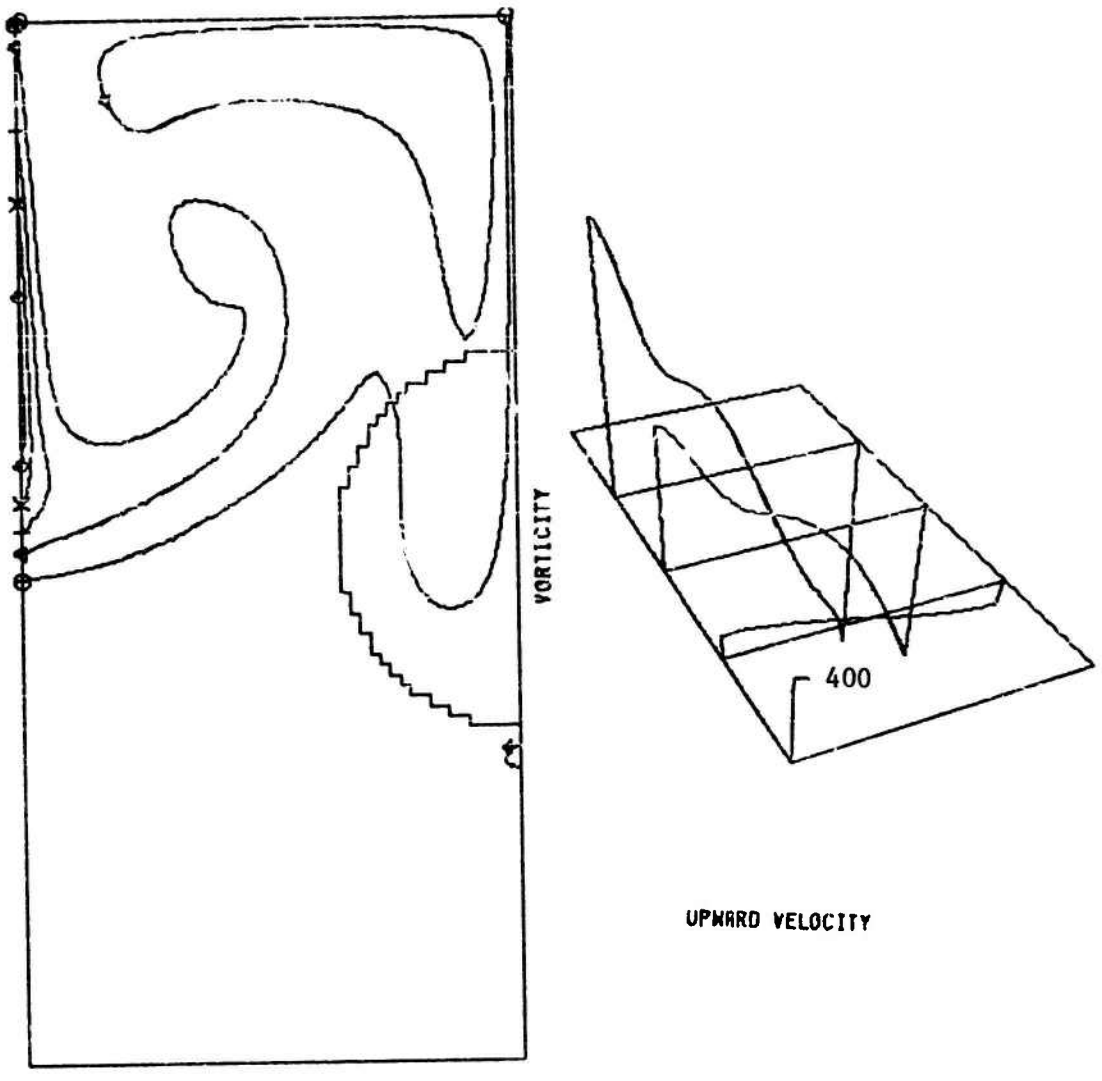

Vorticity (Non-dimensional)	Symbol
621.8	Octagon
1865.4	Triangle
3109.0	+
4352.6	X
5596.2	Diamond
0	Pine Tree

FIGURE 15: VORTICITY AND UPWARD VELOCITY AT .801 SECONDS OF PROBLEM 1

decrease. As with all the other example problems, the maximum temperatures always occur near the intersection of the upper portion of the heated area with the line of symmetry.

At .451 seconds (Figures 10 and 11), the convective forces have significantly affected the isotherms. The hottest region now lies completely outside the heated area, and the maximum temperature has decreased to 850.7°R. Most, and possibly all, of the beam area is now at a lower temperature than it was at .294 seconds. The flow is continuing to accelerate and the maximum upward velocity is 27 inches per second. This maximum velocity is occurring at a point on the line of symmetry above the heated region. Horizontal motion is beginning to alter the flow significantly. The lower portions of the isotherms have become indented and the vorticity plot has changed greatly. The central portion of the streamline and constant vorticity plots have continued their upward movement.

At .601 seconds (Figures 12 and 13), the isotherms have assumed a characteristic "mushroom cloud" shape and there are two regions that have temperatures greater than the 90% isotherm. However, the maximum temperature has decreased to 770°R. The regions of highest stream function and vorticity have moved upward and away from the heated area. The flow is obviously being affected by the upper wall. The maximum upward velocity is still increasing, but more slowly, and is now 30.5 inches/second.

At .801 seconds (Figures 14 and 15), the program is terminated. The gas which was initially heated has cooled significantly and been pushed to the upper portion of the vertical wall. The hottest region now lies within and directly above the central portion of the

beam area, along the line of symmetry. The maximum upward velocity has decreased to about 27 inches/second and the upward velocity profiles have been significantly altered. Apparently, the gas mixture is now passing through the heated region more slowly, as the temperatures in the beam area have now risen slightly. The maximum temperature is now 792.5°R.

Figure 16 is a plot of the pressure rise within the enclosure, and the heating rate per inch of beam path through the enclosure, as a function of time. The variation in the heating rate is due to changes in the average density of the gas mixture in the beam path. The absorption coefficient is assumed to be directly proportional to density. As the density in the heated region decreases due to heating, the absorption coefficient and the heating rate also decrease proportionately. Thus, the time at which the heating rate is lowest (approximately .25 seconds) is also the time at which the density in the heated region is lowest. Since the density increase due to changing pressure is relatively small, this is also the time at which the mass average temperature in the beam path is highest.

C. SAMPLE PROBLEM NO. 2

This problem is identical to problem number 1, except that the laser beam spatial power distribution has been changed to a constant ("flattop beam"). Thus, a heated element on the edge of the beam is being irradiated at the same rate as an element near the center. The input power has been reduced so that the total incident power is the same as in problem number 1. The beam area is also the same. The program utilizes a total power of 57603.1 watts over an area of 7.283 square inches, yielding an average power density of 1226.2 watts per

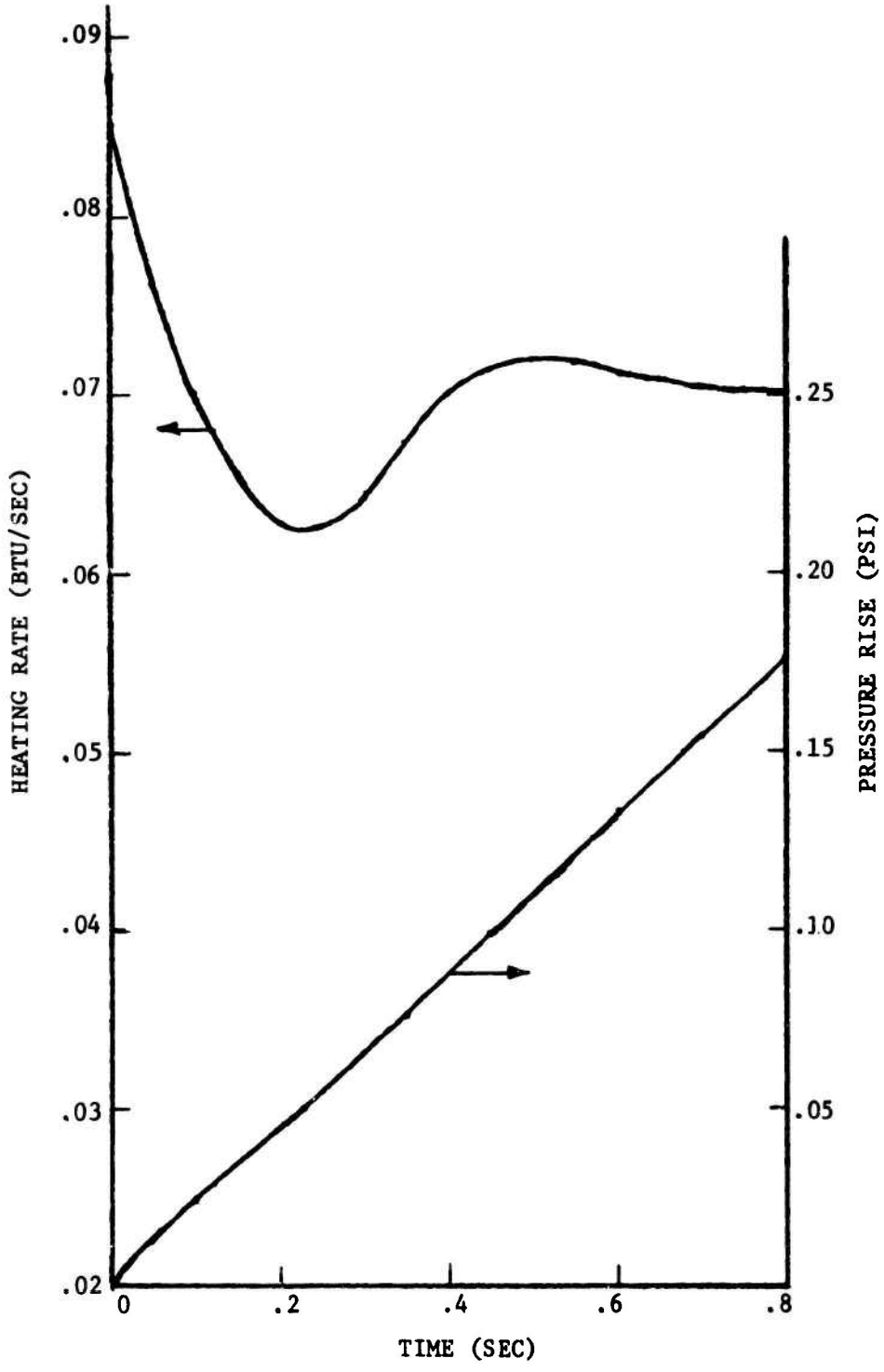

FIGURE 16: HEATING RATE & PRESSURE RISE - SAMPLE PROBLEM NUMBER 1

square centimeter. This is less than .4 watts per sq cm more than the average power density of the Gaussian beam used in the previous sample problem. No other input properties have changed.

Although the only change between sample problems 1 and 2 is the manner in which the power is distributed throughout the beam area, the results are significantly different. At time .151 seconds (Figures 17 and 18), the isotherms are closely grouped near the edge of the heated area. Higher thermal, upward velocity and vorticity gradients exist near the edge of the heated area than at the same time in problem number 1. Also, the maximum temperature rise is only about half that which had occurred at this time in problem 1. The maximum upward velocity is similarly lower and the maximum vorticity is nearly twice as great.

At .301 seconds (Figures 19 and 20), the effects of convection are more pronounced. The ratios of the maximum temperature, upward velocity, and vorticity at this time to the same values at the same time in problem 1 have begun to approach unity; however, the differences are still quite large. For example, the ratio of the maximum temperature in problem 2 to the maximum temperature in problem 1 has increased from .51 at .151 seconds to .66 at .301 seconds.

At .393 seconds (Figures 21 and 22) the maximum temperature value of 822°R occurs. Notice that problem 2 has resulted in a maximum temperature that is 70° lower, and occurs 0.1 seconds later than the maximum temperature of problem 1. As in sample problem number 1, this maximum temperature value has occurred at the top of the heated region near the line of symmetry.

As the heating continues, the isotherms assume the mushroom shaped pattern observed in problem 1, and the pattern is then similarly disturbed by the presence of the upper and the vertical walls. The hottest region lies outside the beam path for a longer time than in problem 1. At .601 seconds the maximum temperatures and vorticities are nearly the same as in problem 1, and the maximum velocity is slightly smaller. The plots of isotherms, streamlines, constant vorticities, and upward velocities at .601 seconds and .801 seconds (Figures 23-26) look quite similar to the plots of problem 1 at those times. The heating rate plot (Figure 27) is slightly different from that of problem 1. The heating rate values are slightly higher for the flattop beam, and the minimum occurs at a later time. The net effect is that slightly more heat is added with the flattop beam, despite the fact that a lower maximum temperature was obtained, and the pressure rise is correspondingly slightly higher.

D. SAMPLE PROBLEM NO. 3

This problem is identical to problem 1 with the exception that the acceleration of gravity (g) has been reduced to 16.1 ft/sec^2. Since the convective force term in the equation of motion is highly dependent on the value of g, it would be expected that this change would reduce the effects of convection. The beam spatial power distribution for this sample problem is the same Gaussian power distribution as was used in example 1.

At .151 seconds (Figures 28 and 29) it is interesting to compare the plots for this example problem with those of problem 1 (Figures 6 and 7). The isotherm values and shapes and the lines of constant vorticity and stream function are nearly identical. However,

the values of vorticity, stream function, and upward velocity are almost exactly half those of problem 1. This indicates that the effects of convection are insignificant up to this time.

By .301 seconds (Figures 30 and 31) the maximum temperature has reached 945°R and is still rising, whereas in problem 1, the maximum temperature attained a maximum value of 892°R at .293 seconds and began decreasing. Throughout this low gravity problem the upward velocities were lower than their corresponding values in the standard gravity problem. However, by .8 seconds the values were much closer than at early times.

At .384 seconds (Figures 32 and 33) the maximum temperature of 976°R was attained. Thus the effect of reducing gravity to one-half of its standard value was to produce a 22% greater temperature rise (obviously due to the lessened convective cooling effect) at a time .09 seconds later. By .601 seconds (Figures 34 and 35) the plots appear almost identical to the plots from problem 1 at .451 seconds (Figures 10 and 11). However, the values of these contours are substantially different. As expected, the motion of the gas has been slowed, thereby allowing the hot gas to remain in the beam path for a longer time and producing a higher local temperature. Since the gas within the beam path is at a higher temperature (e.g., lower density) than in problem 1, and since the absorption coefficient is linearly proportional to density, it is to be expected that the heating rate would be lower for problem 3. And, if Figure 38 is compared with Figure 16, we find that the heating rate is indeed lower for problem 3. Thus, the lower heating rate has produced a higher temperature.

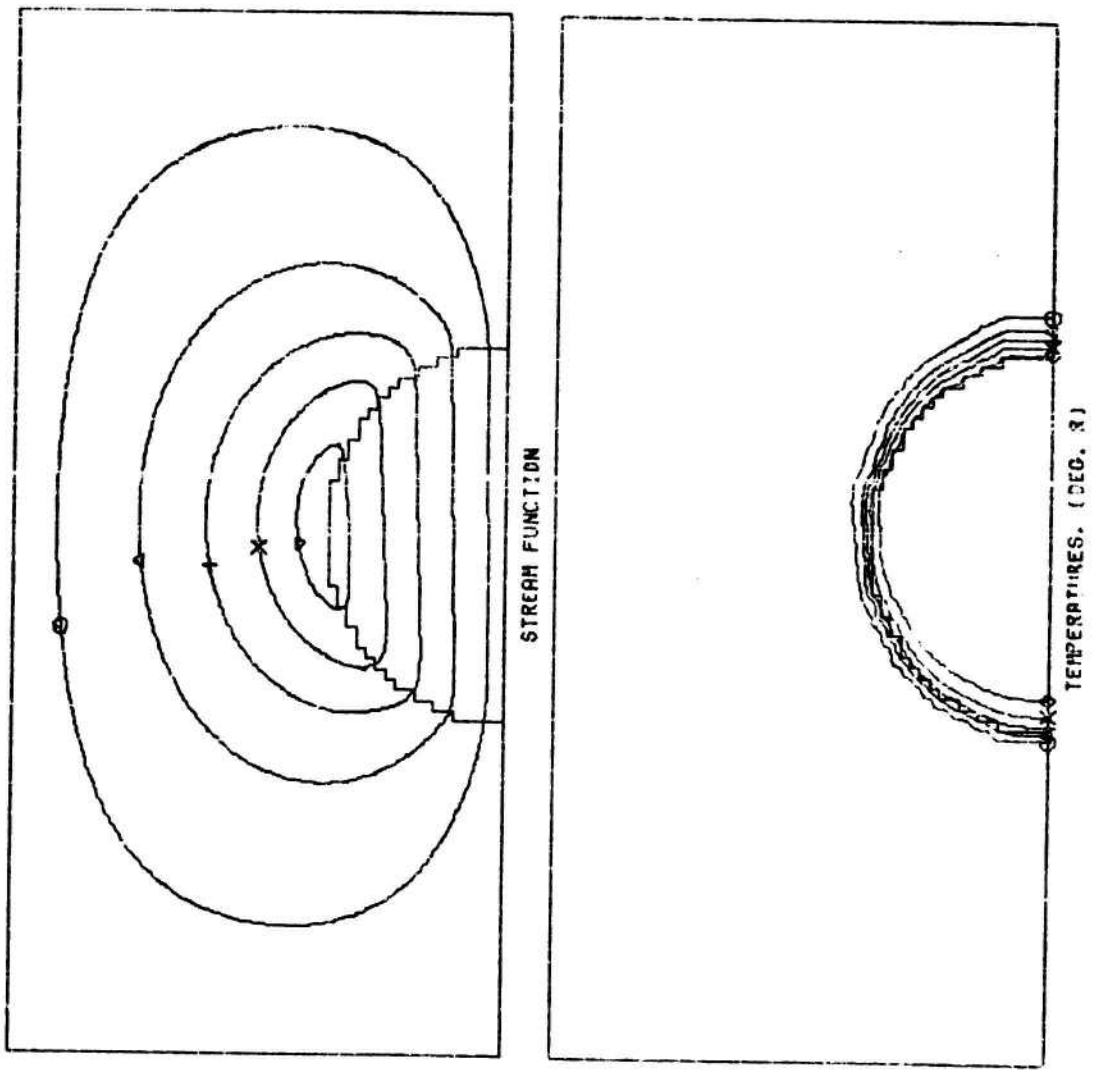

Stream Function (Non-dimensional)	Temperature (°R)	Symbol
15.1	533.5	Octagon
45.3	560.6	Triangle
75.5	587.6	+
105.7	614.6	X
135.9	641.7	Diamond

FIGURE 17: STREAM FUNCTION AND TEMPERATURE AT .15i SECONDS OF PROBLEM 2

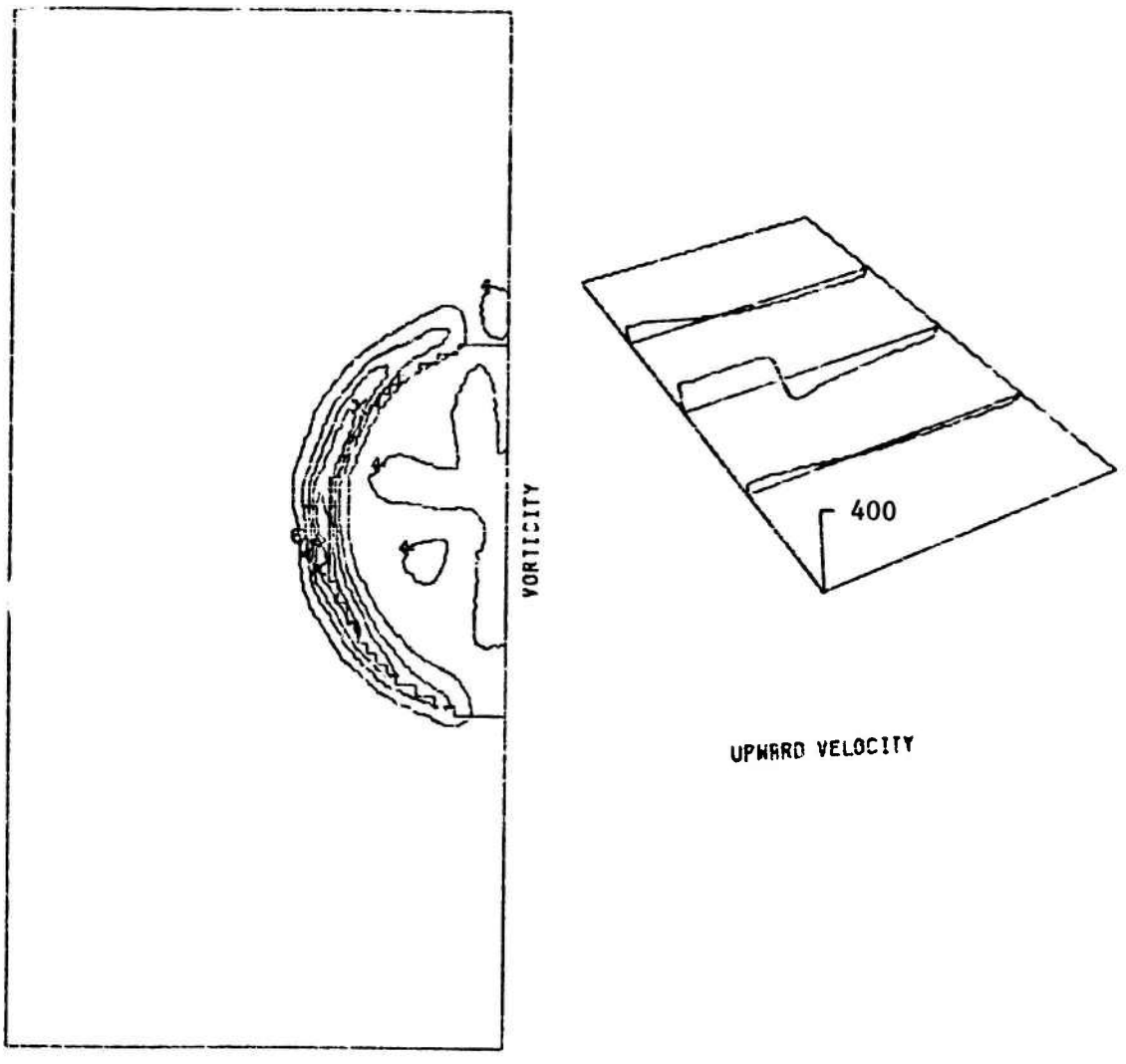

Vorticity (Non-dimensional)	Symbol
229.3	Octagon
713.9	Triangle
1198.5	+
1683.1	X
2167.7	Diamond
0.0	Pine Tree

FIGURE 18: VORTICITY AND UPWARD VELOCITY AT .151 SECONDS OF PROBLEM 2

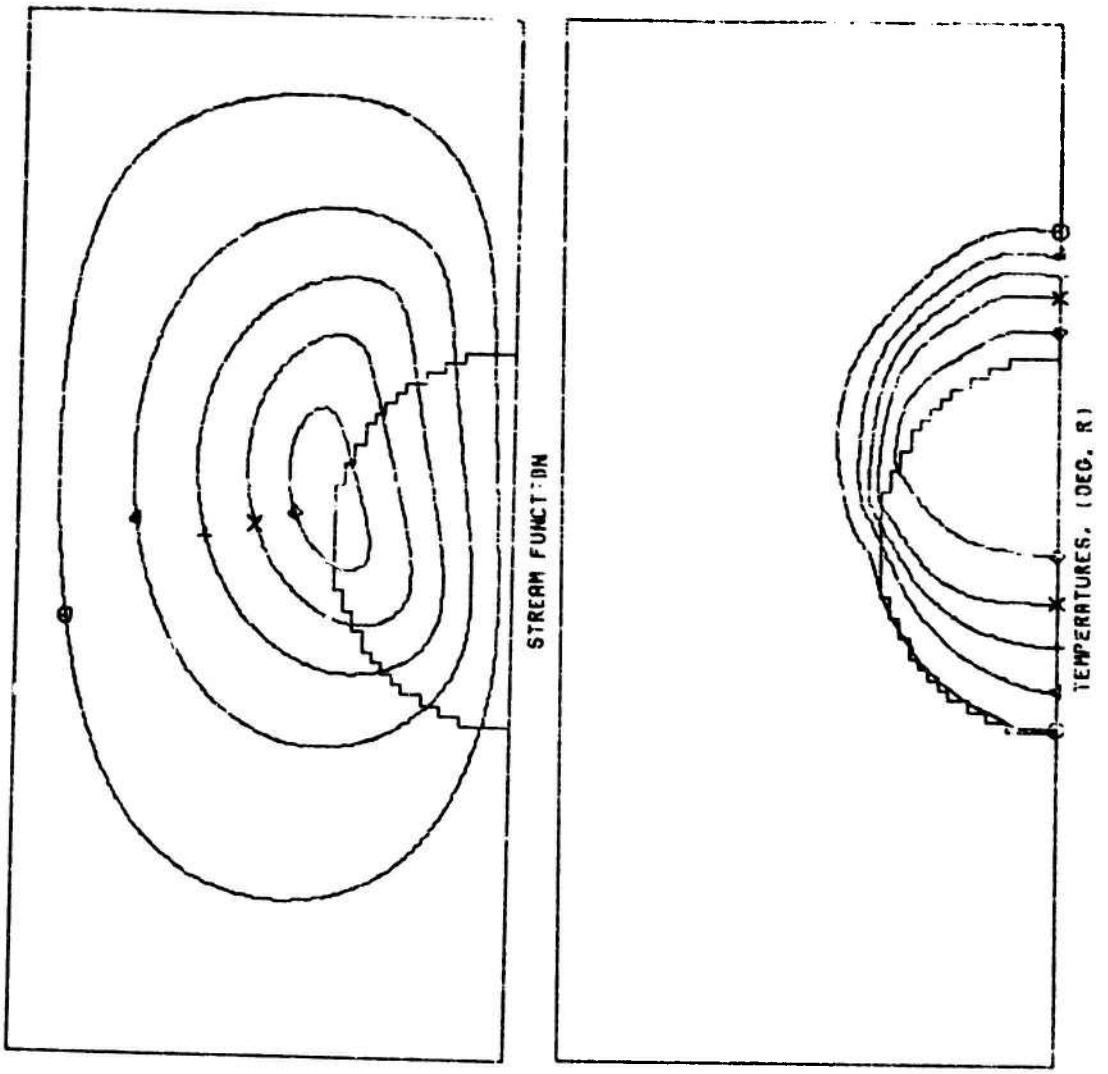

Stream Function (Non-dimensional)	Temperature (°R)	Symbol
45.2	544.5	Octagon
135.6	593.6	Triangle
226.0	642.7	+
316.4	691.8	X
406.8	740.9	Diamond

FIGURE 19: STREAM FUNCTION AND TEMPERATURE AT .301 SECONDS OF PROBLEM 2

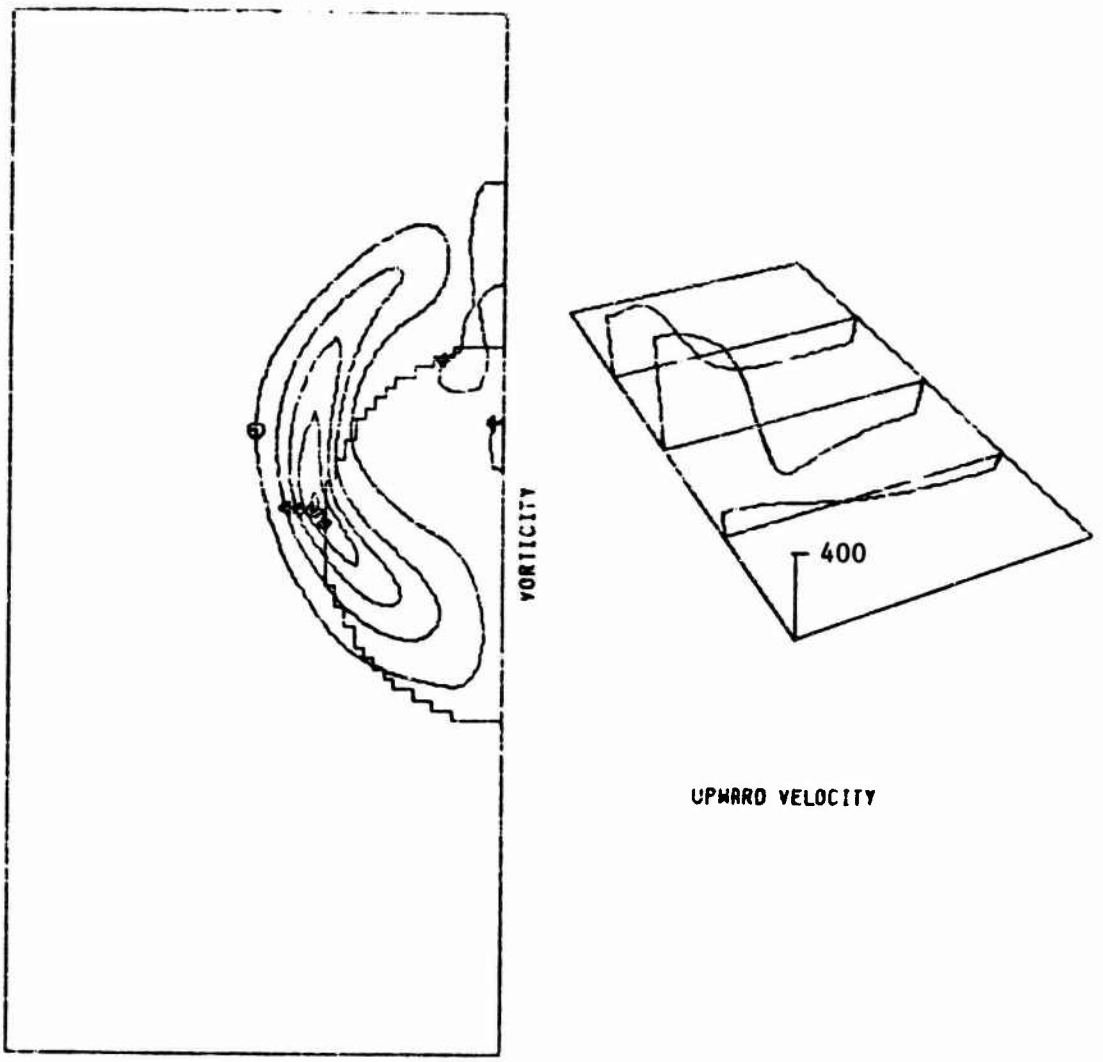

Vorticity (Non-dimensional)	Symbol
394.8	Octagon
1314.4	Triangle
2234.0	+
3153.6	X
4073.2	Diamond
0.0	Pine Tree

FIGURE 20: VORTICITY AND UPWARD VELOCITY AT .301 SECONDS OF PROBLEM 2

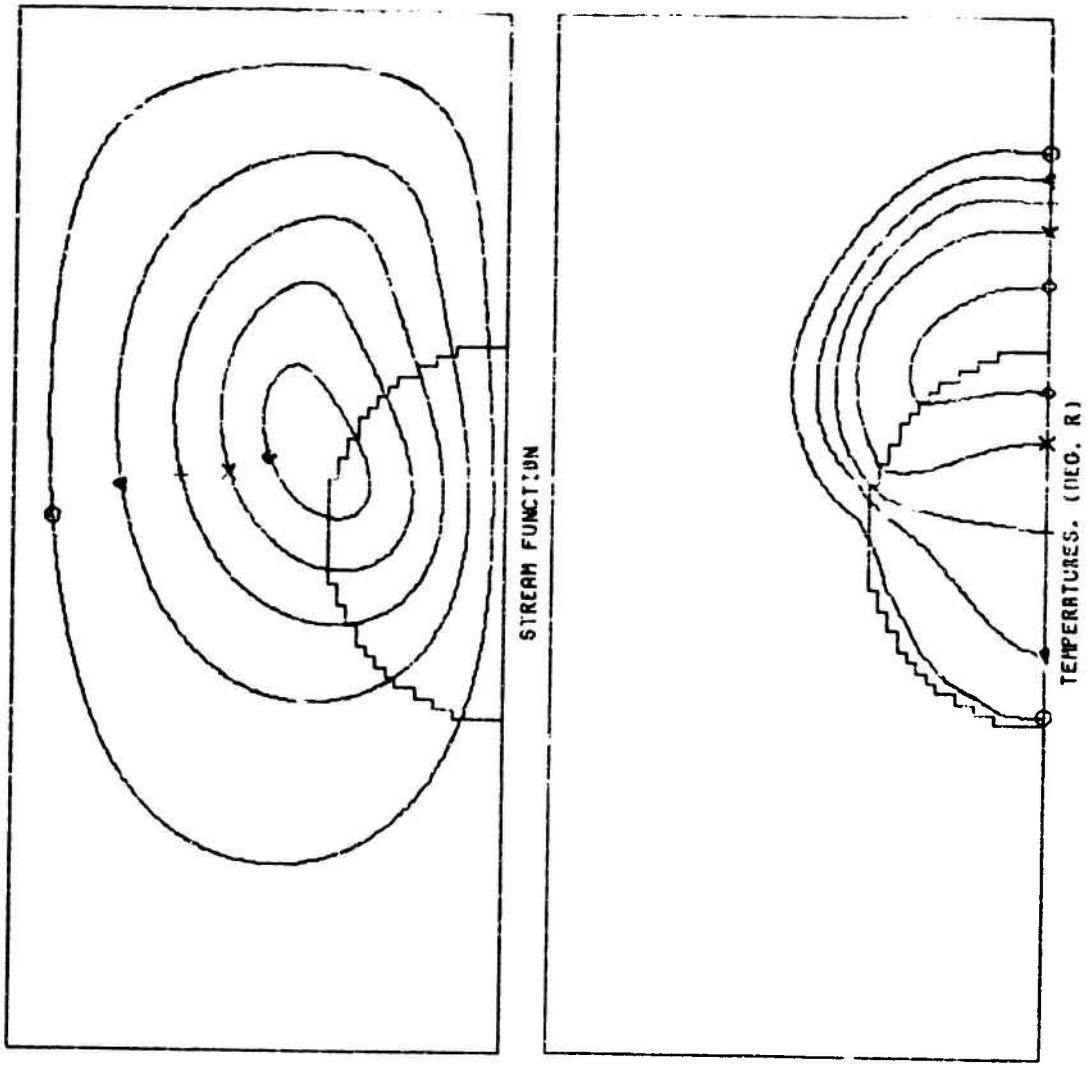

Stream Function (Non-dimensional)	Temperature (°R)	Symbol
64.5	550.2	Octagon
193.5	610.5	Triangle
322.5	670.8	+
451.5	731.1	X
580.5	791.4	Diamond

FIGURE 21: STREAM FUNCTION AND TEMPERATURE AT .394 SECONDS OF PROBLEM 2

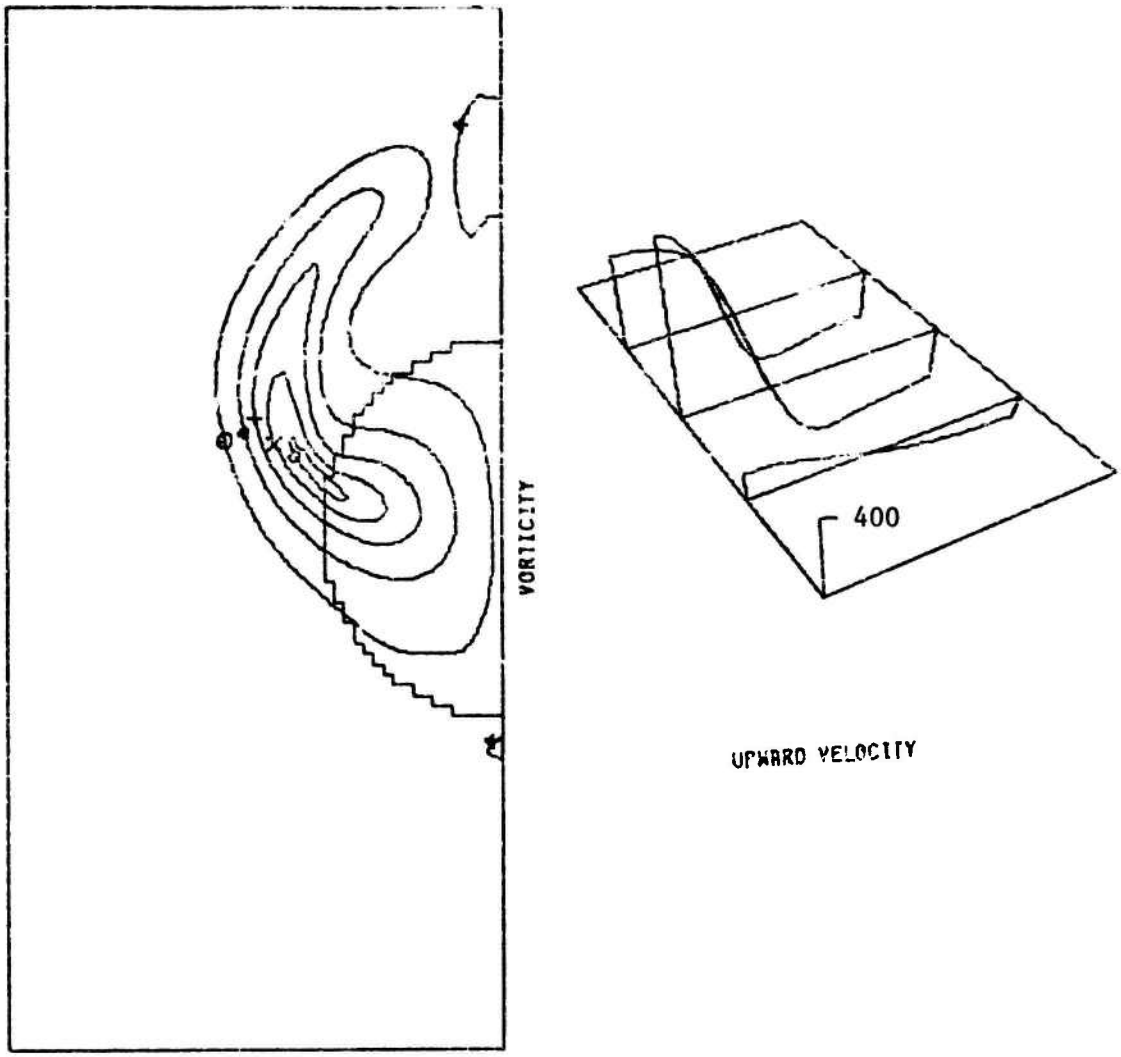

Vorticity (Non-dimensional)	Symbol
351.0	Octagon
1251.0	Triangle
2151.0	+
3051.0	X
3951.0	Diamond
0.0	Pine Tree

FIGURE 22: VORTICITY AND UPWARD VELOCITY AT .394 SECONDS OF PROBLEM 2

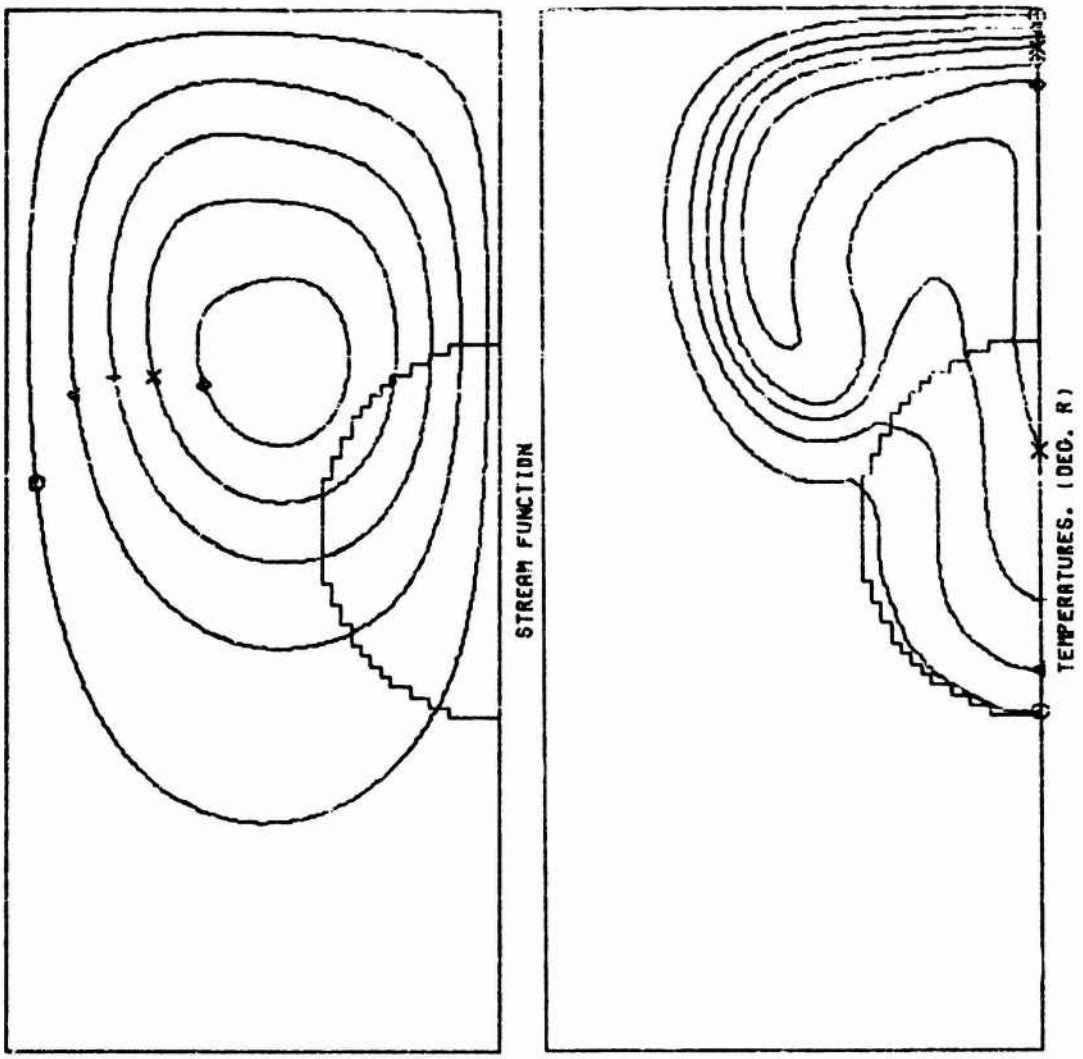

Stream Function (Non-dimensional)	Temperature (°R)	Symbol
95.2	544.9	Octagon
285.6	594.7	Triangle
476.0	644.5	+
666.4	694.4	X
856.8	744.2	Diamond

FIGURE 23: STREAM FUNCTION AND TEMPERATURE AT .601 SECONDS OF PROBLEM 2

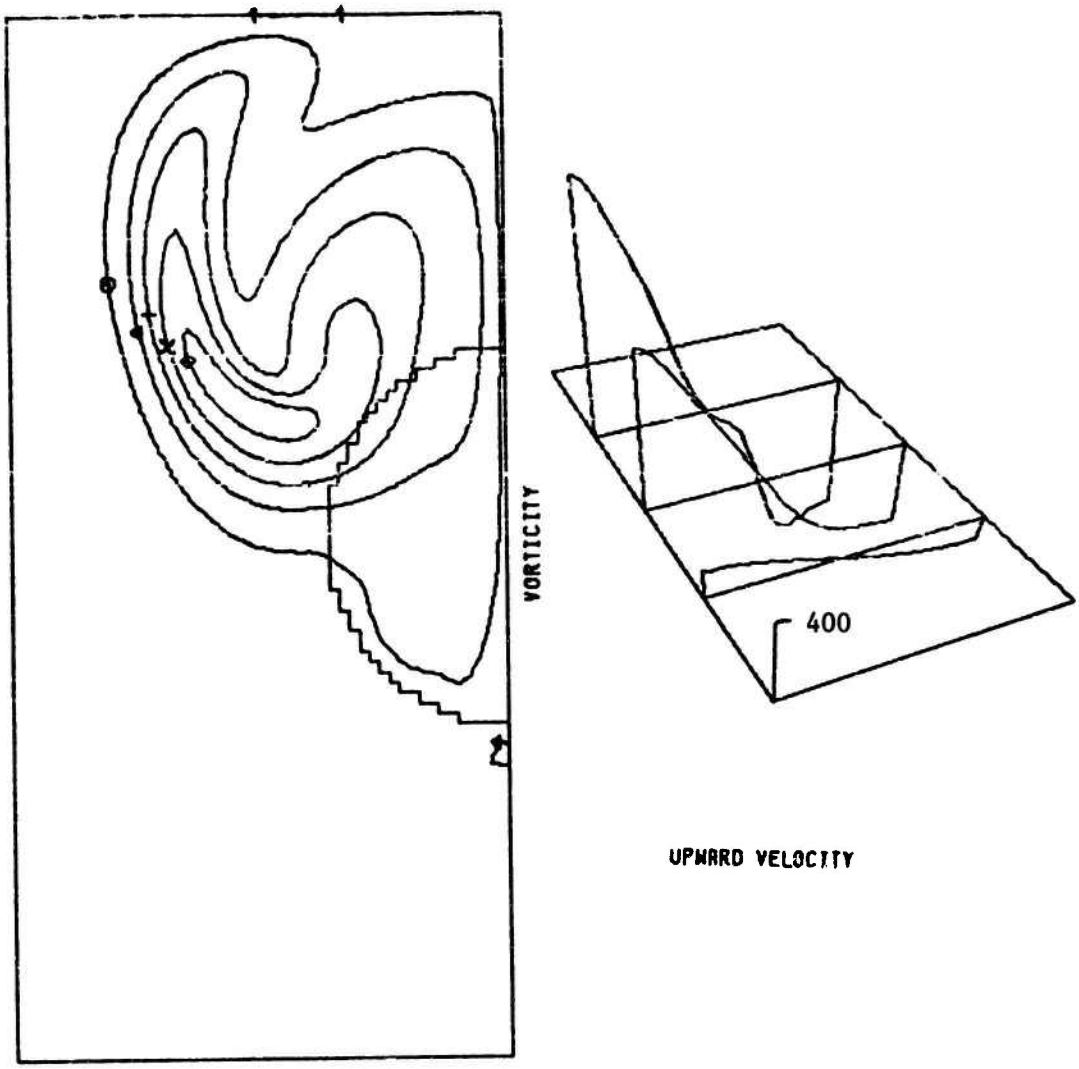

Vorticity (Non-dimensional)	Symbol
289.3	Octagon
987.9	Triangle
1686.5	+
2385.1	X
3083.7	Diamond
0.0	Pine Tree

FIGURE 24: VORTICITY AND UPWARD VELOCITY AT .601 SECONDS OF PROBLEM 2

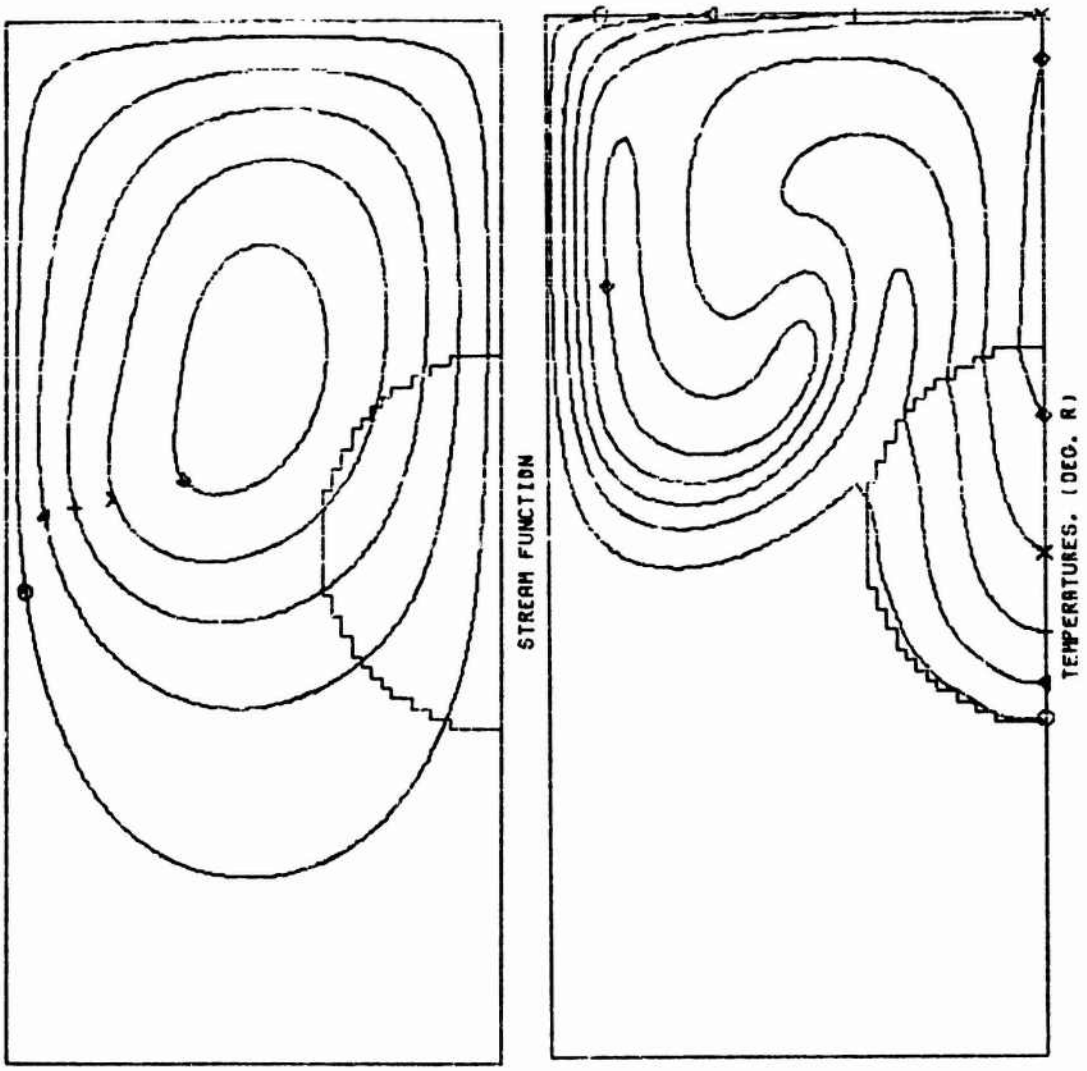

Stream Function (Non-dimensional)	Temperature (°R)	Symbol
95.3	541.1	Octagon
285.9	583.2	Triangle
476.5	625.3	+
667.1	667.4	X
857.7	709.5	Diamond

FIGURE 25: STREAM FUNCTION AND TEMPERATURE AT .801 SECONDS OF PROBLEM 2

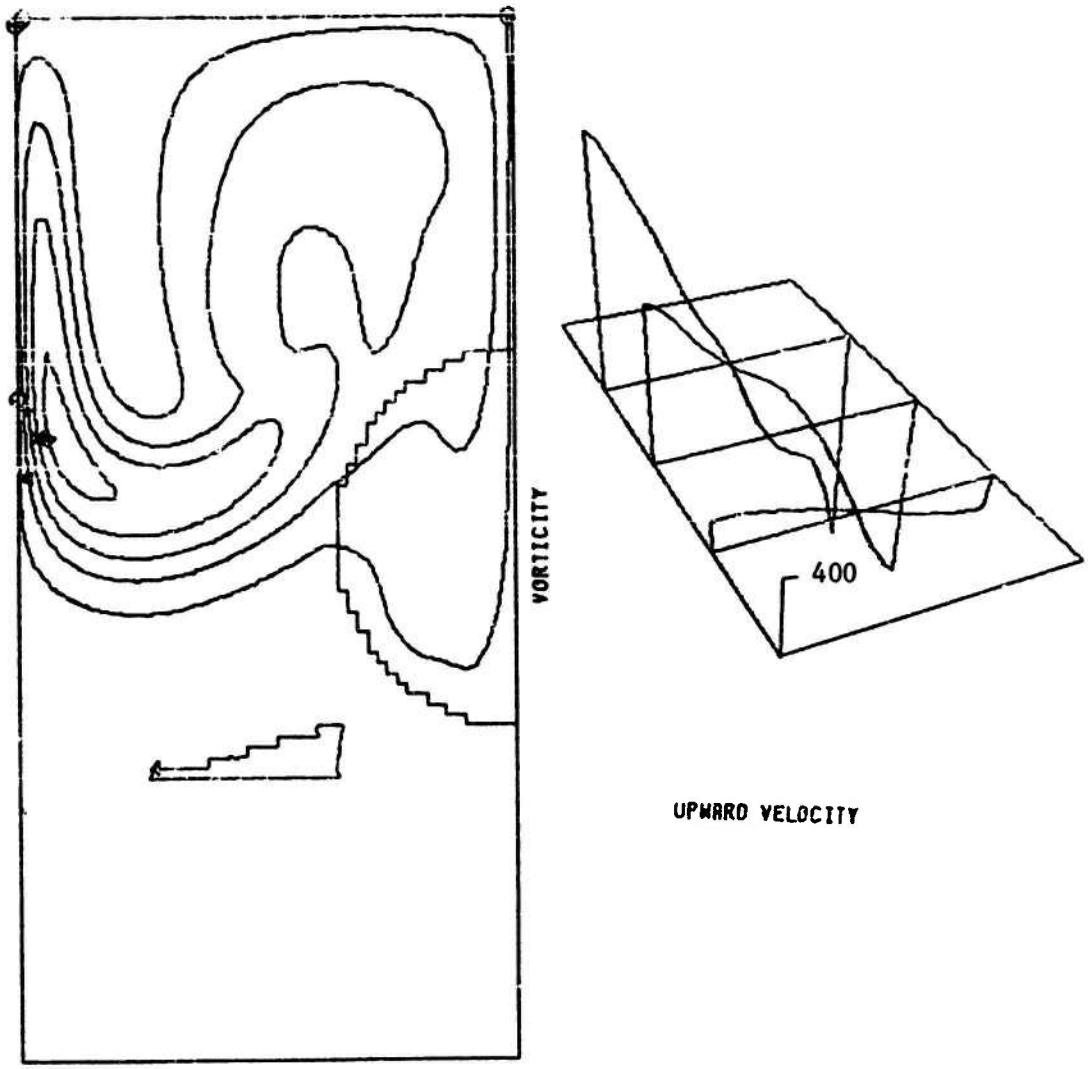

Vorticity (Non-dimensional)	Symbol
309.7	Octagon
929.1	Triangle
1548.5	+
2167.9	X
2787.3	Diamond
0.0	Pine Tree

FIGURE 26: VORTICITY AND UPWARD VELOCITY AT .801 SECONDS OF PROBLEM 2

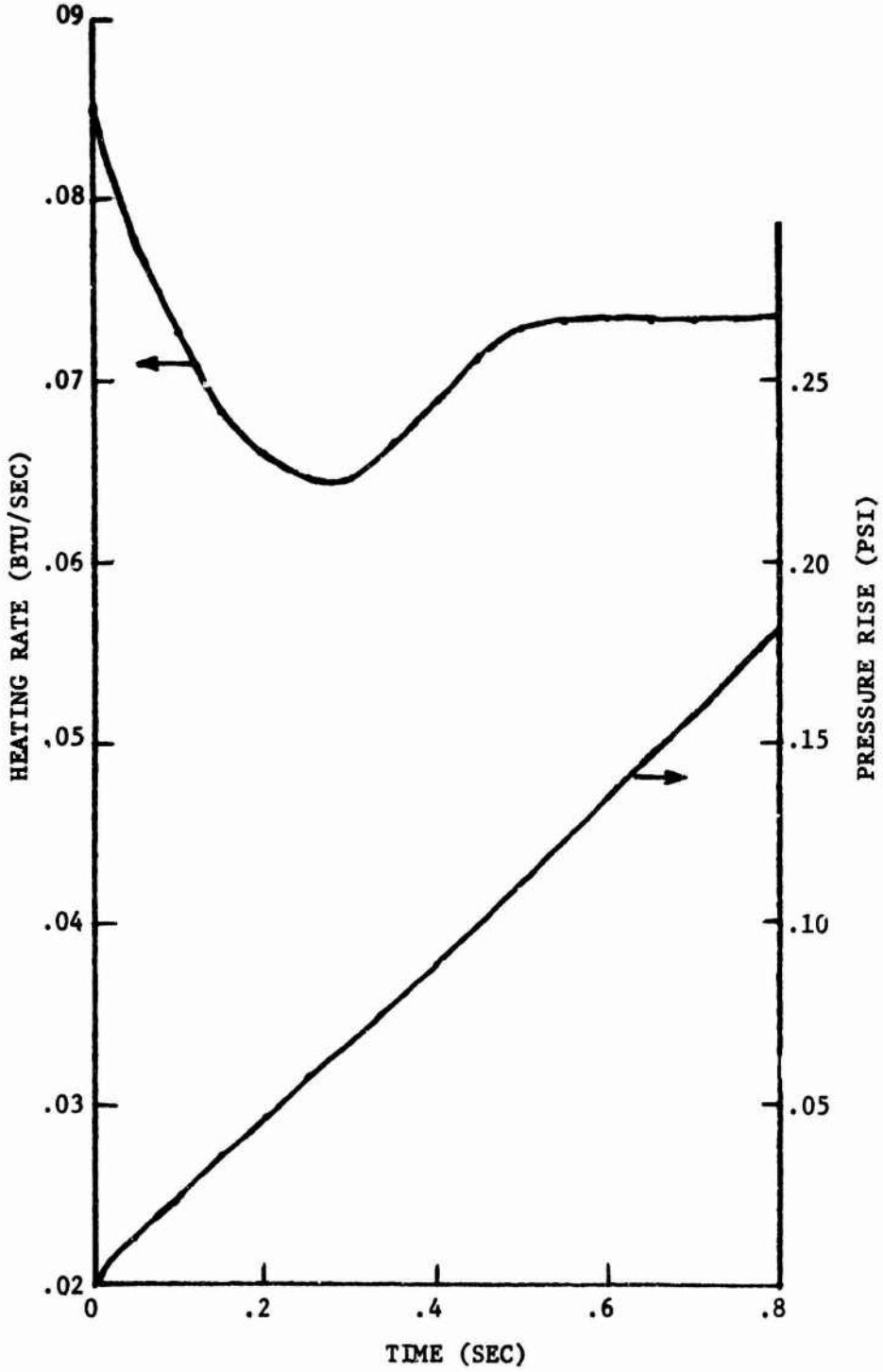

FIGURE 27: HEATING RATE & PRESSURE RISE - SAMPLE PROBLEM NUMBER 2

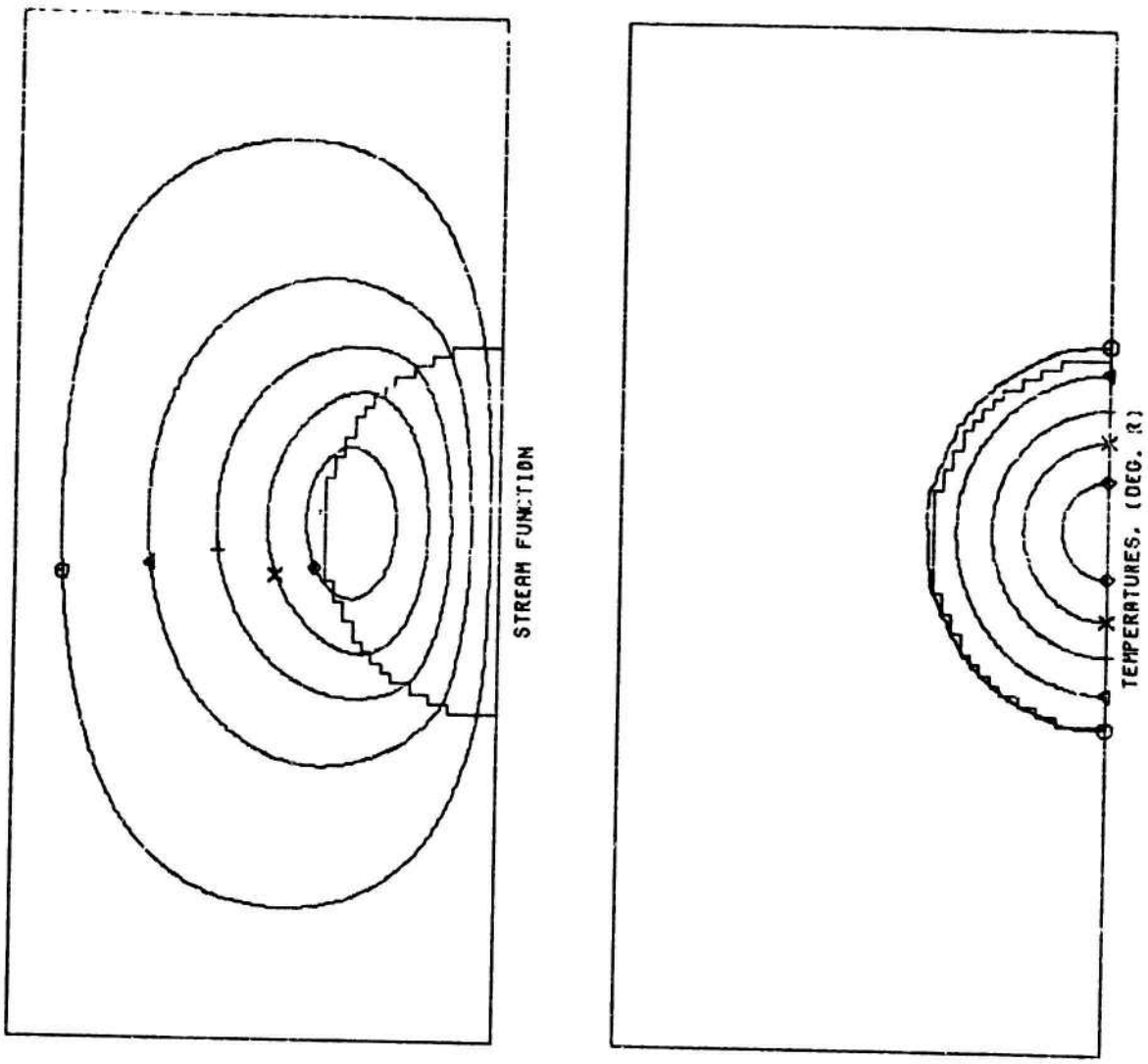

Stream Function (Non-dimensional)	Temperature (°R)	Symbol
7.8	546.9	Octagon
23.4	600.7	Triangle
39.0	654.4	+
54.6	708.2	X
70.2	762.0	Diamond

FIGURE 28: STREAM FUNCTION AND TEMPERATURE AT .151 SECONDS OF PROBLEM 3

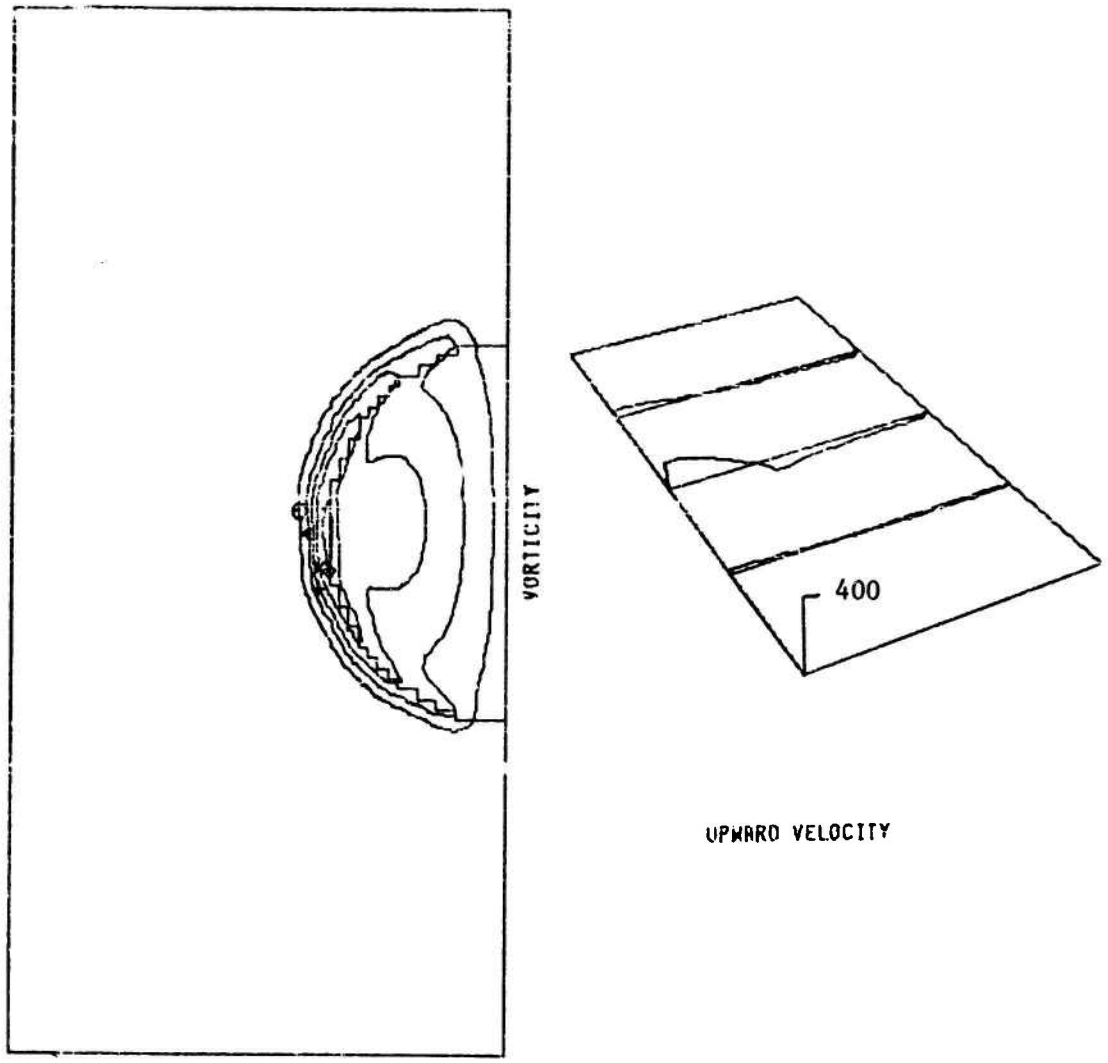

Vorticity (Non-dimensional)	Symbol
63.5	Octagon
190.5	Triangle
317.5	+
444.5	X
571.5	Diamond

FIGURE 29: VORTICITY AND UPWARD VELOCITY AT .151 SECONDS OF PROBLEM 3

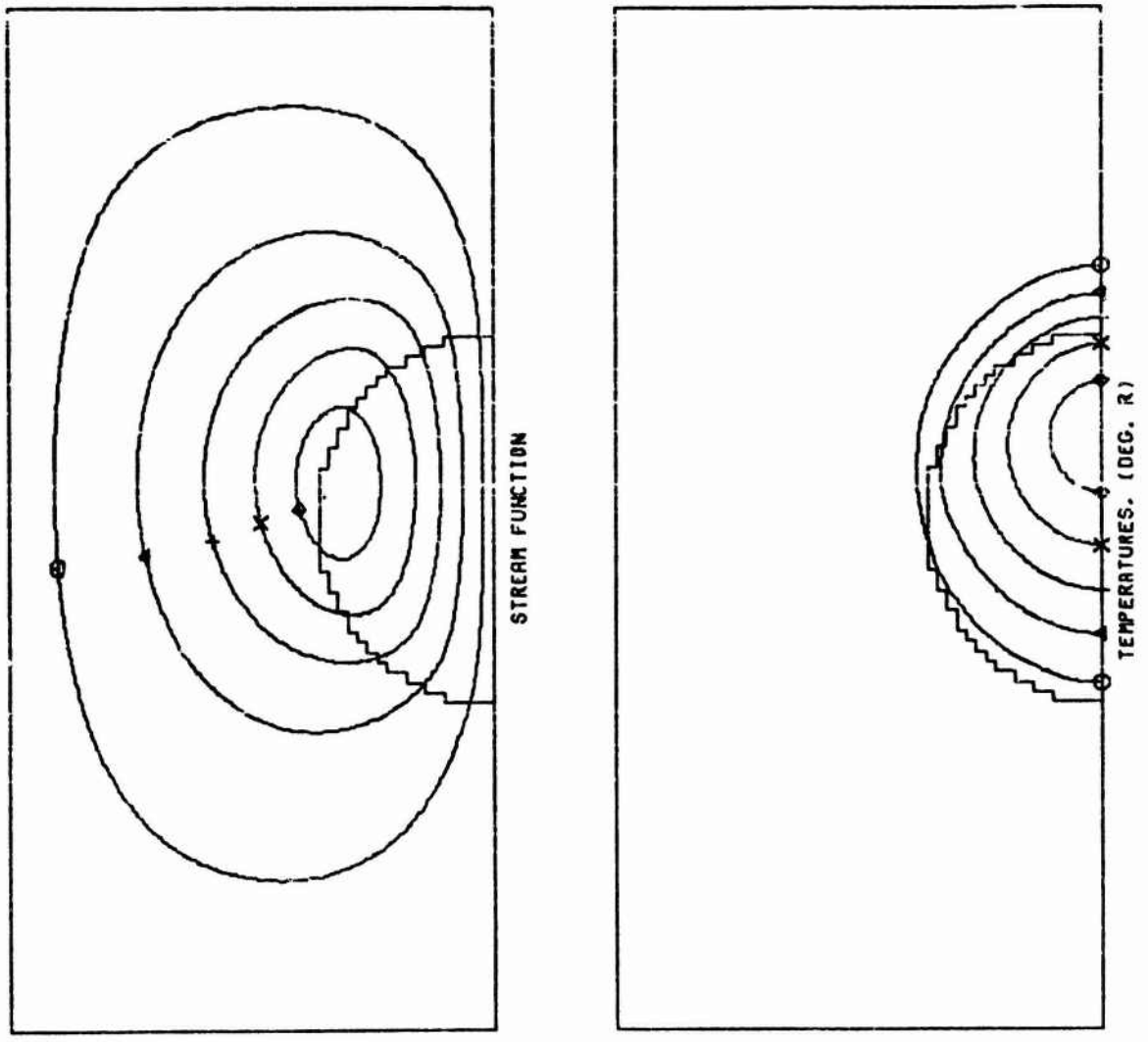

Stream Function (Non-dimensional)	Temperature (°R)	Symbol
24.6	562.7	Octagon
73.8	648.1	Triangle
123.0	733.5	+
172.2	818.5	X
221.4	904.2	Diamond

FIGURE 30: STREAM FUNCTION AND TEMPERATURE AT .301 SECONDS OF PROBLEM 3

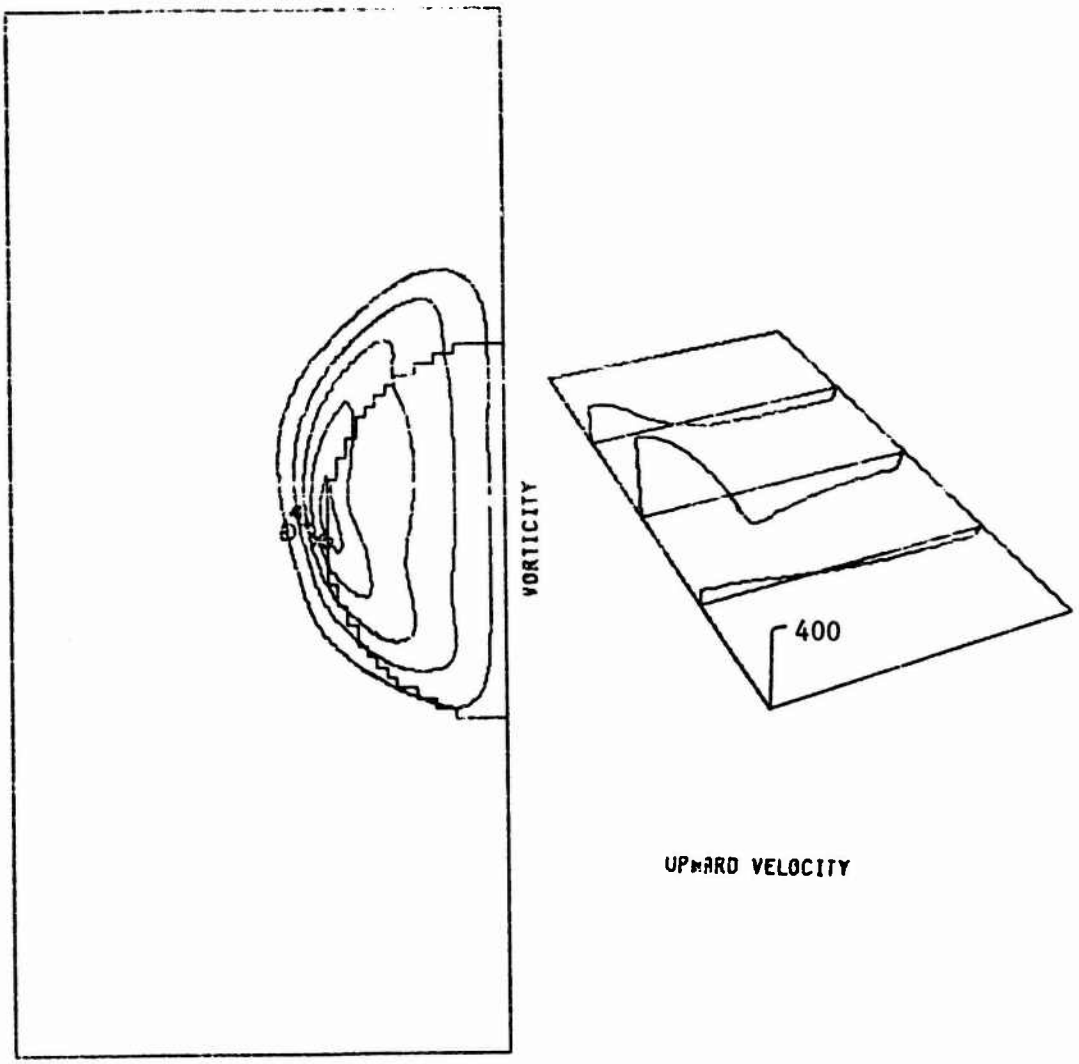

Vorticity (Non-dimensional)	Symbol
164.8	Octagon
494.8	Triangle
824.0	+
1153.6	X
1483.2	Diamond

FIGURE 31: VORTICITY AND UPWARD VELOCITY AT .301 SECONDS OF PROBLEM 3

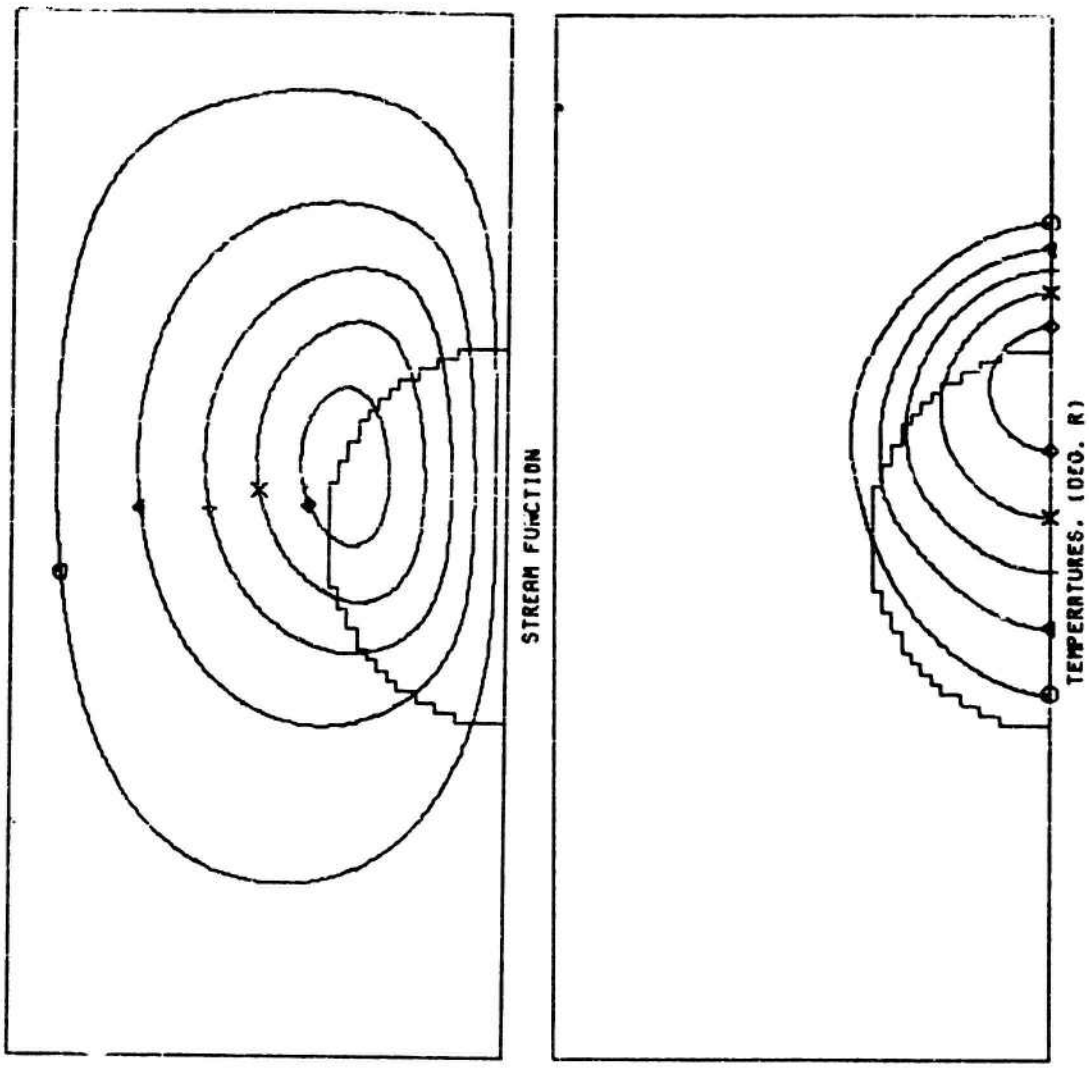

Stream Function (Non-dimensional)	Temperature (°R)	Symbol
35.7	565.6	Octagon
107.1	656.8	Triangle
178.5	748.0	+
249.9	839.2	X
321.3	930.4	Diamond

FIGURE 32: STREAM FUNCTION AND TEMPERATURE AT .385 SECONDS OF PROBLEM 3

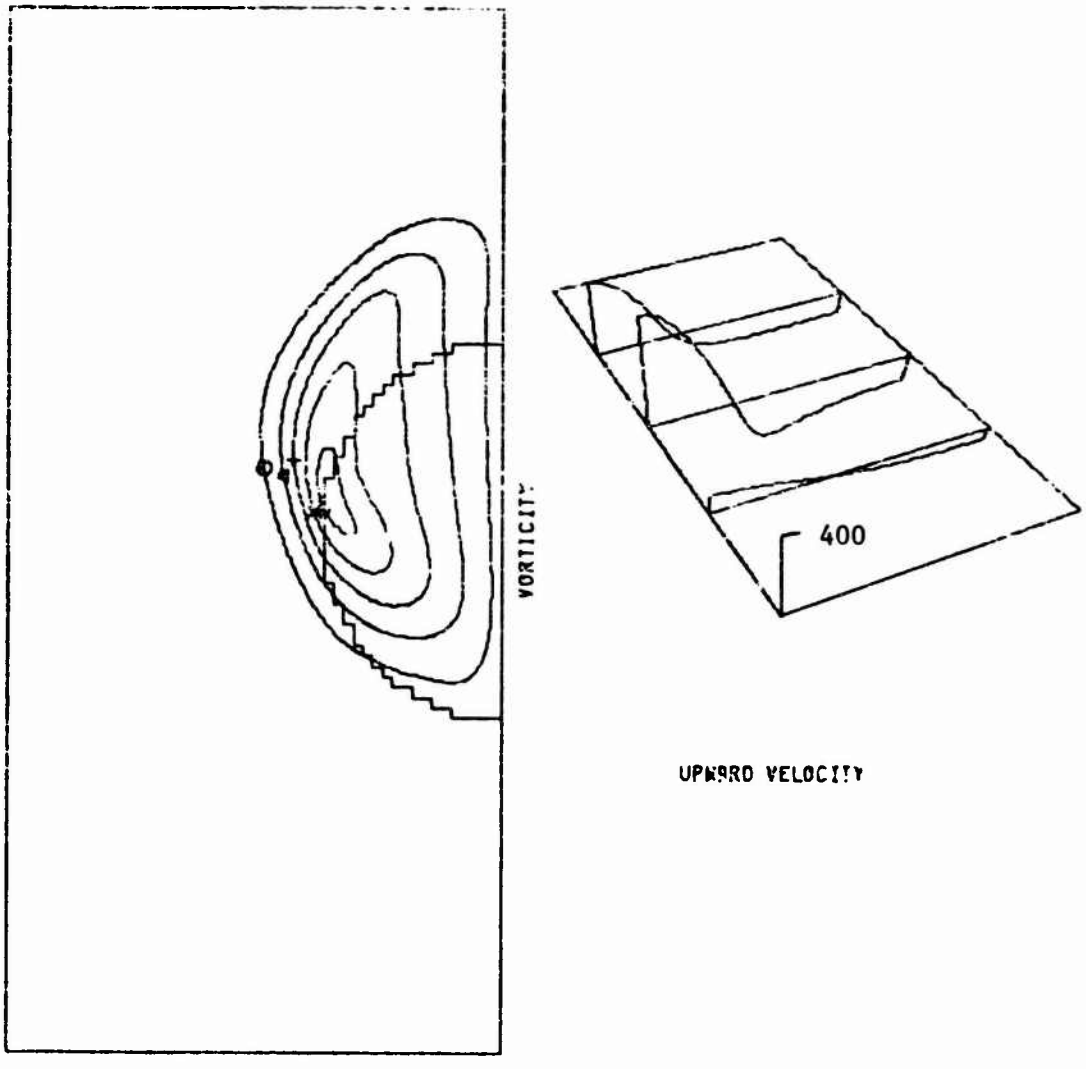

Vorticity (Non-dimensional)	Symbol
211.2	Octagon
633.6	Triangle
1056.0	+
1478.4	X
1900.8	Diamond

FIGURE 33: VORTICITY AND UPWARD VELOCITY AT .385 SECONDS OF PROBLEM 3

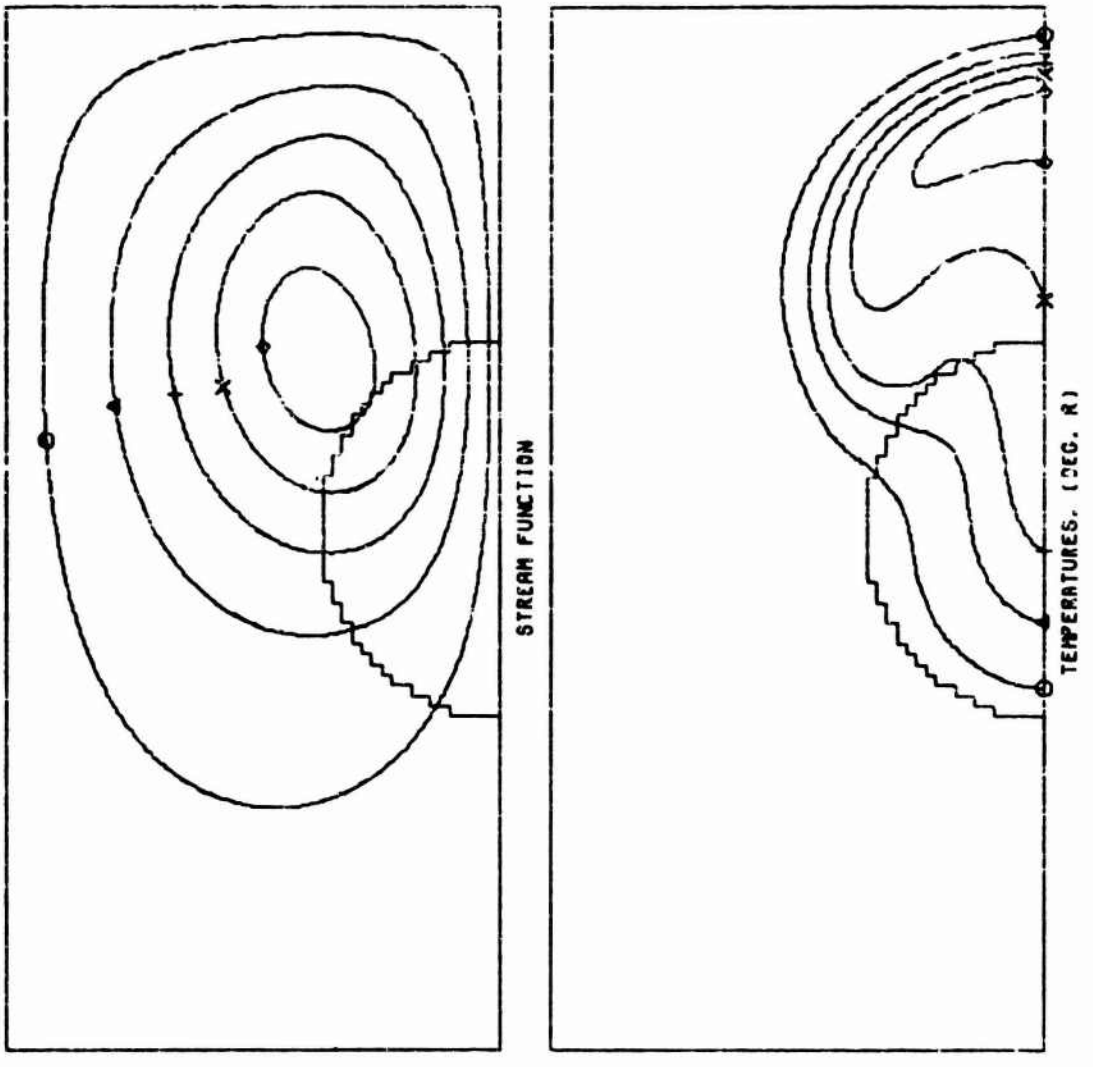

Stream Function (Non-dimensional)	Temperature (°R)	Symbol
63.2	560.1	Octagon
189.6	640.3	Triangle
316.0	720.5	+
442.4	800.6	X
568.8	880.8	Diamond

FIGURE 34: STREAM FUNCTION AND TEMPERATURE AT .601 SECONDS OF PROBLEM 3

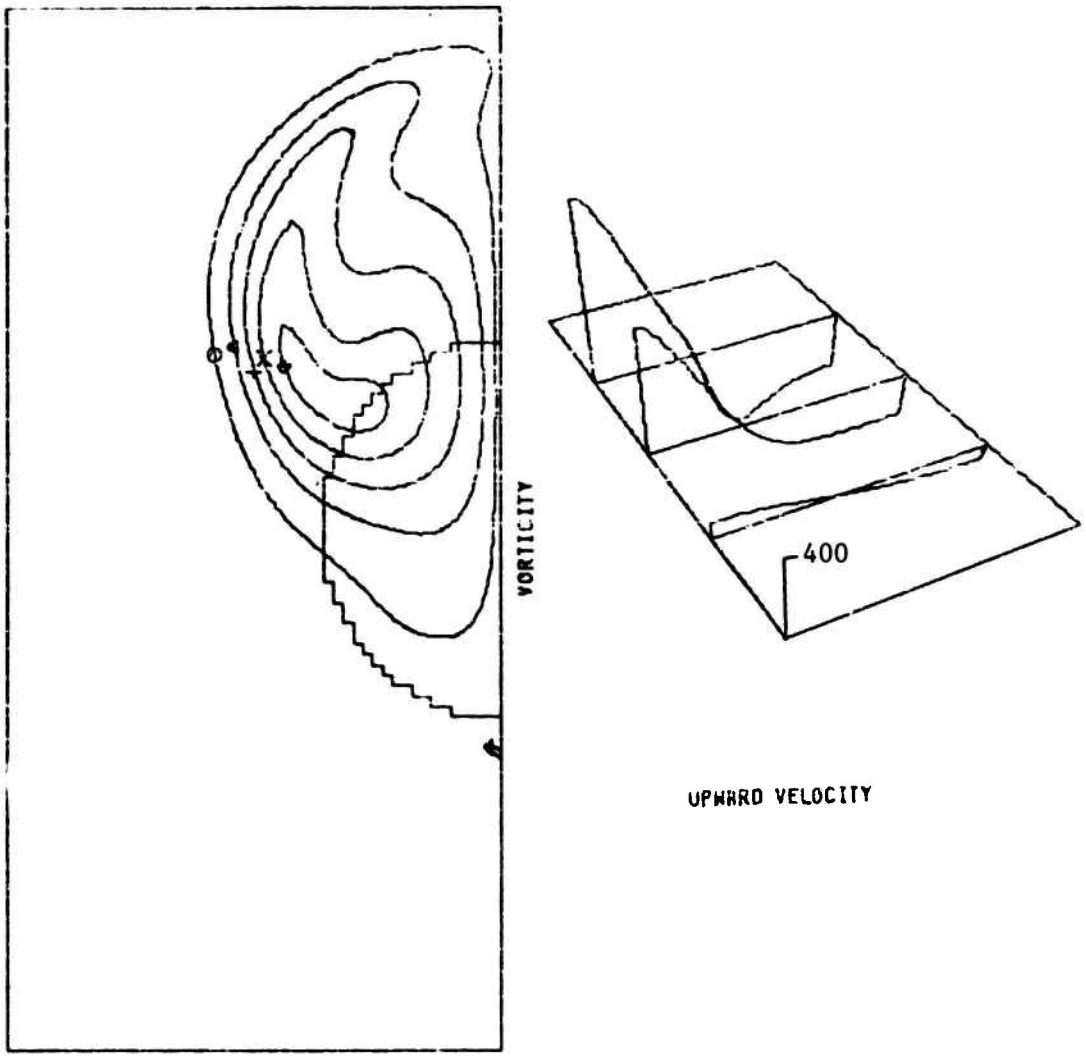

Vorticity (Non-dimensional)	Symbol
259.7	Octagon
779.1	Triangle
1298.5	+
1817.9	X
2337.3	Diamond

FIGURE 35: VORTICITY AND UPWARD VELOCITY AT .601 SECONDS OF PROBLEM 3

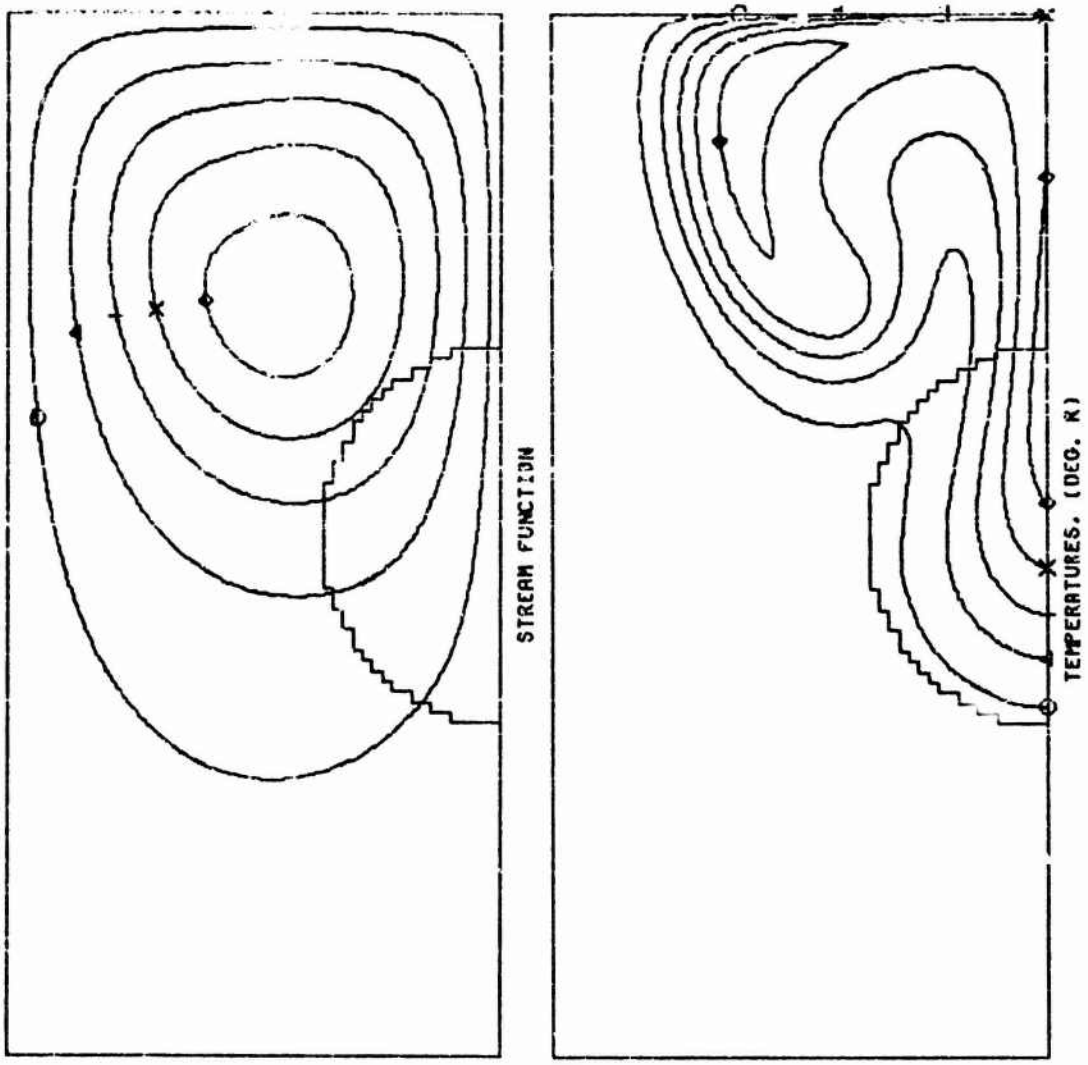

Stream Function (Non-dimensional)	Temperature (°R)	Symbol
76.0	550.8	Octagon
228.0	612.5	Triangle
380.0	674.2	+
532.0	735.9	X
684.0	797.5	Diamond

FIGURE 36: STREAM FUNCTION AND TEMPERATURE AT .801 SECONDS OF PROBLEM 3

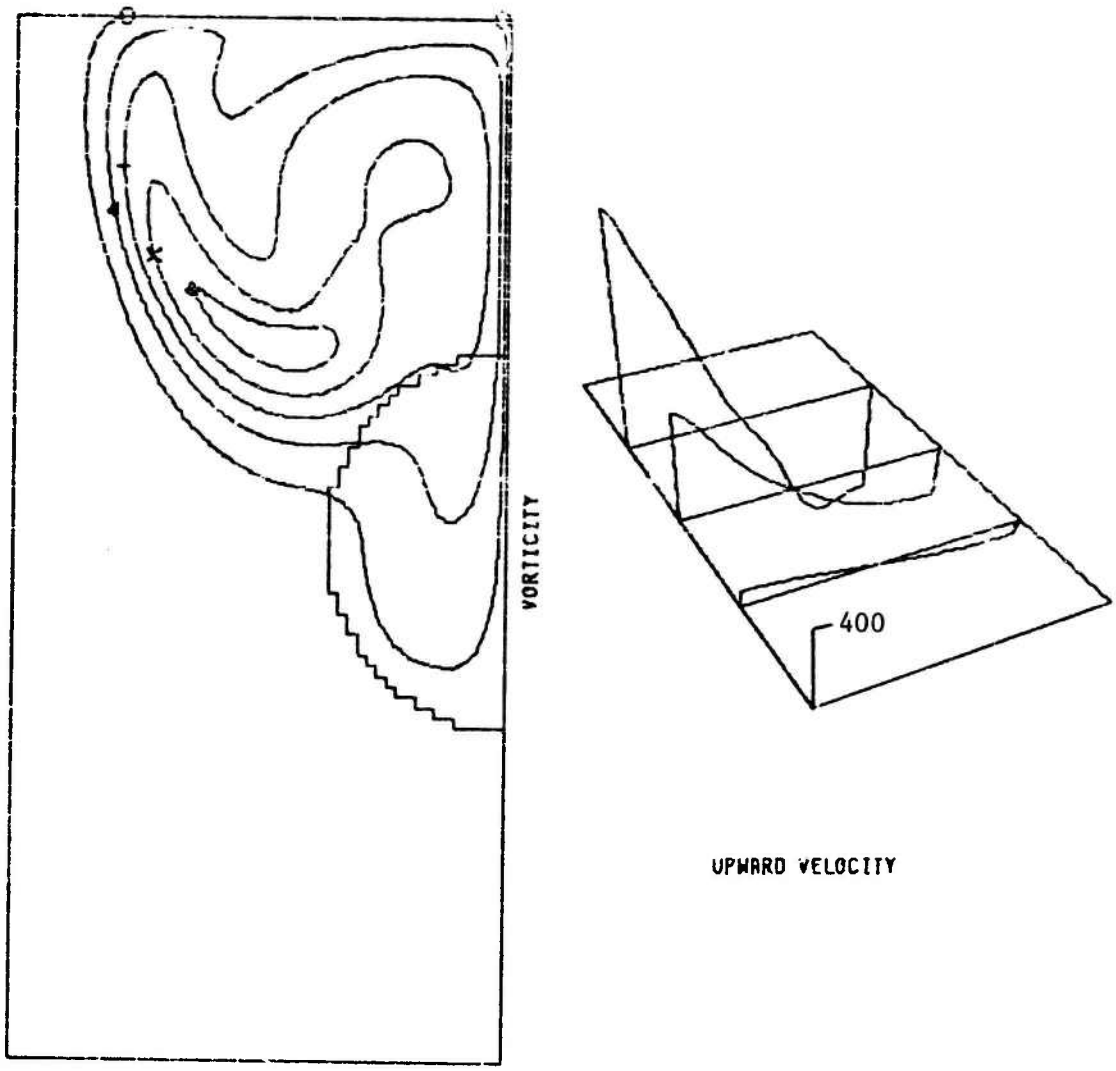

Vorticity (Non-dimensional)	Symbol
245.9	Octagon
737.7	Triangle
1229.5	+
1721.3	X
2213.1	Diamond

FIGURE 37: VORTICITY AND UPWARD VELOCITY AT .801 SECONDS OF PROBLEM 3

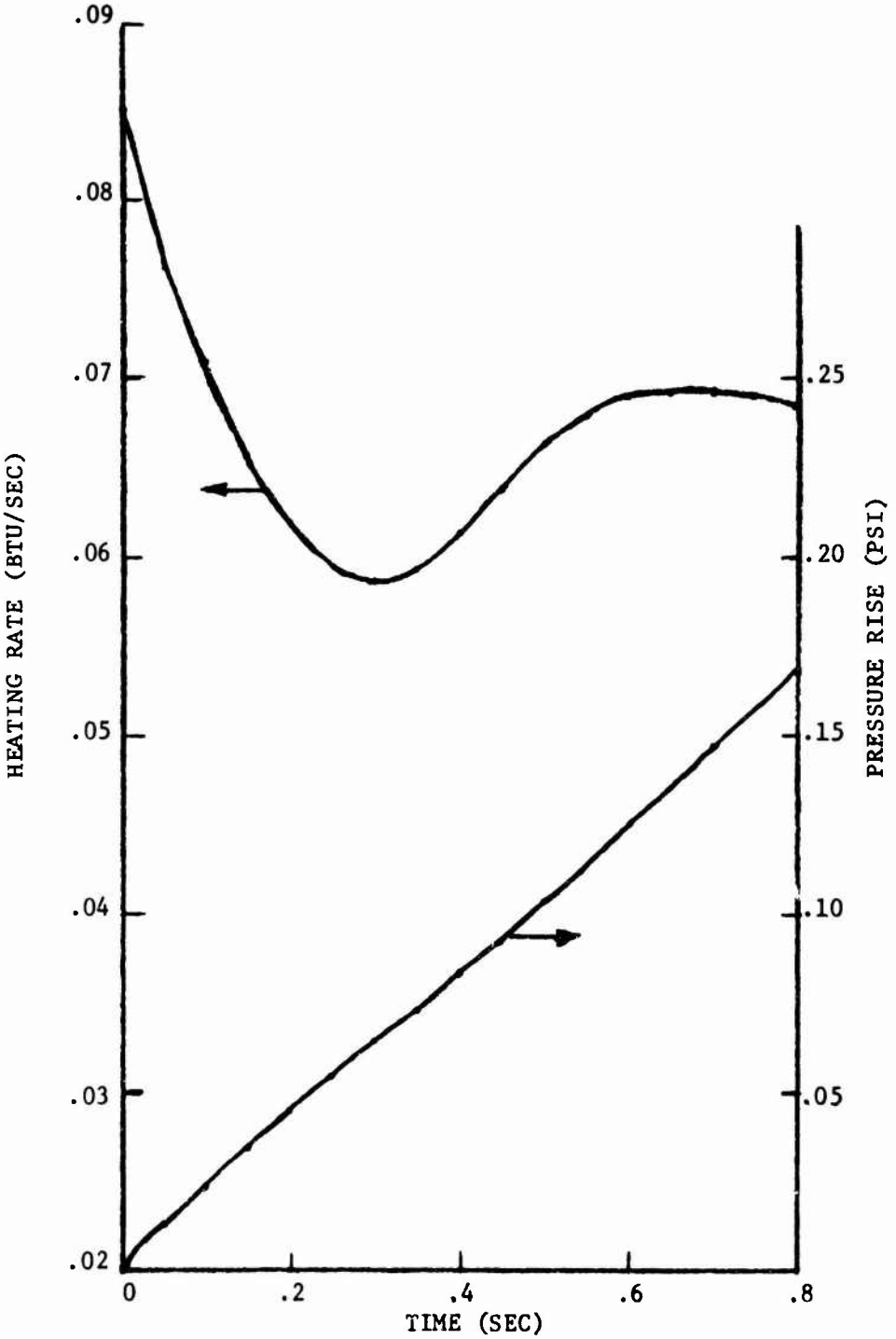

FIGURE 38: HEATING RATE & PRESSURE RISE - SAMPLE PROBLEM NUMBER 3

E. SAMPLE PROBLEM NO. 4

This sample problem is the same as sample problem 2, except that the beam radius has been reduced to 0.5 inches. The beam power has also been reduced in order to maintain the same intensity as in problem 2, and the beam power distribution is "flattop". The actual power and total beam area used in these calculations were 6782.8 watts and .85? sq. inches, respectively. This resulted in an intensity of 1226.2 watts/sq. cm.

At .151 seconds (Figures 39 and 40) the maximum temperature (654°R) is nearly the same as the maximum temperature of problem 2 at .151 seconds. A very simple calculation of the temperature rise of the gas being irradiated was made. This calculation assumed no heat loss, a heating time of .151 seconds, a heating rate which is based upon an average of the heating rates at 0, .05, .1, and .15 seconds, and the gas density at 587°R (one-half the anticipated rise). This simple calculation yielded a temperature rise within five degrees of that calculated by the program. Thus, it appears that very little heat loss from the hottest region of the heated area has occurred at .15 seconds.

At .244 seconds (Figures 41 and 42) the maximum temperature of 712°R was attained. As in all examples, this maximum value occurred near the intersection of the upper portion of the beam with the line of symmetry. Reducing the size of the beam while maintaining intensity resulted in a decrease of approximately 110°R in the maximum temperature attained. Also, this maximum temperature occurred much sooner with the small beam. For approximately the first .15-.20 seconds, the maximum temperature values in problems 2 and 4 are nearly the same.

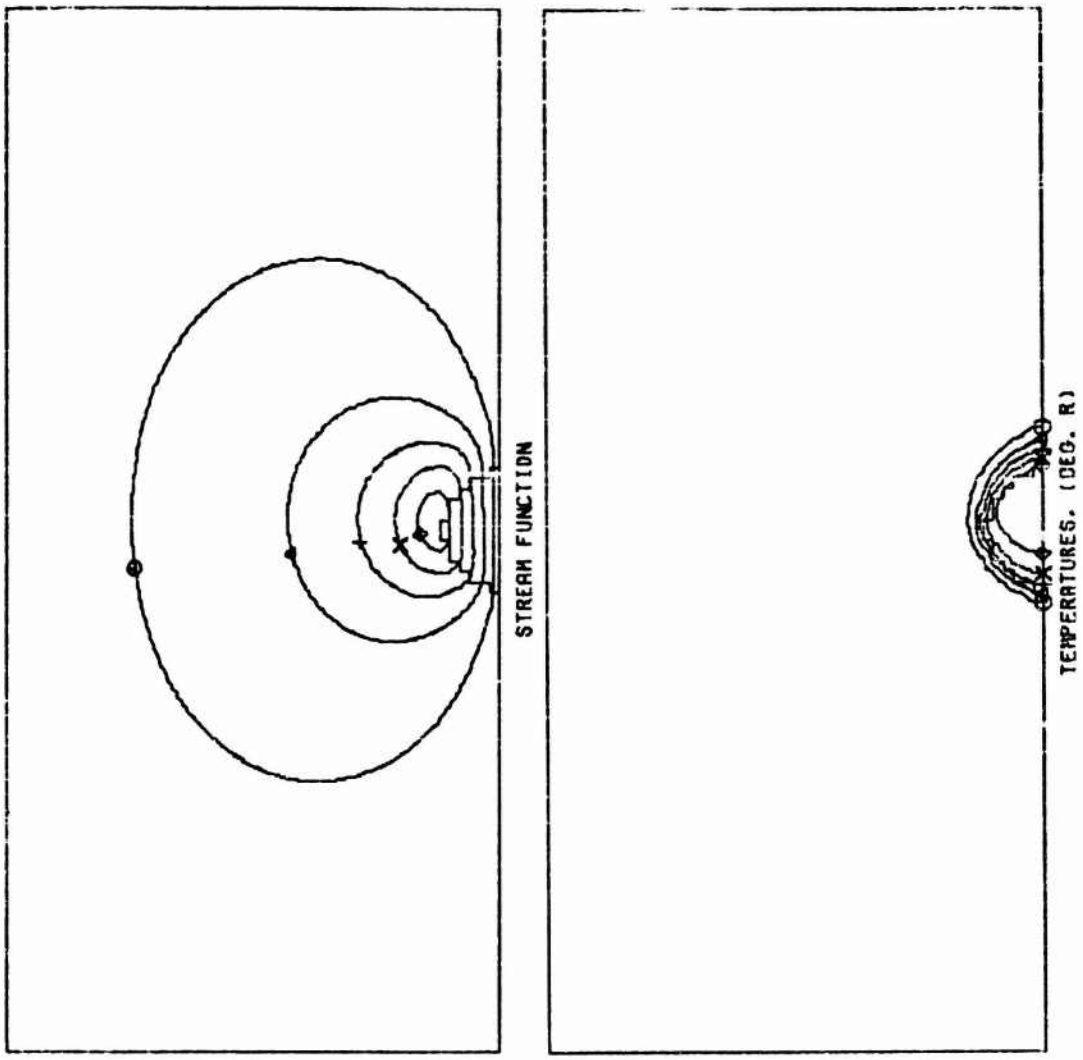

Stream Function (Non-dimensional)	Temperature (°R)	Symbol
5.0	533.4	Octagon
15.0	560.2	Triangle
25.0	587.1	+
35.0	613.9	X
45.0	640.7	Diamond

FIGURE 39: STREAM FUNCTION AND TEMPERATURE AT .151 SECONDS OF PROBLEM 4

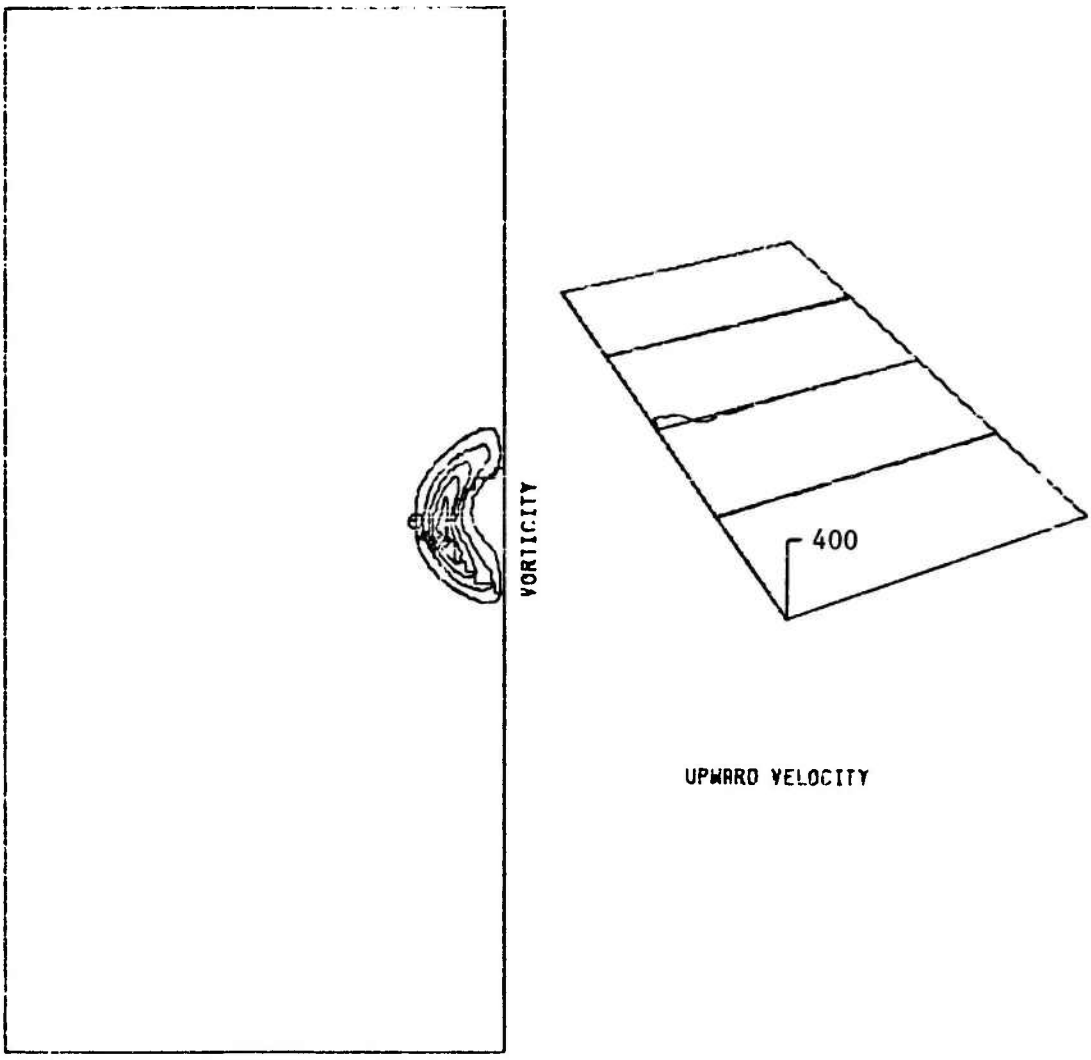

Vorticity (Non-dimensional)	Symbol
23.9	Octagon
71.7	Triangle
119.5	+
167.3	X
215.1	Diamond

FIGURE 40: VORTICITY AND UPWARD VELOCITY AT .151 SECONDS OF PROBLEM 4

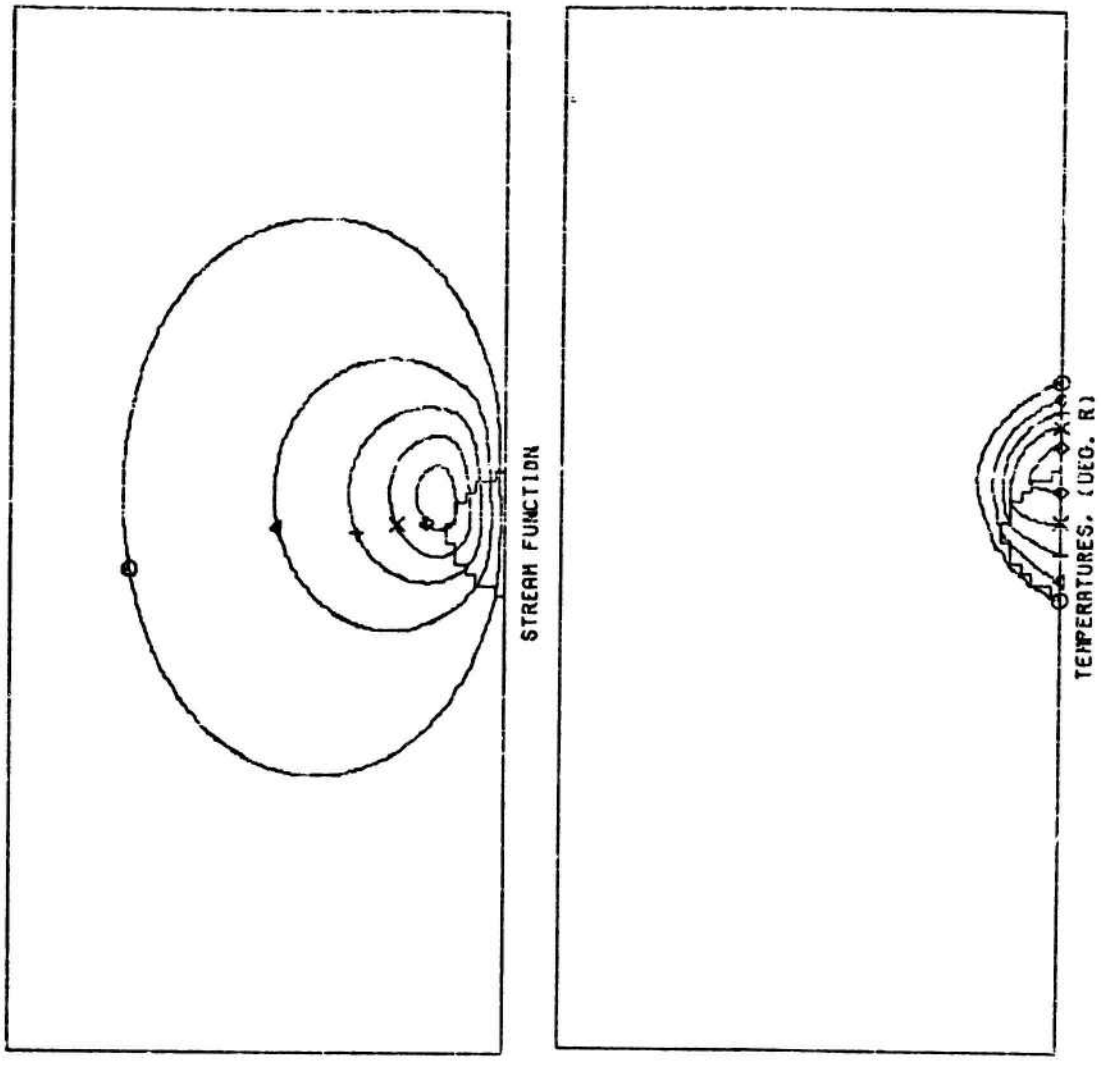

Stream Function (Non-dimensional)	Temperature (°R)	Symbol
10.7	539.2	Octagon
32.1	577.6	Triangle
53.5	615.9	+
74.9	654.3	X
96.3	692.7	Diamond

FIGURE 41: STREAM FUNCTION AND TEMPERATURE AT .245 SECONDS OF PROBLEM 4

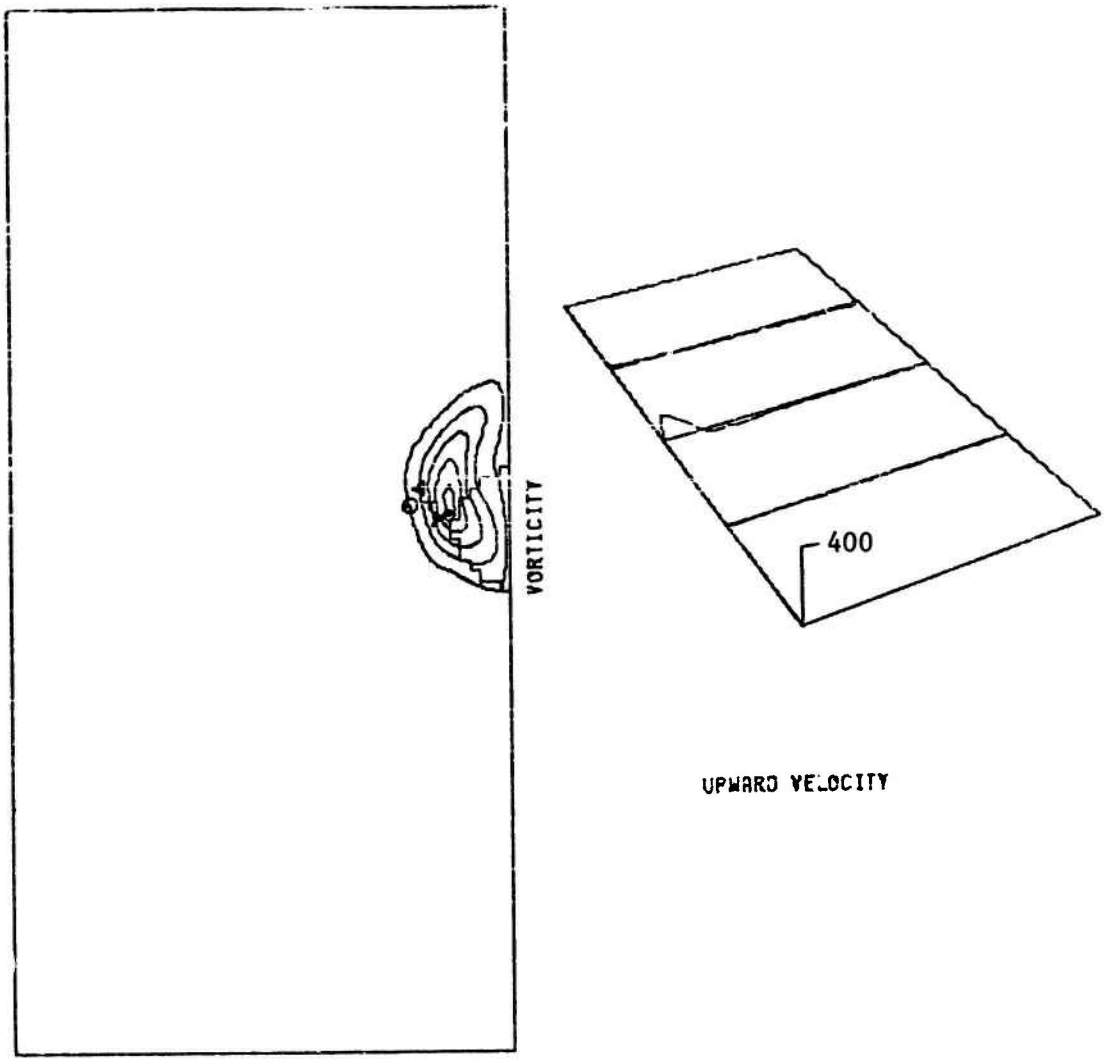

Vorticity (Non-dimensional)	Symbol
38.5	Octagon
115.5	Triangle
192.5	+
269.5	X
346.5	Diamond

FIGURE 42: VORTICITY AND UPWARD VELOCITY AT .245 SECONDS OF PROBLEM 4

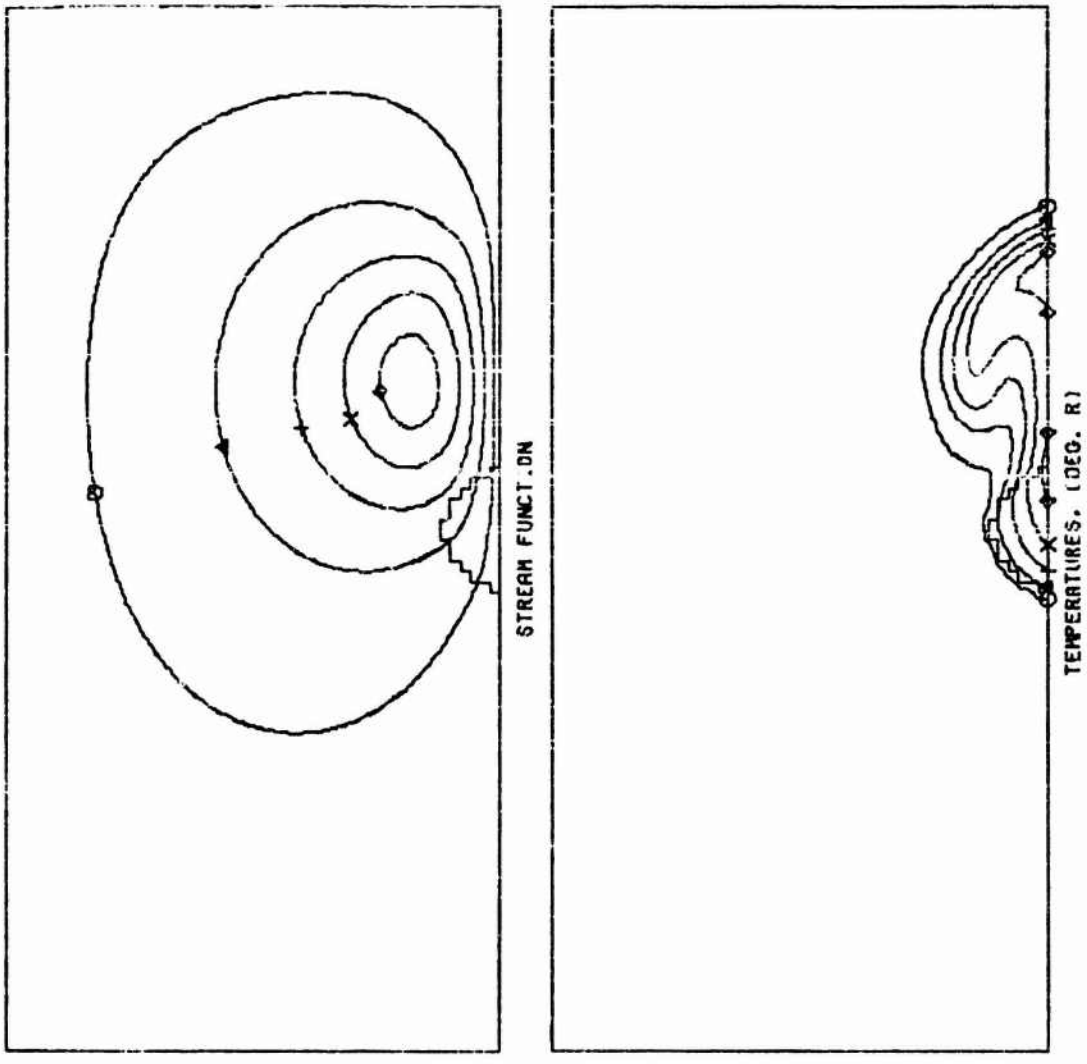

Stream Function (Non-dimensional)	Temperature (°R)	Symbol
23.2	533.0	Octagon
69.6	559.0	Triangle
116.0	585.0	+
162.4	611.0	X
208.8	637.0	Diamond

FIGURE 43: STREAM FUNCTION AND TEMPERATURE AT .451 SECONDS OF PROBLEM 4

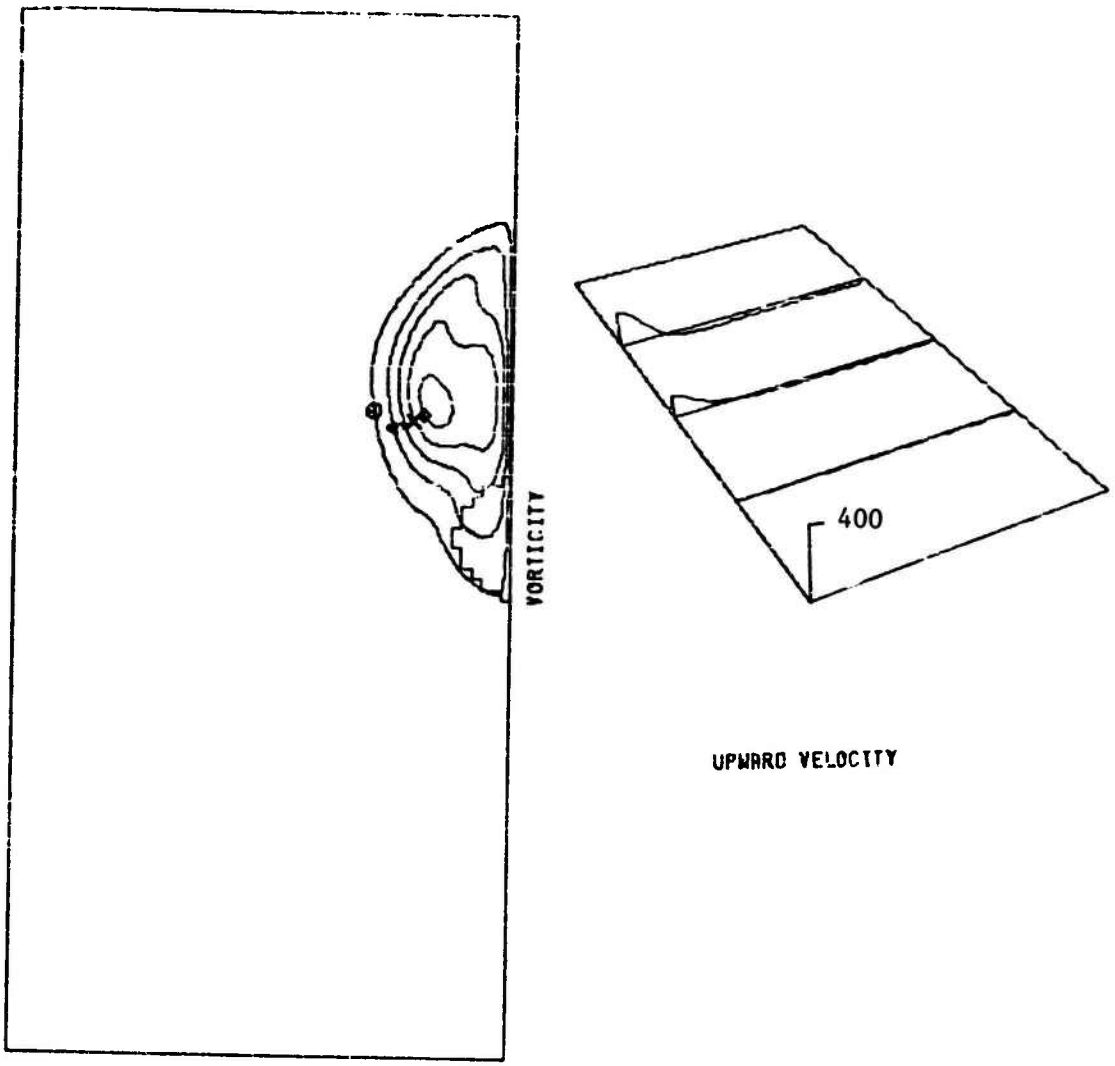

Vorticity (Non-dimensional)	Symbol
34.6	Octagon
103.8	Triangle
173.0	+
242.2	X
311.4	Diamond

FIGURE 44: VORTICITY AND UPWARD VELOCITY AT .451 SECONDS OF PROBLEM 4

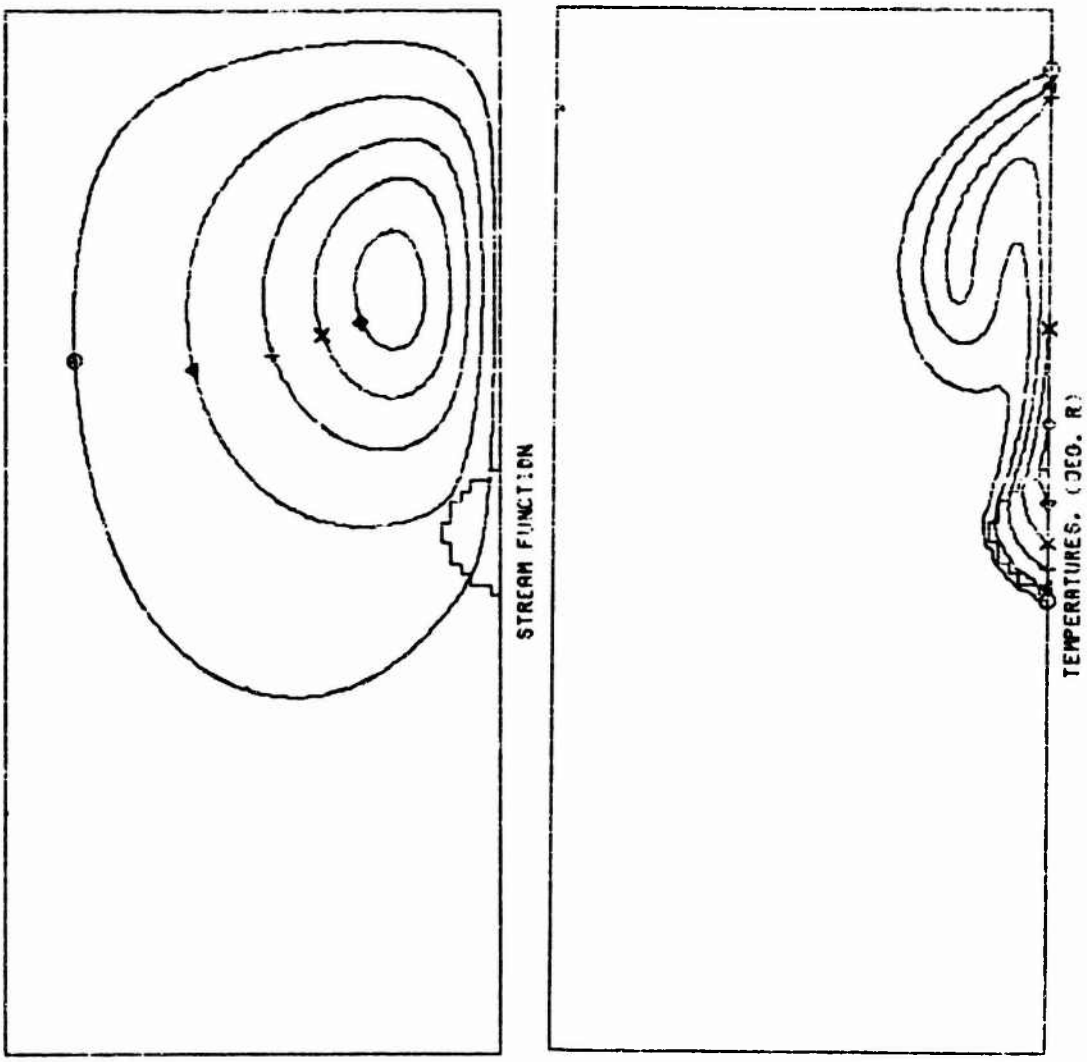

Stream Function (Non-dimensional)	Temperature (°R)	Symbol
30.7	534.5	Octagon
92.1	563.5	Triangle
153.5	592.5	+
214.9	621.6	X
276.3	650.6	Diamond

FIGURE 45: STREAM FUNCTION AND TEMPERATURE AT .601 SECONDS OF PROBLEM 4

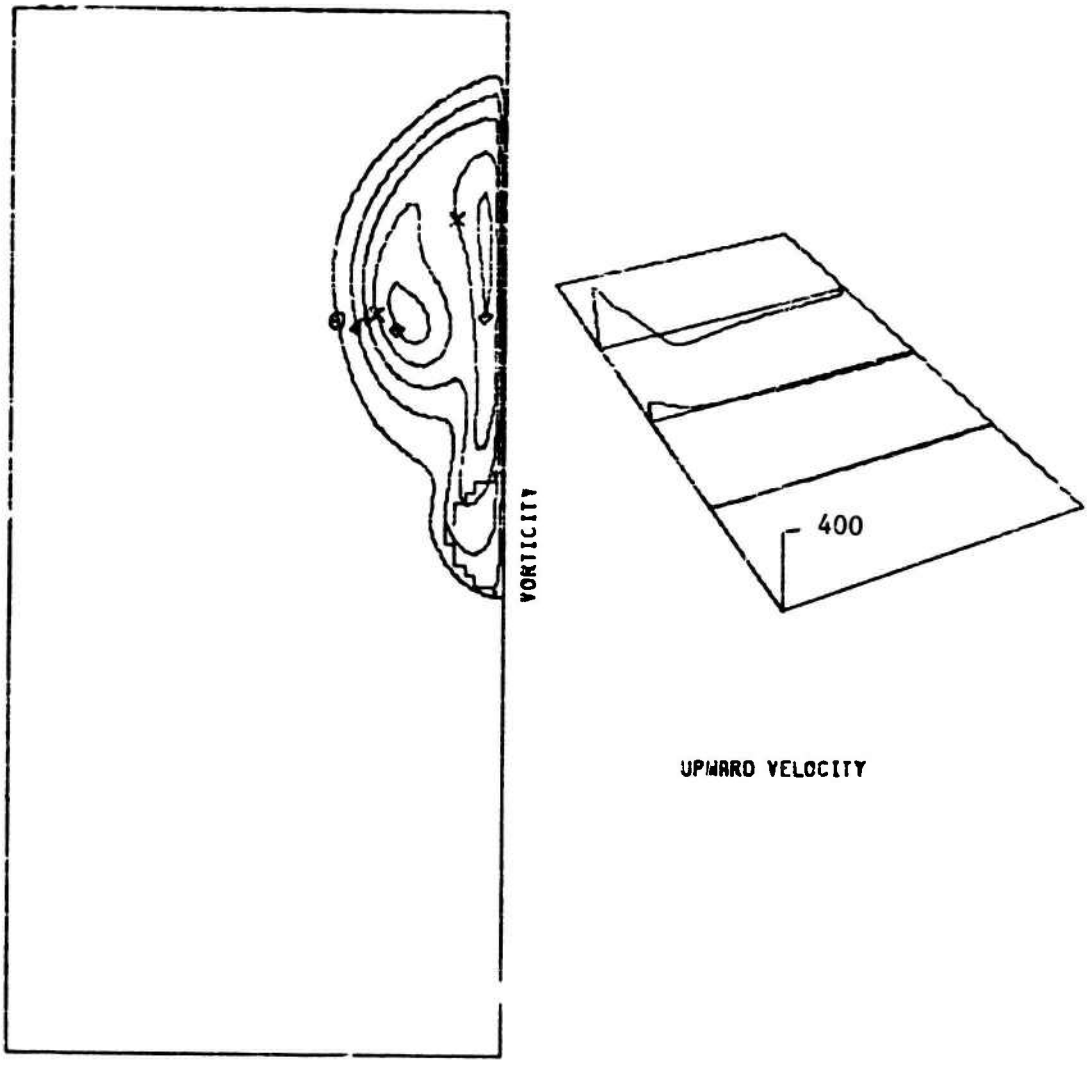

Vorticity (Non-dimensional)	Symbol
31.3	Octagon
93.9	Triangle
156.5	+
219.1	X
281.7	Diamond

FIGURE 46: VORTICITY AND UPWARD VELOCITY AT .601 SECONDS OF PROBLEM 4

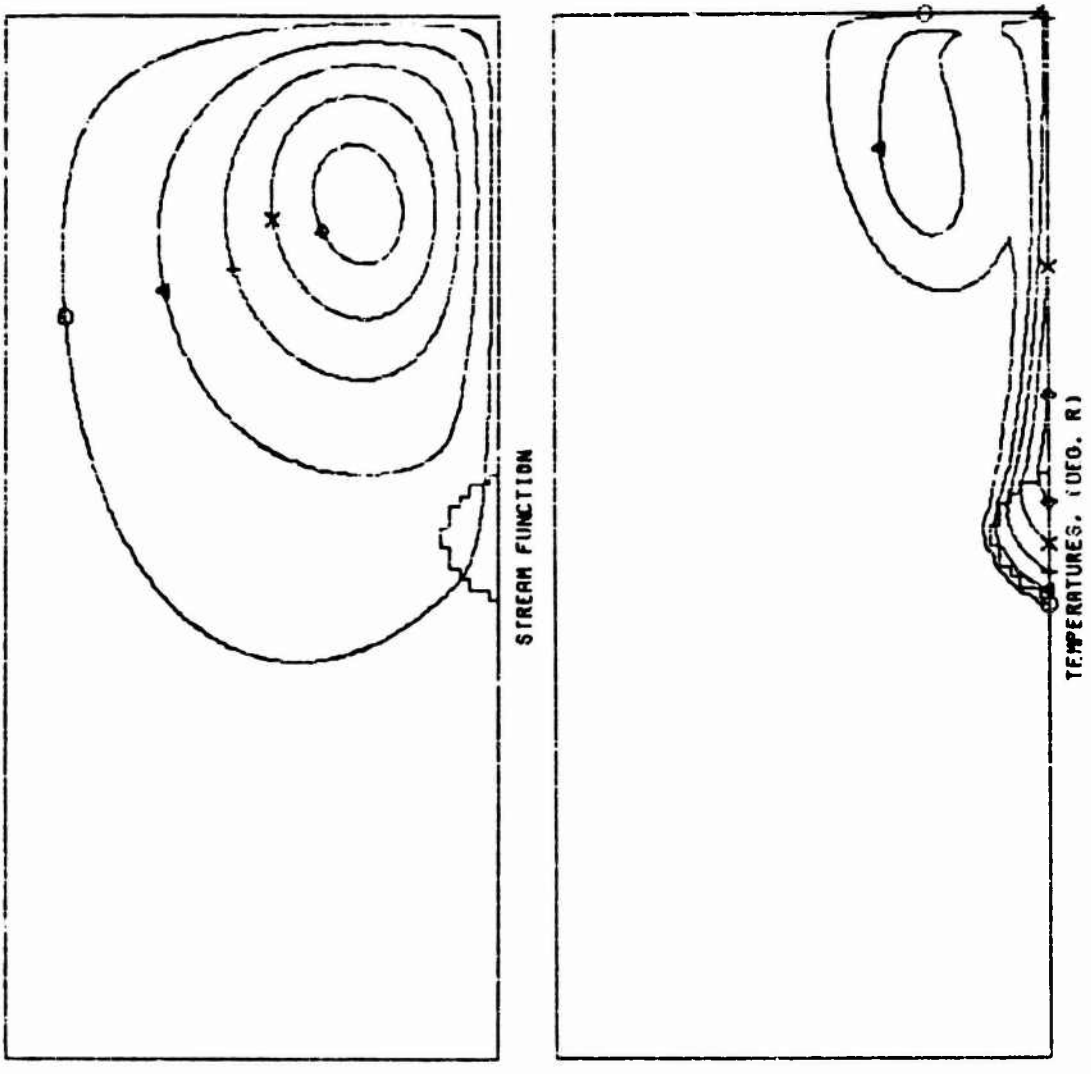

Stream Function (Non-dimensional)	Temperature (°R)	Symbol
38.3	535.1	Octagon
114.9	565.2	Triangle
191.5	595.4	+
268.1	625.6	X
344.7	655.7	Diamond

FIGURE 47. STREAM FUNCTION AND TEMPERATURE AT .801 SECONDS OF PROBLEM 4

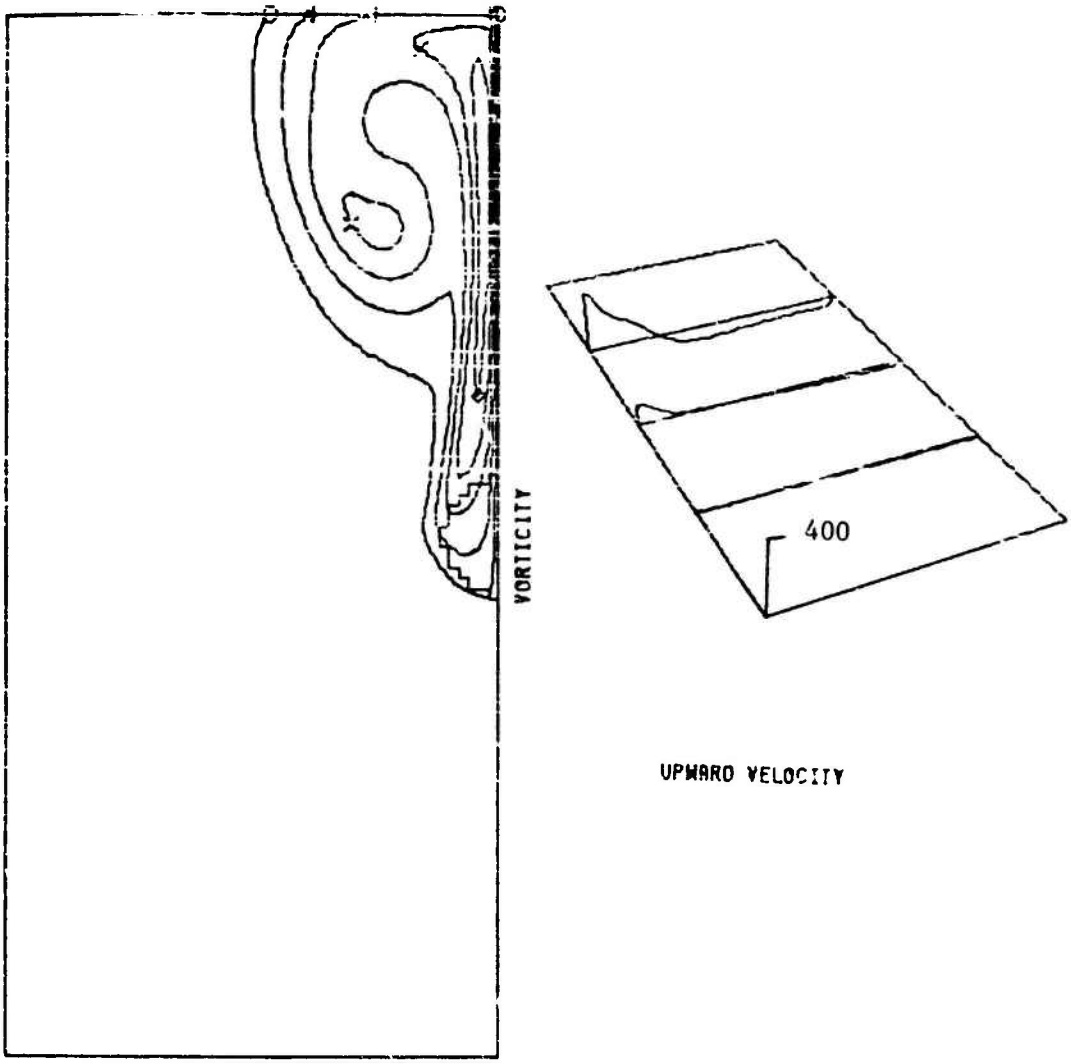

Vorticity (Non-dimensional)	Symbol
35.3	Octagon
105.9	Triangle
176.5	+
247.1	X
317.7	Diamond

FIGURE 48: VORTICITY AND UPWARD VELOCITY AT .801 SECONDS OF PROBLEM 4

However, after .244 seconds the maximum temperatures for the problem with the large beam continue increasing for an additional .15 seconds, while the maximum temperatures for the small beam problem decrease. The upward velocities are very low and slowly developed for the small beam.

At .451 seconds (Figures 43 and 44) the characteristic mushroom cloud shape is forming. The temperatures in the beam area have decreased by a considerable amount. After this time, the temperatures in the beam area gradually increase at a steadily decreasing rate. The ratios of the total beam power and area for problems 2 and 4 are the same, .1178. The ratio of the initial heating rates is also .1178, and the final heating rate ratio, which is approximately steady-state, is also .1178.

V. CONCLUSIONS, APPLICATIONS, AND RECOMMENDATIONS FOR IMPROVEMENT

A. CONCLUSIONS

The computer model described in this report produces results which appear reasonable and reliable for a two-dimensional heating model. However, experimental verification has not been accomplished. Due to inaccuracies and estimations in some of the input parameters and assumptions, exact agreement with experimental results cannot be expected. Some of these inaccuracies and estimations will be discussed later. However, except for the effects of chemical changes/reactions in the gas mixture, the model should produce at least a preliminary estimation.

Based upon the results of the sample problems presented in this report, and other similar but unreported runs that were made,

it appears that the effects of convection are minimal during an initial heating period. The duration of this initial heating period is dependent upon such parameters as the beam area and intensity. During this heating period the primary mechanism by which the absorbed energy is removed from the heated region is conduction. For intensities and beam sizes such as the ones considered in the sample problems, conductive heat loss is negligible for the gas in the central portion of the heated area. However, once sufficient energy has been deposited and sufficient time has passed, the heated gas begins to rise rapidly enough to begin to remove itself from the beam area. It appears that the highest temperatures occur just before the initially heated gas is swept from the heated area. By this time, convection is the dominant mode of heat removal. Prior to this time of highest temperatures the gas has been becoming increasingly hotter, and therefore less dense. As this occurs, the heating rate correspondingly decreases, due to the decrease in the number of potentially absorbing molecules in the beam path. The heating rate is linearly proportional to the average density of the gas in the beam diameter. As the convection motion of the gas begins to remove the hot gas from the upper portions of the beam and supplies cooler gas from below the heated area, the average density in the beam area increases. This results in an increase in the heating rate. Eventually, a near steady-state condition within the beam area is established. Decreasing the acceleration of gravity retards this convective motion which then allows the initially heated gas to remain within the beam area for a longer time. This, of course, results in higher temperatures in the heated region. Increasing the viscosity of the gas mixture should

have a similar effect. The Gaussian power distribution results in higher temperatures near the center of the beam, as would be expected. And finally, decreasing the beam size (at constant intensity) results in less convective motion and increases the importance of conduction. However, due to the small beam size, much less convective motion is required to remove the hot gas from the beam path. The net effect of decreasing beam size at constant intensity is to reduce the temperature.

B. APPLICATIONS

This model can be used to determine how best to maximize or minimize the heating rate, total heat input, maximum temperature and the time required to attain it, pressure rise, and reduction in the laser beam power as it is transmitted through the gas. These studies may in turn be utilized to investigate such parameters as ignition of gases by laser radiation and propagation of high energy laser beams through the atmosphere, within lasing gases, and/or in absorbing gases. The gas mixture evaluated in this problem (3% pentane in air) is a highly flammable mixture. At some temperature in excess of 960°R, this mixture would be ignited. The exact temperature at which auto-ignition would occur is unknown. Perhaps this model, coupled with experimental results, could be used to determine this temperature. However, any such endeavor would require a careful examination of the potential chemical changes which may be occurring as the ignition temperature is approached. Also, the potential occurrence of photochemical effects must be investigated. As a part of any application of this model, the following variables should be investigated.

1. Initial pressure and temperature.
2. Beam parameters such as size, spatial power distribution,

and power. With very slight modifications, the beam shape or temporal power distribution (e.g., pulsed laser) can also be investigated.

3. The acceleration of gravity. This could be a variable for moving systems such as aircraft.
4. Various gas mixture constituents, as long as suitable physical property data can be obtained.
5. Size of the enclosure. This variable is probably not very important for short irradiation times, and the results should be applicable to non-enclosed (constant pressure) situations.
6. Initial motion of the gas. At the start of the irradiation, it may be possible (via modification of the program) to give the gas an initial upward or downward velocity. The initial horizontal velocity must be zero to be consistent with the original assumption of symmetry across the vertical centerline. This capability may be useful for flowing systems.
7. Location of the laser beam within the enclosure. The analysis described in this report assumes that the laser beam axis is coincident with the axis of the enclosure, and assumes that the enclosure has a square cross-section. If the laser beam is displaced vertically, the program can be easily modified to account for this. If the laser beam is displaced horizontally, the assumption of symmetry about a central vertical plane is destroyed, and major changes in the program will be required. It is anticipated that

moving the beam closer to the walls will reduce convective motion and thereby affect the heating and temperature distribution of the gas mixture. The effects of the walls should increase as the beam is brought closer to the walls and should also increase with irradiation time.

C. RECOMMENDATIONS FOR IMPROVEMENT

Potential thermally induced chemical effects and photochemical effects must be considered. These are very briefly discussed in Section I. If the absorbed energy does not quickly manifest itself as an increase in the translational motion (temperatures) of all the molecules in the beam area, then these effects may be significant. Also, if the absorbed energy causes some chemical change in the absorbing molecules, or increases their reactivity independent of temperature, then this must also be considered. Finally, as the gas becomes heated, certain chemical reactions may begin to occur which release energy and change the chemical composition and physical properties of the gas mixture. When this is of concern, it may be possible to couple some chemical kinetic model with this heat transfer model.

Another improvement which would be of value involves a more accurate approximation of the absorption coefficient. For some gases, the absorption coefficient may be a strong function of the total absolute pressure, the partial pressure of each constituent in the mixture, and the temperature. These variations of the absorption coefficient are in addition to the dependence on density. Only the effect of density on absorption coefficient is evaluated in this model. Finally, variations of thermal conductivity, viscosity, and specific heat with temperature could be incorporated into this model.

REFERENCES

1. Capt R. J. Skaar, Analysis of the Thermal Response of a Hydrocarbon Fuel When Subjected to a High Intensity Laser, Air Force Institute of Technology, Wright-Patterson AFB, Ohio, GAW/MC/74-9, March 1974.
2. J. O. Wilkes and S. W. Churchill, "The Finite-Difference Computation of Natural Convection in a Rectangular Enclosure," A.I. Ch. E. Journal, 12, No. 1 (January 1966), page 161.
3. K. Mach, An Analytical Study of Subsonic Inviscid Flow in Diffusers and Ducts of Varying Cross Section, Ph.D. Dissertation, Ohio State University, 1971.
4. R. Bird, W. Stewart, and E. Lightfoot, Transport Phenomena, John Wiley & Sons, Inc., New York, 1960.
5. P. J. Roache, Computational Fluid Dynamics, Hermosa Publishers, Albuquerque, New Mexico, 1972.

APPENDIX 1 - LIST OF TERMS

c = specific heat at constant pressure (Btu/lbm°R)

g = acceleration of gravity (ft/sec^2)

I = local beam intensity or power density ($watts/cm^2$)

k = thermal conductivity

L = width of enclosure

m = mass of gas in the enclosure

M = molecular weight

n = mole fraction

N_{PR} = Prandtl number = $\frac{\mu c}{k}$

N = number of components in gas mixture

P = pressure (psi)

q = volumetric heating rate (Btu/sec) of element

Q = non-dimensional volumetric heating rate = $\frac{q}{\rho c} \frac{r^2}{\nu \theta_o}$

r = beam radius

R = universal gas constant

T = non-dimensional temperature = $\frac{\theta}{\theta_o} - 1$

t = time after irradiation has begun

u = velocity in upward direction

U = non-dimensional upward density = $\frac{ur}{\nu} = \frac{\partial \psi}{\partial Y}$

v = horizontal velocity

V = non-dimensional horizontal velocity = $\frac{vr}{\nu} = -\frac{\partial \psi}{\partial X}$

X = non-dimensional vertical coordinate = $\frac{x}{r}$

Y = non-dimensional horizontal coordinate = $\frac{y}{r}$

α = absorption coefficient (cm^{-1})

ζ = dimensionless vorticity = $-\nabla^2 \psi$

θ = temperature

$\bar{\theta}$ = mass average temperature of gas in the enclosure

ν = kinematic viscosity

μ = viscosity

ρ = density (lbm/ft^3)

$\bar{\rho}$ = average density within the enclosure

ρ_o = initial density within the enclosure ($\rho_o = \bar{\rho}$)

τ = dimensionless time = $\frac{t\nu}{r^2}$

γ = dummy variable, analogous to time

ϕ = dimensionless density = $\frac{\rho}{\rho_o}$

ψ = dimensionless stream function

Subscript o refers to initial conditions

APPENDIX 2 - PROGRAM LISTING

```
      PROGRAM LSPM(INPUT,OUTPUT,TAPE 5=INPUT,TAPE 6=OUTPUT,PLOT)
      DIMENSION R(101),AL(101),PTIME(10)
      COMMON //  HOI(10),ALPHA(10),COMBI(10),W(10),COND(10),CP(10),
     1        NAME(10,2),EMU(10),VNU (10),RX(120),RY(120),
     2 UN(101,51),VN(101,51),TN(101,51),RHON(101,51),
     3 PN(101,51),TF(101,51),VORTP(101,51),VORT(101,51),SI(101,51)
      LOGICAL UNUSED(101,51)
      EQUIVALENCE (UNUSED(1,1),PN(1,1))
      DIMENSION  PX(101), PY(51)
      DIMENSION TA(6),TD(6),SC(6),UNC(6),ZC(6),MARKER(6)
      COMMON/CNL/ DELNSR,GAM,CP,BB,B,AL
      DIMENSION IUN(10)
      DATA IUN,ITN / 3,20,50,75,7*1/
      DATA MARKER  / "OCTAGON","TRIANGLE","+","X","DIAMOND",
     1 "PINE TREE" /
      DATA SC(6),UNC(6),ZC(6) / 3*0.0 /
      DATA PTIME/.1002,.2002,.4002,.6002,.8002,.9999,4*2.0/
C    PTIME VALUES SHOULD BE SLIGHTLY SMALLER THAN DESIRED PRINT-OUT TIMES
      READ(5,10) T0,POWER,RA,DELT,PO,N,DEL,S,TIME
   10 FORMAT (F8.0,F8.0,F8.2,F8.4,F8.2,I8,F8.4,F8.2,F8.1)
C     MULTIPLY POWER BY 1.132 TO GET SAME POWER FOR TRUNCATED GAUSSIAN
C        BEAM AS FOR FLATTOP
      WRITE(6,25)T0,POWER,RA,DELT,PO,N,DEL,S,TIME
   25 FORMAT (1H1,29HINITIAL TEMPERATURE (DEG. R)-,16X,F8.1/15H POWER (W
     1ATTS)-,29X,F9.1/22H BEAM RADIUS (INCHES)-,24X,F7.2/22H TIME INTERV
     2AL (SEC.)-,27X,F7.2/22H INITIAL PRESSURE (PSIA)-,21X,F7.2/22H NUMB
     3ER OF COMPONENTS-,29X,I3/22H GRID DIMENSIONS (INCHES)-,24X,F7.5/22H
     4 GRID SIZE (INCHES)-,26X,F7.2/22H BEAM DURATION (SEC.)-,24X,F7.2)
C   DEL MUST BE .GT. . 1*S
      WRITE(6,40)
   40 FORMAT (///2X,12HELEMENT NAME,5X,7HDENSITY,4X,10HABSORPTION,5X,7HT
     1HERMAL,6X, 9HMOLECULAR,5X,13HCONCENTRATION,5X,9HKINEMATIC,5X,13HSPE
     2CIFIC HEAT/20X,36H  COEFFICIENT  CONDUCTIVITY      WEIGHT,24X,9HVISCO
     3SITY/14X,11H(LB/CU FT),2X,8H(1/CM),5X,15H(BTU/HR-FT-DEG),15X,15H(V
     4OLUME PERCENT),3X,11H(SQ FT/SEC),5X,12H(BTU/LB-DEG)/20X,15HPER PSI
     5 PERCENT)
```

```
      DO 70 M=1,N
      READ(5,50)(NAME(M,J),J=1,2),RHOI(M),ALPHA(M),CONDI(M),W(M),CONC(M)
     1,VMUE(M),CP(M)
   50 FORMAT (A1 ,A7,7F8.0)
   60 WRITE(6,65) (NAME(M,J),J=1,2),RHOI(M),ALPHA(M),CONDI(M),W(M),CONC(
     1M),VMUE(M),CP(M)
   65 FORMAT (1H ,A1 ,A7,F8.5,3X,F9.7,3X,F7.5,5X,F8.3,7X,F7.4,10X,F .6,
     1 8X,F8.5)
   70 CONTINUE
      GRAV=32.2
      F=32.77
C***CALCULATE AVERAGE PROPERTIES***
      AVRHO=0.
      AVALPH=0.
      AVCON=0.
      AVW=0.
      AVMUE=0.
      VCP=0.
      AVMU=0.
      DO 5  I=1,N
    5 EMU(I)=RHOI(I)*VMUE(I)
      DO 100  I=1,N
      AX=CONC(I)*W(I)
      AVRHO=(FO/(F*TO))*AX +AVRHO
      ALPH=CONC(I)*ALPHA(I)*FO*100.
      AVALPH=AVALPH + ALPH
      AVW=AVW + CONC(I)*W(I)
      PHI =0.
      DO 85  J=1,N
      PHI=PHI+(CONC(J)/SQRT(8.*(1.+W(I)/W(J))))*(1.+SQRT(EMU(I)/EMU(J)
     1)*(W(J)/W(I))**.25)**2
   85 CONTINUE
      AVCON=AVCON + CONC(I)*CONDI(I)/PHI
      AVMU=AVMU + CONC(I)*EMU(I)/PHI
      VCP=CP(I)*W(I)*CONC(I)+VCP
  100 CONTINUE
```

```
      AVCP=WCP/AVV
      AVMUE=AVMU/AVGRO
      WRITE(6,110)
  110 FORMAT (1H ,4CX,37HAVERAGE PROPERTIES OF THE GAS MIXTURE )
      WRITE(6,120) AVGRO,AVALPH,AVCOND,AVM,AVMU,AVCP
  120 FORMAT (1H ,4CX,17HAVERAGE DENSITY,F8.5/4CX,26HTOTAL ABSORPTION C
     1OEFFICIENT,F8.7/4CX,24HAVERAGE THERMAL CONDUCTIVITY,F10.5/4CX,24HA/
     2VERAGE MOLECULAR WEIGHT,F8.3/4CX,27HAVERAGE KINEMATIC VISCOSITY,F1
     3.8/4CX,21HAVERAGE SPECIFIC HEAT,F8.5)
C     DEFINE NONDIMENSIONAL VARIABLES
C     U=U/RA/VMU     V=V*RA/VMU     X=X/RA     Y=Y/RA     T=(T/TO)-1
C     TAU=TAU*VMU/RA**2     RHO=RHO/RHOI     PP=P*RA**2/(RHOI*GE*V**2*TI)
C     DEFINE GRID SIZE
      XMAX=S/CEL+1.01
      JMAX=IMAX/2+1.01
C     INITIAL CONDITIONS
      DO 200  I=1,IMAX
      DO 200  J=1,JMAX
      UN(I,J)=200.
        VN(I,J)=0.
        RHO(I,J)=1.
        TN(I,J)=0.
      GR(I,J)=0.
      TF(I,J)=0.
      VORTS(I,J)=0.
      SI(I,J) =  .
  200 CONTINUE
      NPOINT=1
      NMOV =  0
      SI=RO
      TEMAX=0.
      TSLOPE=0.
C
C     ESTABLISH PLOTTER GRID
      PX(1) = PY(1) = 0.
      DO  I = 2,IMAX
```

```
      FX(I) = FX(I-1) + DEL
  205 CONTINUE
      DO  207    J=2,JMAX
      FY(J) = FY(J-1) + DEL
  207 CONTINUE
      KNTIME = 1
      CALL PLOT (0.0,0.3,-3)
C     FACTOR DETERMINES THE SIZE OF THE PLOTS
      F=.67
      CALL FACTOR(F)
      TMAXMAX=0.
      ITIME=1
      JRANG=RA/DEL+2.
      XCENT=(FLOAT(IMAX)+1.)/2.
      IRANG=XCENT-RA/DEL-2.
      IRTRNG=XCENT+RA/DEL+2.
      ITOP=IRTRNG
      IBOTM=IRANG
      IMAXP=IMAX-1
      JMAXP=JMAX-1
      ICHEK=IMAX/2+1
      JCHEK=JMAX*3/4
      DTAUM=DELT*AVANT/(RA*RA)*144.
      DELM=DEL/RA
      FRANT=AVNT*AVNT*3600./AVCON
      HALF=RF*.5*F/144.
      TERM2=GRAV*RA**3/(AMU**2*1728.)
      DELMSQ=DELM**2
      TERMA=DTAU/(ANU*DELM*DELM)
      TERM3 = DT/DELM
      TERMF=DTAU/(2.*DELM)
      TERM4=TERM*TIME
      TERM5 = TERM
      TERME=DTAU/DELMSQ
      TERMH=1./(2.*DELM)
      POWDEN=POWER/(3.14*RA**2*6.45)
```

```
      POWDEL=POWDEN*6.45
      QCONV=54*R**12./(AVRHO*AVGP*AVNUS*TO)
      GAM = 1.85
      CC = 2.*(C_LNSO/GAM-1.)
      BB = 2.*(1.+DELNSO/GAM)
      DO  170    I=1,IMAX
      P(I)=-BB
      AL(I) = 1.
  150 CONTINUE
  210 CONTINUE
      CALL HEAT (SA,DEL,AVALPH,POWDEN,POWDEL,QCONV,
     1 QTH,XCENT,IMAX,JMAX,IK,IBEDG,IBTEDG,JBEDG,ITIME)
      CALL TERME (IMAXR,IMAX,JMAXR,JMAX,ITOP,IBOTM,IBTEDG,
     1 QTAUM,TERMA,TERMB,TCHECK,JCHEK)
C    CALCULATE PRESSURE AND DENSITY
      EN=EI+(DEL)*R*QTH)/(AVH*HALFV*AVGP)
      DO  520    I=1,IMAX
      DO  520    J=1,JMAX
      RHON(I,J)=EN/(EO*(TE(I,J)+1.))
  520 CONTINUE
      CALL MOTION (IMAXR,IMAX,JMAXR,JMAX,NUCY,DELN,
     1 TERMC,TERME,TERMF,TERMH)
      ITIME=ITIME+1
      CLOCK=FLOAT(ITIME)*DELT
      IF(CLOCK .GE. TIME) GO TO 522
      CALL TIMREM (TLEFT)
      IF (TLEFT .LT. 10.0)    GO TO 522
      IF(ITIME .NE. NPRINT) GO TO 2005
      NPRINT=NPRINT+50
  522 CONTINUE
      QTH=2.*QTH
      WRITE(6,500)  EN,QTH
  500 FORMAT(20X, 15HPRESSURE (PSIA),5X,F10.5,20X,21HHEATING RATE(BTU/SE
     1C), 5X, F10.5)
  503 CONTINUE
      WRITE(6,2000)  CLOCK
```

```
 2000 FORMAT (//40X,8HTIME(SEC), 10X,F10.5////)
 2009 PI=PN
C    DETERMINE MAX TEMP AND OFFSET TEMPERATURES
      TEMAXP=TEMAX
      TEMAX=0.
      DO  2010    I=1,TMAX
      DO  2009  J=1,JMAX
      TEMAX=AMAX1(TEMAX,TF(I,J))
      TN(I,J)=TF(I,J)
      IF (TF(ICHECK,JCHEK) .GT. .0001)  GO TO 2009
      IF (ABS(TF(I,J)) .LT. .0001)   GO TO 2010
 2009 CONTINUE
 2010 CONTINUE
C    DETERMINE WHETHER MAXIMUM TEMPERATURE HAS REACHED A MAXIMA
      TSLOP=TEMAX-TEMAXP
      IF(TSLOP .GE. 0.) GO TO 2013
      IF(TSLOPP .LE. 0.) GO TO 2013
      TSLOPP=TSLOP
      GO TO 2025
 2013 TSLOPP=TSLOP
 2015 CONTINUE
      IF (TLAST .LT. 10.0)   GO TO 2020
      IF(CLOCK .LT. PTIME(KPTIME))  GO TO 2100
 2020 CONTINUE
      KPTIME = KPTIME + 1
      GO TO 2029
 2025 TMAXPP=(TEMAXP+1.)*TO
      IF(TMAXMAX .GT. TMAXPP)  GO TO 2015
      CLOCKP=CLOCK-DELT
      WRITE(6,2027)  CLOCKP, TMAXPP
 2027 FORMAT(30X,20HMAX TEMP ATTAINED AT, F9.5,2X7HSECONDS/40X,
     1 11HMAX TEMP =, 2XF9.2)
C      GRAPHS ARE ONLY DRAWN FOR MAX TEMPS EXCEEDING PREVIOUS
C      MAX TEMP BY TWO PERCENT
      IF(TMAXMAX .GT. .98*TMAXPP) GO TO 2015
      TMAXMAX=TMAXPP
```

```
 2029 CONTINUE
      KP = 1
C
C
C         FIND MAX AND MIN VORTICITY, TEMPERATURE, STREAM
C         FUNCTION AND UPWARD VELOCITIES FOR CONTOUR PLOTS
C
      ZMAX = TMAX = UMAX = SMAX = -1000.0
      ZMIN = TMIN = UMIN = SMIN =  1000.0
      DO 2030 I = 1,IMAX
      DO 2030 J = 1,JMAX
      ZMAX = AMAX1(ZMAX,VORT(I,J))
      TMAX = AMAX1(TMAX,TE(I,J))
      UMAX = AMAX1(UMAX,UN(I,J))
      SMAX = AMAX1(SMAX,SI(I,J))
      ZMIN = AMIN1(ZMIN,VORT(I,J))
      TMIN = AMIN1(TMIN,TE(I,J))
      UMIN = AMIN1(UMIN,UN(I,J))
      SMIN = AMIN1(SMIN,SI(I,J))
 2030 CONTINUE
C         SELECT CONTOURS FOR PLOTTING
      TMAX = AINT(TMAX*1000.0)/1000.0
      TMIN = AINT(TMIN*1000.0)/1000.0
      ZMAX = AINT(ZMAX) $ ZMIN = AINT(ZMIN)
      UMAX = AINT(UMAX) $ UMIN = AINT(UMIN)
      SMAX = AINT(SMAX) $ SMIN = AINT(SMIN)
      DELT = TMAX - TMIN
      DELZ = ZMAX - ZMIN
      DELU = UMAX - UMIN
      DELS = SMAX - SMIN
      DO 2040 I = 1,5
      FIE = 0.1*FLOAT(2*I-1)
      TC(I) = TMIN + FIE*DELT
      SC(I) = SMIN + FIE*DELS
      ZC(I) = ZMIN + FIE*DELZ
      UNC(I) = UMIN + FIE*DELU
```

```
      TA(I) = (TC(I)+1.0)**0
 2040 CONTINUE
      WRITE (6,2045) CLOCK,(TA(I),SC(I),UNC(I),ZC(I),MARKER(I),I=1,5)
 2045 FORMAT(*0  AT TIME =*F7.5,* SECONDS, PLOTTED CONTOURS ARE*/
     1 15X,4HTEMP,13X,2HST,13X,3HMUN,11X,4HMACH,9X,6HSYMBOL/
     2 (4X,4F15.4,8X,A10))
      WRITE (6,2047) SC(6),UNC(6),ZC(6),MARKER(6),TMIN,SMIN,UMIN,ZMIN,
     1 TMAX,SMAX,UMAX,ZMAX
 2047 FORMAT(15X,3F13.4,8X,A10/*0MIN*,4F15.4/* MAX*,4F15.4///)
C    PLOT 4 INCHES HIGH, 8 INCHES WIDE
C    DRAW BOX
 2050 CALL PLOT( .0,BY(JMAX),2)
      CALL PLOT(BX(IMAX),BY(JMAX),2)
      CALL PLOT(BX(IMAX),0.0,2)
      CALL PLOT( 0.0, 0.0, 2)
      CALL PLOT(BX(1),BY(1),3)
      DO 2055 I=2,IK
      CALL PLOT(BX(I),BY(I),2)
 2055 CONTINUE
      UNUSED(1,1)= .FALSE.
      IF (KP - 2) 2060,2070,2080
C    PLOT ISOTHERMS
 2060 CALL LEVEL2(BX,BY,TF,TC,UNUSED,IMAX,JMAX,5)
      CALL SYMBOL (2.90,-0.25,0.1,22HTEMPERATURES, (DEG. R),0.0,22)
      KP = 2
      CALL SYMBOL (-0.25,3.60,0.10,18HTIME =          SEC.,90.0,18)
      CALL NUMBER (-0.25,4.30,0.10,CLOCK,90.0,4)
      CALL PLOT (0.0,5.0,-3)
      GO TO 2050
C    PLOT STREAMLINES
 2070 CALL LEVEL2(BX,BY,SI,SC,UNUSED,IMAX,JMAX,6)
      CALL SYMBOL (3.2,-0.25,0.1,15HSTREAM FUNCTION,0.0,15)
      KP = 3
      CALL PLOT (10.0,-5.0,-3)
      GO TO 2050
 2080 CALL LEVEL2 (BX,BY,VJET,ZC,UNUSED,IMAX,JMAX,6)
```

```
      CALL SYMBOL (3.5,-0.25,0.10,9HVORTICITY,0.0,9)
      CALL PLOT (10.0,0.0,-3)
C     PLOT UPWARD VELOCITIES
      CALL TABASD (FY,FX,UN,IMAX,JMAX,IUN,JUN)
      CALL SYMBOL (3.2,0.750,0.1,15HUPWARD VELOCITY,0.0,15)
      CALL PLOT (10.0,0.0,-3)
 2100 CONTINUE
      IF (TLEFT .LT. 10.0)  GO TO 2120
      IF(CLOCK .LT. TIME)  GO TO 210
 2120 CONTINUE
      CALL PLOTE
      CALL TIMREM (TLEFT)
      WRITE (6,2200) TLEFT
 2200 FORMAT(1H0,F9.3,' SECONDS LEFT')
      STOP
      END
```

```
      SUBROUTINE HEAT (RA,DEL,AVALPH,POWDEN,POWDEL,QCONV,
     1 QTH,XCENT,IMAX,JMAX,IK,IBEGG,IRTEGG,JBEGG,ITIME)
      COMMON // RHOI(10),ALPHA(10),CONDI(10),W(10),CONC(10),CP(10),
     1         NAME(10,2),EMU(10),VNUE(10),PX(120),PY(120),
     2  UN(101,51),VN(101,51),TN(101,51),RHON(101,51),
     3  QN(101,51),TE(101,51),VORTP(101,51),VORT(101,51),SI(101,51)
C    DETERMINE HEATING RATE
C    ALPHA NOT INFLUENCED BY TEMPERATURE
C    GAS DENSITY VARIATIONS INCLUDED (ALPHA IS DIRECTLY PROPORTIONAL
C      TO DENSITY)
C    HEATING OCCURS IN A SECTION ONE INCH THICK
      DO  300  I=IBEGG,IRTEGG
      DO  300  J=1,JBEGG
      RADSQ=(ABS(XCENT-FLOAT(I))*DEL)**2+((FLOAT(J)-1.)*DEL)**2
      RAD=SQRT(RADSQ)
C    IF CENTERPOINT OF CELL LIES WITHIN BEAM, HEATING OCCURS
      IF(RAD .GT. RA) GO TO 300
      ALPH=AVALPH*RHON(I,J)*2.54
C
C     GAUSSIAN BEAM TRUNCATED AT DEFINED RADIUS
      QN(I,J)=2.*POWDEL*EXP(-.5*RADSQ/(.25*RA*RA))*ALPH/1055.*QCONV
C
  300 CONTINUE
C       DETERMINE ACTUAL ENERGY INPUT RATE
      QTH=0.
      AREA=0.
      DO 350  I=IBEGG,IRTEGG
      DO 350  J=1,JBEGG
      IF(QN(I,J) .EQ. 0.) GO TO 350
      QTH=QTH+QN(I,J)/QCONV*DEL*DEL
      AREA=AREA+DEL*DEL
  350 CONTINUE
      IF(ITIME .NE. 0)  GO TO 365
      IA=XCENT
      DO 354 I=IA,IRTEGG
      QRATP = QN(I,1) / QN(IA,1)
```

```
      WRITE(6,353) I,QPROP
  353 FORMAT(20X,1HI,5X,I4,10X,14HPROP INTENSITY,3X,E16.8)
  354 CONTINUE
C     DETERMINE  BEAM BOUNDARY
      IK=0
      KEDGE=1
      WRITE(6,931)
  931 FORMAT(///20H HEATED EDGE OF BEAM )
      DO  355  I=IBEDG,IREDG
      DO  355  J=1,JBEDG
      IF (KEDGE .NE. 2)  GO TO 910
      JR = JMPHE + 1 - I
      IF (JR .LT. 1)  GO TO 355
      IF (QN(I,JR) .LQ. 0.)  GO TO 356
      IF (QN(I-1,JR+1) .LQ. 0.)  GO TO 905
      IF (QN(I+1,JR+1) .LQ. 0.)  GO TO 905
      GO TO 355
  905 X=(I-1)*DEL
      Y = (JR-1)*DEL
      GO TO 930
  910 IF (QN(I,J) .EQ. 0.)  GO TO 355
      IF (QN(I-1,J+1) .EQ. 0.)  GO TO 920
      IF (QN(I+1,J+1) .EQ. 0.)  GO TO  920
      GO TO 356
  920 X=(I-1)*DEL
      Y=(J-1)*DEL
  930 CONTINUE
      WRITE(6,900)  X,Y
  900 FORMAT(1H ,20X,F10.5,5X,F10.5)
      IK=IK+1
      PX(IK)=X
      PY(IK)=Y
      IF (KEDGE .EQ. 2)  GO TO 356
      IF (QN(I+2,J) .NE. 0.)  GO TO 356
      JMPHE = J
      KEDGE = 2
```

```
      GO TO 355
  356 CONTINUE
  355 CONTINUE
  990 CONTINUE
      WRITE(6,310) POWDEN
  310 FORMAT(///20X,35HAVERAGE POWER DENSITY (WATTS/S) C4),10X,F9.4///)
C     DETERMINE ACTUAL POWER AND AREA-----ONLY WORKS FOR CONSTANT ALPHA
      AREA=2.*AREA
      QT=QTH/ALPH*1.05E.*2.
      ACPOWD=QT/(AREA*4.89)
      WRITE(6,360)QT,AREA,ACPOWD
  360 FORMAT(62X,18HACTUAL VALUES USED///41X,5HPOWER,20X,4HAREA,20X,18HP
     1OWER DENSITY/35X,F9.1,2X,5HWATTS,9X,F9.3,2X,6HSQ. IN.,3X,F1..3,2X,
     212HWATTS/SQ. CM ///)
  365 CONTINUE
      RETURN
      END
```

```
      SUBROUTINE TEMP (IMAXP,IMAX,JMAXP,JMAX,ITOP,IBOT+1,IBEDG,
     1 DTAUN,TERMA,TERMB,ICHEK,JCHEK)
      COMMON // RHOI(10),ALPHA(10),CONDI(10),W(10),CONC(10),CP(10),
     1         NAME(10,2),EMU(10),VNUE(10),BX(120),BY(120),
     2  UN(101,51),VN(101,51),TN(101,51),RHON(101,51),
     3  QN(101,51),TE(101,51),VCRTE(101,51),VORT(101,51),SI(101,51)
      DO 100  I=IBOTM,ITOP
      G  = SIGN(0.5,UN(I,1))
      TE(I,1)=TERMA*(TN(I+1,1)+TN(I-1,1)+TN(I,2)*2.-4.*TN(I,1))+DTAUN*
     1 QN(I,1)-TERMB*((0.5-G)*UN(I+1,1)*TN(I+1,1)+2.0*GUN(I,1)*TN(I,1)-
     2 (0.5+G)*UN(I-1,1)*TN(I-1,1)+VN(I,2)*TN(I,2))+TN(I,1)
      TE(I,JMAX)=TERMA*(TN(I+1,JMAX)+TN(I-1,JMAX)+2.*TN(I,JMAXM)-4.*
     1           TN(I,JMAX))+DTAUN*QN(I,JMAX)+TN(I,JMAX)
      DO  99  J=2,JMAXM
      F  = SIGN(0.5,VN(I,J))
      G  = SIGN(0.5,UN(I,J))
      TE(I,J)=TERMA*(TN(I+1,J)+TN(I-1,J)+TN(I,J+1)+TN(I,J-1)-4.*TN(I,J))
     1 +DTAUN*QN(I,J)-TERMB*((0.5-G)*UN(I+1,J)*TN(I+1,J)+2.0*G*
     2 UN(I,J)*TN(I,J)-(0.5+G)*UN(I-1,J)*TN(I-1,J)+(0.5-F)*VN(I,J+1)+
     3 TN(I,J+1)+2.0*F*VN(I,J)*TN(I,J)-(0.5+F)*VN(I,J-1)*TN(I,J-1))+
     4 TN(I,J)
      IF (TE(I,J) .GT. .0001)  GO TO 99
      IF (TE(ICHEK,JCHEK) .LT. .0001)  GO TO 100
   99 CONTINUE
  100 CONTINUE
C   EDGES
      DO 120  J=2,JMAXP
      TE(1,J)=TERMA*(TN(2,J)*2.+TN(1,J+1)+TN(1,J-1)-4.*TN(1,J))+DTAUN*
     1        QN(1,J)+TN(1,J)
      TE(IMAX,J)=TERMA*(TN(IMAXM,J)*2.+TN(IMAX,J+1)+TN(IMAX,J-1)-4.*
     1           TN(IMAX,J))+DTAUN*QN(IMAX,J)+TN(IMAX,J)
      IF(TE(IMAX,J) .LT. .0001)  GO TO 130
  120 CONTINUE
  130 CONTINUE
C   CORNER POINTS
      TE(1,1)=TERMA*(2.*TN(2,1)+2.*TN(1,2)-4.*TN(1,1))+DTAUN*QN(1,1)+
```

```
     1          TN(1,1)
      TF(1,JMAX)=TERMA*(2.*TN(1,JMAXR)+2.*TN(2,JMAX)-4.*TN(1,JMAX))+
     X1           DTAUN*GN(1,JMAX) +TN(1,JMAX)
      TF(IMAX,1)=TERMA*(2.*TN(IMAXR,1)+2.*TN(IMAX,2)-4.*TN(IMAX,1))+
     1           DTAUN*QN(IMAX,1)+TN(IMAX,1)
      TF(IMAX,JMAX)=TERMA*(2.*TN(IMAXR,JMAX)+2.*TN(IMAX,JMAXR)-4.*
     1             TN(IMAX,JMAX)+DTAUN*QN(IMAX,JMAX)+TN(IMAX,JMAX))
  200 CONTINUE
      IF(ITOP .EQ. IMAXR)GO TO 255
      IMAXR=IMAXR-1
      DO 250  I=IBTOM,IMAXR
      IF(TF(I,1) .GT. .0001)GO TO 250
      ITOP=I+2
      IF(I .LT. IMAXR)  GO TO 255
      ITOP=IMAXR
      GO TO 255
  250 CONTINUE
  255 CONTINUE
      IF(IBOTM . EQ. 2) GO TO 265
  258 CONTINUE
      DO 260 J=1,JMAX
      IF(TF(IBOTM,J) .LT. .0001) GO TO 260
      IBOTM=IBOTM-1
      GO TO 258
  260 CONTINUE
      IF(IBOTM .LT. 2) IBOTM=2
  265 CONTINUE
      RETURN
      END
```

```
      SUBROUTINE MOTION (IMAXR,IMAX,JMAXR,JMAX,NNCY,DELN,
     1 TERMU,TERMF,TERME,TERMH)
      COMMON // RHOI(10),ALFHA(10),CONDI(10),W(10),CONC(10),CP(10),
     1            NAME(10,2),AMU(10),VNUT(10),DX(120),DY(120),
     2  UN(101,51),VN(101,51),TN(101,51),RHON(101,51),
     3  OM(101,51),TF(101,51),VORTP(101,51),VORT(101,51),SI(101,51)
      DIMENSION  D(101),V(101),AL(101),B(101)
      COMMON/ONE/ DELNSQ,GAM,CC,JR,D,AL
      SIMAX=.001
C     CALCULATE VORTICITY (CORNER POINTS NOT R.D.FIELD-VORT(I,1)=0)
      DO 90  I=2,IMAXR
      DO 90  J=2,JMAXR
      F  =  SIGN( .5,VN(I,J))
      G  =  SIGN(.5,UN(I,J))
      VORT(I,J)  =  VORTP(I,J)-TERMU*((0.5-G)*UN(I+1,J)*VORTP(I+1,J)+
     1 2.0*G*UN(I,J)*VORTP(I,J)-(0.5+G)*UN(I-1,J)*VORTP(I-1,J)+
     2 (0.5-F)*VN(I,J+1)*VORTP(I,J+1)+2.0*F*VN(I,J)*VORTP(I,J)-
     3 (0.5+F)*VN(I,J-1)*VORTP(I,J-1))+
     1TERMF*(RHON(I,J+1)-RHON(I,J-1))+TERMH*(VORTP(I+1,J)+
     3              VORTP(I-1,J)+VORTP(I,J+1)+VORTP(I,J-1)-4.*VORTP(I,J))
      SIMAX=AMAX1(SIMAX,ABS(SI(I,J)))
   90 CONTINUE
      DO 110  I=2,IMAXR
      VORT(I,JMAX)=3.*(VORT(I,JMAXR)-VORT(I,JMAX-2))+VORT(I,JMAX-3)
  110 CONTINUE
      DO 130  J=2,JMAXR
      VORT(IMAX,J)=3.*(VORT(IMAXR,J)-VORT(IMAX-2,J))+VORT(IMAX-3,J)
      VORT(1,J)=3.*(VORT(2,J)-VORT(3,J))+VORT(4,J)
  130 CONTINUE
      NCYCLE=0
      XCHEK=.001
C     SI IS ZERO ON ALL 4 BOUNDARIES
  155 CONTINUE
      DO  300   J=2,JMAXR
      DO  200   I=2,IMAXR
      D(I)=-DELNSQ*VORT(I,J)-CC*SI(I,J)-SI(I,J+1)-SI(I,J-1)
```

```
280 CONTINUE
    CALL TRIDAC(2,IMAXP,AL,B,AL,D,V)
    DO  280   I=2,IMAXP
    UN(I,J) = V(I)
280 CONTINUE
300 CONTINUE
    EMAX=0.0
    DO  400   I=2,IMAXP
    DO  350   J=2,JMAXP
    D(J)=-FLN.C*VORT(I,J)-C*UN(I,J)-UN(I+1,J)-UN(I-1,J)
350 CONTINUE
    CALL TRIDAC(2,JMAXP,AL,B,AL,D,V)
    DO  380   J=2,JMAXP
    EMAX=AMAX1(EMAX,ABS((SI(I,J)-V(J))/SIMAX))
    SI(I,J) = V(J)
380 CONTINUE
400 CONTINUE
    NCYCL  = NCYCLE + 1
    IF (NCYCLE .LT. 300)  GO TO 410
    WRITE (6,405)
405 FORMAT(10X,29HCONVERGENCE PROBLEM IN SOTION  )
410 CONTINUE
    IF(EMAX .GT. XCHCK)  GO TO 155
422 CONTINUE
    DO  430 I=1,IMAX
    DO  430  J=1,JMAX
    VORTP(I,J) = VORT(I,J)
    IF(ABS(VORTP(I,J)) .LT. 1.E-7)  VORTP(I,J)=0.
430 CONTINUE
C   CALCULATE  VELOCITY
C   ALONG  AXIS  UN=VN=0
C   ALONG  CENTERLINE  UN=DUN/DY=0
    DO  500  I=2,IMAXP
    UN(I,1)=(SI(I,2)-SI(I,1))/DELN
    DO  460   J=2,JMAX
    UN(I,J)=(SI(I,J+1) - SI(I,J-1))*TERMN
```

```
      VV(I,J)=TE**2*(SI(I-1,J)-SI(I+1,J))
  400 CONTINUE
  500 CONTINUE
      RETURN
      END
```

```
      SUBROUTINE TRIDAG (IF,L,A,B,C,D,V)
C         SUBROUTINE FOR SOLVING A SYSTEM OF LINEAR
C         SIMULTANEOUS EQUATIONS HAVING A TRIDIAGONAL
C         COEFFICIENT MATRIX.
C         THE EQUATIONS ARE NUMBERED FROM IF THROUGH L,
C         AND THEIR SUBDIAGONAL, DIAGONAL, AND SUPER-
C         DIAGONAL COEFFICIENTS ARE STORED IN THE ARRAYS
C         A, B, AND C.  THE COMPUTED SOLUTION VECTOR
C         V(IF)...V(L) IS STORED IN THE ARRAY V.
      DIMENSION A(1),B(1),C(1),D(1),V(1),F(101),G(101)
C
C         COMPUTE INTERMEDIATE ARRAYS F AND G.
C
      IFP1   = IF+1
      F(IF)  = B(IF)
      G(IF)  = C(IF)/B(IF)
      DO 1 I = IFP1,L
      F(I)   = B(I)-A(I)*C(I-1)/F(I-1)
      G(I)   = (D(I)-A(I)*G(I-1))/F(I)
    1 CONTINUE
C
C         COMPUTE SOLUTION VECTOR V
C
      V(L)   = G(L)
      LAST   = L-IF
      DO 2 K = 1,LAST
      I      = L-K
      V(I)   = G(I)-C(I)*V(I+1)/F(I)
    2 CONTINUE
      RETURN
      END
```

APPENDIX 3

GAS DENSITY VARIATION ASSUMPTION

In the equations of motion, the gas density is assumed to be constant except in the bouyancy force term. This assumption simplifies the solution of the equations and produces only minimal error if the variations in gas velocities and temperatures are small. However, for some of the problems considered here, local absolute temperature values nearly doubled. This, of course, results in a fifty percent decrease in density. This change in density due to heating is considered in the calculation to determine the amount of energy absorbed from the laser beam, but is not taken into account on the left side of the equations of motion. Since the magnitude of the error introduced by this assumption will vary spatially with temperature, its effects should be most significant near the heated region. Unfortunately, this is also the area of greatest interest. It is recommended that future attempts to solve this problem incorporate variable density throughout.

APPENDIX 4

PROGRAM USERS' INSTRUCTIONS

Figure 5 lists the input data, and the appropriate units for this data, which must be provided. Appendix 2 is a listing of the main program and the four primary subroutines. Several other subroutines, used only for plotting purposes, are not shown. The following is a list of important terms along with some discussion of each term as necessary. These are presented in the approximate order in which they are encountered in the program.

Variable	Function
Main Program	
IUN (array-card 17)	This defines the X values of the velocity vs. horizontal distance plots. The location of these X values is IUN*DEL
PTIME (array-card 17)	This defines the times at which plots will be drawn
Read statement (card 19) - first data card	
TO	Initial temperature
POWER	Power of laser beam
RA	Beam radius
DELT	Size of time steps
PO	Initial pressure
N	Number of components in the gas mixture
DEL	Size of spatial steps
S	Length of side of cross-section of the square enclosure
TIME	Irradiation time

Read statement (card 38) - next N data cards. Each subscript M refers to a different component in the gas mixture. Each variable is an array of size N.

NAME	Name of component
RHOI	Initial density of component at TO and PO
ALPHA	Absorption coefficient per psi and per volume percent of that component
CONDI	Thermal conductivity
W	Molecular weight
CONC	Concentration (mole fraction)
VNUE	Kinematic viscosity
CP	Specific heat
GRAV (card 46)	Acceleration of gravity in feet per second^2
R (card 47)	Universal gas constant in (psia-ft^3/ mole °R)
AVRHO (card 49)	Gas mixture initial density
AVALPH (card 50)	Gas mixture total absorption coefficient ($c.^{-1}$) at the initial conditions
AVCON (card 51)	Gas mixture thermal conductivity
AVW (card 52)	Gas mixture molecular weight
AVNUE (card 53)	Gas mixture kinematic viscosity
AVMU (card 55)	Gas mixture viscosity
AVCP (card 73)	Gas mixture specific heat
IMAX (card 86)	Number of grid spaces or elements in vertical (X) direction
JMAX (card 87)	Number of grid spaces or elements in horizontal (Y) direction
UN (array-card 91)	Non-dimensional local vertical velocity
VN (array-card 92)	Non-dimensional local horizontal velocity

RHON (array-card 93)	Non-dimensional local density
TN (array-card 94)	Non-dimensional local temperature at start of a time step
QN (array-card 95)	Non-dimensional local volumetric heating rate
TF (array-card 96)	Non-dimensional local temperature at end of a time step
VORIP (array-card 97)	Non-dimensional local vorticity at the start of a time step
SI (array-card 98)	Non-dimensional local stream function
NPRINT (card 100)	Whenever the number of time steps taken is equal to NPRINT (i.e., ITIME .EQ. NPRINT) then the pressure, total heating rate, and time will be printed.
PI (card 102)	Initial pressure
PX & PY (card 107)	Used to establish plotter grid. All points in the plots can be identified by coordinates (PX, PY).
KPTIME (card 114)	This defines the subscript value for the PTIME array
F (card 117)	This term determines the size of the plots. For F=1, the plots are 4" x 8". The size of plots is proportional to F.
ITIME (card 120)	This defines the number of time steps preceding the current one.
XCENT (card 122)	This determines the vertical distance from the bottom edge of the enclosure to the center of the enclosure.
DTAUN (card 131)	Non-dimensional time step ($\Delta\tau$)
DELN (card 132)	Non-dimensional spacial step (ΔX)
PRAND (card 133)	Prandtl number
POWDEN (card 144)	Average power density (watts/cm^2) based on input beam power and radius.
GAM (card 147)	This is the "dummy" variable used in subroutine MOTION to solve the equation of motion via the ADI method.

PN (card 160)	Pressure at the end of each time step
QTH (card 175)	The actual heating rate per inch of thickness over the entire beam area. This is calculated in subroutine HEAT for one-half of the beam area.
TMAXPP (card 206)	The maximum temperature attained at any point in the array. The program determines this value, prints it, and automatically plots the graphs at the next time step.

Subroutine HEAT

This subroutine determines which grid elements are to be heated (e.g., whether they be in beam path) and calculates the local heating rate at each element. The proportional intensity of the beam and the coordinates of the heated edge of the beam are also determined and printed. The total volumetric heating rate (QTH) for one-half of the beam and per inch thickness is also determined. Finally, the actual power and actual beam area used in the calculations, which differs from input data due to beam truncation, and numerical approximation errors, is determined and printed. Cards 20 and 21 are changed when a "flat-top" beam is considered.

RAD (card 15)	This is the distance from an element to the center of the beam. This is used to determine if, and how much, heating will occur at that element.
ALPH (card 18)	Local absorption coefficient per inch
AREA (card 26)	One-half of the actual cross-sectional area in the beam path. Converted to total actual beam area at card 80.
QPROP (card 31)	Ratio of the intensity of the beam at any point to its intensity at the beam center.

BX & BY (arrays-cards 62 & 6)	These define the heated elements which lie on the edge of the heated (beam) area.
QT (card 81)	Actual beam power used in program
ACPOWD (card 82)	Actual power density

Subroutine TEMP

This subroutine solves the energy equation in order to find the new temperature array TF.

Subroutine MOTION

This subroutine solves the motion equation to find the new vorticity array VORT. This new VORT array is used to find the SI array (stream function) via the ADI method described in the report. Finally, the SI array is converted to local velocity arrays UN and VN. The variable XCHEK at card 31 is the value used to determine if suitable convergence has occurred in the ADI method calculations.

Subroutine TRIDAG

This subroutine solves the system of linear equations encountered in the ADI method calculation of stream function (SI) from vorticity (VORT) in subroutine MOTION.